Bridging further animal and human memory function using functional magnetic resonance imaging in awake rats and molecular imaging

Thesis

for the degree of

doctor rerum naturalium (Dr. rer. nat.)

approved by the Faculty of Natural Sciences of
Otto-von-Guericke-University Magdeburg

by M.Sc. Liv Mahnke
born on 26.11.1987 in Wuppertal

Examiner: Prof. Dr. Magdalena Sauvage
Assoc. Prof. Dr. Jan Pieter Konsman

submitted on: 21.10.2021
defended on: 07.04.2022

Table of Content

Table of Figures

List of Abbreviations

Arc	activity-regulated cytoskeletal-associated gene, Arg3.1
BOLD	blood-oxygen-level-dependent
CA1/CA3	cornu ammonis field 1 / 3
CgCx	cingulate cortex
DNMS	delay non-matching-to-sample
EPI	echo-planar imaging
FISH	fluorescent in situ hybridization
fMRI	functional magnetic resonance imaging
IEG	Immediate Early Gene
GLM	general linear model
GP	globus pallidus
HIP	hippocampus
HRF	hemodynamic response function
MTL	medial temporal lobe
MR	magnetic resonance
OB	olfactory bulb
LEC	lateral entorhinal cortex
PER	perirhinal cortex
ROI	region of interest
SPM	Statistical Parametric Mapping
T	Tesla
TE	echo time
TR	repetition time
VPL/VPM	ventral posterolateral/-medial thalamic nucleus

Abstract

The Medial Temporal Lobe (MTL) of the brain has been established to be crucial for memory function. Damage to this area, as seen, for example, in aging or patients suffering from amnesia, leads to severe memory deficits. The MTL comprises the Hippocampus (HIP) and cortical areas surrounding the HIP: the parahippocampal areas. Despite decades of research on memory function, the specific role of these subareas in episodic memory, as well as their functional relationship, remains unclear. Partly because MTL damage in patients often extends to more than one MTL subregion, thereby preventing a dissociation of their function. Notably, the function and cytoarchitecture of the MTL are conserved across a various range of species, including rodents. This allows for the use of rodent models, in which invasive targeted manipulations can be implemented, to tackle questions under debate in humans. Yet, principally because of different modus operandi, findings are transferable between species only to a limited extent. For example, in functional magnetic resonance imaging (fMRI) studies, rats are usually tested under sedation while humans are awake during testing. In the present thesis, the use of two different human-to-rat translational approaches to study the role of the HIP in episodic memory was proposed.

A 9.4 Tesla (T) functional MRI approach in awake rats to achieve the standard whole-brain analyses conducted in human fMRI studies was established, and a human-to-rat behavioral paradigm with a cellular resolution imaging technique based on Immediate Early Gene detection combined. Using a high throughput MRI-compatible olfactometer (Chapter 2) and a memory paradigm for awake rats that was adapted to 9.4T fMRI, we report results similar to those observed in humans, including a more important role of the HIP in processing odors for which memory could be formed in contrast to odors newly experienced (Chapter 3). Furthermore, we showed that only the contribution of some parahippocampal areas to recognition memory (such as the lateral entorhinal cortex) is inversely correlated to hippocampal function (Mahnke et al., 2021). Here we used an imaging technique with a spatial resolution high enough to dissociate the source of activity even between adjacent brain areas.

The findings emerging from these two studies suggest that even though very challenging, human-to-rat translational approaches open up very promising avenues for future cross-species studies.

Chapter 1

1. General Introduction

1.1 Episodic recognition memory

Episodic recognition memory, the ability to identify an item, an event, or a person that has been encountered previously 'comes in handy' for coping with day-to-day routines for both humans and animals. The ongoing debate on whether episodic memory is present in animals to a comparable extent as in humans is still a subject of debate. Yet, evidence has accumulated that rodents can remember specific episodes from their past in a restricted but comparable manner as humans (Babb & Crystal, 2006; Binder et al., 2015; Crystal, 2009; Fouquet et al., 2010), thereby implying a possible bridging of rodent and human memory function.

Recognition memory is suggested to be supported by two memory retrieval processes, namely familiarity and recollection. Familiarity is described as a vague feeling of "déjà vu", for example, when one recognizes a person as familiar, without being able to retrieve additional information about the person´s life or their name. In contrast, the recollection process allows for retrieving additional details about this person, including spatial and temporal information, i.e., when and where you meet this person for the first time (for a review, see Yonelinas, 2002). The contribution of familiarity and recollection to recognition memory has been extensively studied. Two models have prevailed to date: the dual-process model and the one-process model (for reviews, see Yonelinas & Parks, 2007; Squire et al., 2007; respectively). Both models agree in the Medial Temporal Lobe (MTL) being critical for the recognition memory and in the hippocampus (HIP), part of the MTL, supporting recollection. However, what remains a matter of debate is if the HIP also supports familiarity and if the parahippocampal areas, also part of the MTL, are segregated into areas supporting familiarity: the lateral entorhinal (LEC) and the perirhinal (PER) cortices and areas supporting recollection: the medial entorhinal (MEC) and the postrhinal (POR) cortices (see **Figure 1**). This is

important because recollection is affected explicitly in aging or patients suffering from amnesia presenting memory deficits while familiarity is spared (Jennings & Jacoby, 1997; Koen & Yonelinas, 2014). Hence, identifying which specific areas of the MTL support familiarity and recollection might rescue memory deficits seen in these populations, possibly by boosting areas supporting familiarity. Moreover, it is still unclear whether the contribution of the parahippocampal areas to familiarity is entirely independent of hippocampal function or whether these areas are functionally tied within this frame.

1.2 The Medial Temporal Lobe

Due to extensive research over the past decades, the MTL has been identified as one major brain area involved in recognition memory (see review by Eichenbaum et al., 2007). The MTL, a structure consisting of the hippocampal formation and the parahippocampal areas, can be found bilaterally both in humans and rodents (one hemisphere displayed in **Figure 1**).

The hippocampal formation is subdivided into four distinct subregions: the subiculum, the cornu ammonis fields (CA1, CA2, CA3; the CAs), and the dentate gyrus. These regions were subdivided based on their neuroanatomy and cytoarchitecture (see Chapter 3 by Amaral & Lavenex in Andersen et al., 2007). In this thesis, I will refer to the hippocampus as composed of the CAs and the dentate gyrus unless stated otherwise. The parahippocampal areas, a set of cortical structures, namely the perirhinal (PER), parahippocampal (called postrhinal in rodents), medial and lateral entorhinal cortices (MEC and LEC), surround the hippocampus.

Between the subregions of the MTL, a high anatomical and functional connectivity was found over the past decades (see, e.g., Burwell, 2000; Van Strien et al., 2009). One anatomical pathway frequently investigated is the perforant pathway, a circuit

describing the major cortical input of the entorhinal cortex (EC) to the hippocampal formation (i.e., all subregions). In addition to the connectivity within the MTL, further connections can be found from the HIP to other brain regions, e.g., the cingulate cortex (CgCx) through the Papez circuit or the globus pallidus (GP) (Aggleton & Brown, 1999; Packard & Knowlton, 2002).

1.3 Structural and functional conserved MTL across rodents and humans

Despite an extensive investigation in both humans and rodents over the past decades of the role of the MTL areas in recognition memory, the contribution of the individual MTL subregions to recognition memory remains unclear. Given that in humans with MTL damage following, e.g., brain trauma or heart attack, the damage extends typically to several of the MTL subareas (for a review, see, e.g., Eichenbaum et al., 2007), the most promising approach to address this question is the use of rodent models. These models allow for targeted and controlled manipulations of specific subareas, which is not the case in humans. Such manipulations require to date invasive approaches that cannot occur in humans. Tackling questions related to human memory function is enabled because it has been shown that humans and rats share similar types of memory (Babb & Crystal, 2006; Binder et al., 2015; Crystal, 2009; Fouquet et al., 2010). Also, various studies have reported the structural and functional conservation of the MTL subregions between rodents and humans (for the HIP, see Chapter 3 in Andersen et al., 2007; Manns & Eichenbaum, 2006).

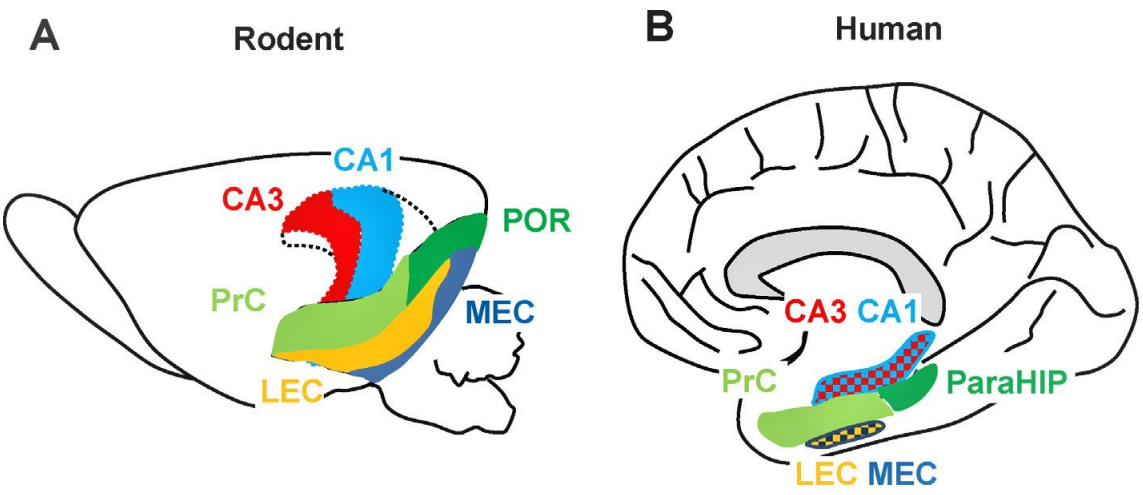

Figure 1: The medial temporal lobe is conserved across species. Subregions of the MTL are shown in **A** rodents and **B** humans. The figure was taken with permission from (Sauvage et al., 2013).

1.4 Memory impairments due to aging or diseases

As previously mentioned, identifying the neuroanatomical network supporting memory function and especially the neural substrates of familiarity are of high societal impact given the memory deficits experienced in aging and patients suffering from 'related' pathologies. Indeed, age-related cognitive decline has become a major burden in our society [for a review see, e.g., World health report 2001 (World Health Organisation, 2001)]. Aging and pathological conditions, such as amnesia or Alzheimer´s disease, correlate with hippocampus dysfunction, manifesting as episodic memory impairments (Bäckman et al., 2001). Finding a treatment to help reduce, stop the decline of, or even improve the memory performance, requires knowledge about the role of each brain region within this frame. Therefore, understanding the specific contribution of each brain area during recognition memory is an important and growing field of research in Neuroscience (Eichenbaum et al., 2007; Yonelinas et al., 2005). Several studies with patients suffering hippocampal damage or damage in other

parts of the MTL reported various levels of memory decline (Aggleton et al., 2005; Brandt et al., 2016; Rempel-Clower et al., 1996; Yonelinas et al., 2002). This decline could be a deficit in recollection but sparing the familiarity process or vice versa, or with a broad MTL damage include both processes. Progress in unraveling the specific role of each area is, however, heavily hindered by the fact that invasive approaches can be implemented only under particular conditions in humans (i.e., implantation of electrodes in epileptic patients, etc.).

1.5 Translational approaches between humans and rodents

Considering the above-mentioned conservation of the MTL and the somewhat comparatively less problematic access to laboratory rodents, human-to-rat translational approaches to study recognition memory are a useful tool. Such translational approaches consist of establishing experimental conditions for rats as similar as possible to those used in humans, intending to collect similar data and analyze them with the same tools and models to yield results more readily comparable between these species. This approach and the ability to target specific brain areas and control for the damage/changes can be very instrumental for investigating recognition memory. Using such human-to-rat translational paradigms, primarily behavioral to date, has already yielded essential findings, especially regarding the role of the hippocampus, in recognition memory (Clark et al., 2001; Fortin et al., 2004; Nakamura & Sauvage, 2016).

A successful translational approach for similarly testing recognition memory in rodents as in humans was developed by Fortin and colleagues (2004). A list of words or pictures is typically presented to the subject during a 'study phase' to test for recognition memory in humans. After a delay, the previously shown stimuli

(words/pictures) are presented again during a recognition phase (they constitute the `old´ stimuli), but this time intermixed with new words/pictures (i.e., the `new´ stimuli; see **Figure 2**). Memory performance is assessed during the recognition phase by asking subjects to identify as `old´ the stimuli they encountered during the study phase, and as `new´ stimuli they did not encounter (used for example by Kim et al., 1999; Stark & Squire, 2000). To identify brain regions activated during recognition memory using fMRI in humans, scanning occurs upon presenting the stimuli in the MR scanner. In some studies, stimuli are viewed 'passively' and memory performance assessed upon scanning completion (i.e., outside of the scanner), while in others, memory performance is taxed inside the scanner.

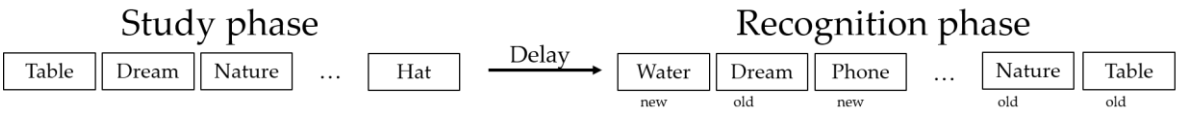

Figure 2: One example of a simple recognition memory task used in human fMRI. In the scanner, during the study phase, a series of words displayed on a screen (one at a time) is presented to the subjects (pictures or faces are also used). After a delay, subjects are presented the previously shown list of words (old) intermixed with a list of new words during the recognition phase. Memory performance is assessed by asking subjects to identify stimuli as `old´ (stimuli viewed during the study phase) or `new´ (not viewed during the study phase).

Fortin and colleagues adapted this behavioral paradigm to rats by using neutral odors such as household scents (thyme, lemon peel, etc.) instead of visual stimuli, given that the primary sense of rodents is olfaction and not vision. In this paradigm, similar as in humans, transparent cups filled with sand mixed with an odor stimulus were presented to the rats during the study phase while remaining in their home-cage. One cup at a time was presented; it was ensured they smelled the odor because a small piece of cereal they like was buried in the scented sand. After a delay, the memory for these odors was tested by presenting either the odor experienced during the study

phase (`old´ odor) or a new odor they had not been presented with (`new´ odor) to the rats. The rats were trained to respond following a non-matching-to-sample rule, according to which they should refrain from digging, turn around, and go to the back of the cage to receive a food reward when presented with an `old´ odor: a correct response for an `old´ odor. Conversely, when the odor was not part of the study list (a `new´ odor), animals could retrieve a buried reward by digging in the test cup: a correct response for a `new´ odor. As was the case in humans, memory performance was assessed as a percentage of correct choice. Further, in the case of the rats, detection of the brain activity was performed by using a molecular imaging technique based on the detection of Immediate Early Genes (IEG). This technique has the advantage to yield cellular spatial resolution but at the cost of making whole-brain analyses very laborious and time-consuming, if not impossible.

On the other hand, even though fMRI studies focusing on cognitive functions in rodents are virtually lacking to date, a growing number of studies have used fMRI in sedated rodents to investigate resting-state or functional connectivity (Kalthoff et al., 2011; Scherf & Angenstein, 2017; for a review, see Jonckers et al., 2015). Yet, very few have used awake rodents (see, e.g., Brydges et al., 2013; Harris et al., 2015; Stenroos et al., 2018). Some of the reasons for this shortcoming are the challenges that present the optimal conditions necessary for studying cognition within an fMRI setting. These would include imaging animals ***awake***, defining the appropriate ***fMRI scanning sequence*** for this purpose, and putting together an fMRI-compatible setup that can deliver a ***high number of stimuli*** as required in human fMRI studies focusing on memory function. However, developing such an approach is crucial to bridge further human and animal recognition memory by making findings more readily comparable across species.

Using such a human-to-rats translational fMRI paradigm and in parallel translational behavioral paradigms combined with high-resolution IEG imaging constitutes an optimal approach to embrace the complexity of a whole-brain analysis of the neural substrates of memory function. Yet, it still yields the high spatial resolution of analysis

necessary to, for example, evaluate the role of the HIP in recognition memory and whether its integrity is necessary to ensure the optimal contribution of the LEC and the PER to familiarity signals during recognition memory.

1.6 Aim and outline of the thesis

The main goal of this thesis is **to bridge further human and animal recognition memory** by using experimental conditions in rats as similar as possible as those used in humans to make findings more readily comparable between species.

In the present study, a focus was set on the **hippocampus**. Its **role in recognition memory** was investigated using a whole-brain level of analysis by establishing a **9.4T fMRI-compatible memory paradigm** similar to those used in humans to test rats in an **awake** state (Chapters 2 and 3). In addition, using a translational human-to-rat behavioral paradigm combined with IEG imaging provided the spatial resolution necessary to **investigate the reliance of the LEC and the PER on hippocampal function** during recognition memory (Chapter 4).

To achieve the *first goal*, in line with human studies, **a fMRI-compatible hardware** that was necessary to **deliver a high number of stimuli** was built, and its function was tested. This was done by duplicating a 40 channels olfactometer designed in our lab for a 7T scanner. Then the fMRI sequence was adapted, and its function was tested with the 9.4T scanner by detecting BOLD activation patterns (odor maps) in the olfactory bulb (Chapter 2). This olfactometer was subsequently used to perform **a whole-brain analysis of BOLD activation patterns occurring during recognition memory with the hippocampus as a focus** by adapting the 7T memory paradigm developed in our lab for awake rats to the 9.4T scanner (Chapter 3). This translational study is the first allowing for contrasts similar to those performed in humans to be

analyzed in awake rats and leading to results similar to those reported in humans, opening up very promising new avenues for future cross-species studies.

To achieve the *second goal* of the study, **the influence of hippocampal function on the contribution of LEC and PER familiarity signals to recognition memory** was investigated using a higher spatial resolution imaging technique (IEG imaging). This technique allows to dissociated the source of activity even between adjacent brain areas, which is the case of the LEC and the PER (Chapter 4). This study suggests that the contribution of the PER to recognition memory within this frame is independent of the hippocampus. But not that of the LEC, its contribution is inversely correlated to hippocampal function (Mahnke et al., 2021).

Finally, a summary and integration of the findings can be found in the last chapter of the thesis, together with a discussion of the challenges encountered, limitations of the studies, and an outlook on future experiments (Chapter 5).

Chapter 2

2. Obtaining odor-specific activation maps in the olfactory bulb verifies the functionality of the 40-channel olfactometer at 9.4T

2.1 Introduction

Besides the use of electrophysiological and optogenetic techniques, the use of olfactory stimuli while performing fMRI experiments has increased over the past years. For testing memory function, a high number of stimuli (at least 30-40) have to be delivered to be comparable to human experimental conditions. Additionally, the olfactometer has to be fMRI compatible. To date, however, only a small number of rodent studies are present that delivered different odors during an fMRI scan. These studies presented at most 4 distinct odors within a scan and are therefore not compatible with the investigation of memory function (Chen et al., 2020; Fonseca et al., 2020; Han et al., 2019). In addition, these studies used artificial odors (chemicals) and not naturalistic odors such as household odorants, as it is the case in our study. In humans, a 24-channel fMRI-compatible olfactometer is available, a number of channels that is however not high enough to readily compare human and animal data (Bestgen et al., 2016). For this reason, a previous Ph.D. student of the lab (Caroline Chwiesko) developed a versatile (i.e., more channels can be added) 40-channels fMRI-compatible olfactometer together with a custom build odor delivery mask. Using this setup, animals could be scanned under awake conditions at a later time point with 7T fMRI (Chwiesko, 2017), following the aim of enabling human to rodent translational approaches for investigating memory.

The main aim of the present study is to duplicate and test the olfactometer designed in Bochum and adapt it to the needs of 9.4T fMRI scanning. This required building the olfactometer 'anew' at the LIN (Leibniz Institute for Neurobiology), adapting the

7T scanning sequence to a 9.4T scanner, and testing the functionality of the olfactometer within this frame. To do so, we conducted two experiments focusing on validating the delivery of odors by the olfactometer by studying odor maps in the olfactory bulb (the first olfactory relay in the brain) of rats scanned under medetomidine sedation. Experiment 1 aimed at demonstrating that delivering (5) distinct odors with the olfactometer (short odor presentations) elicits distinct odor maps within a single 9.4T scan. The second experiment demonstrates the ability of the olfactometer to deliver odors from a high number of channels (ca 40) within one scan. The data collected in these two studies are part of a manuscript shortly submitted to the Journal of Neuroscience Methods.

2.2 Material and Methods

Duplicating the olfactometer was achieved by building anew the control unit, located outside the MR (magnetic resonance) scanner room, and the delivery unit containing only nonmagnetic components, located inside the MR scanner room (see **Figure 3**). On the one hand, the magnetic environment of the MR scanner requires that the parts of the olfactometer containing metal or electrical components be placed outside of the MR test room. This includes the valves delivering the airflow to the odorant pots and the computer and software, including the converter that converts the output trigger sent by the scanner. On the other hand, to ensure a precise temporal stimulus presentation, the distance between the pots which contain the odors and the odor delivery mask needs to be as short as possible. Therefore, the nonmagnetic odorant pots are located within the MR testing room.

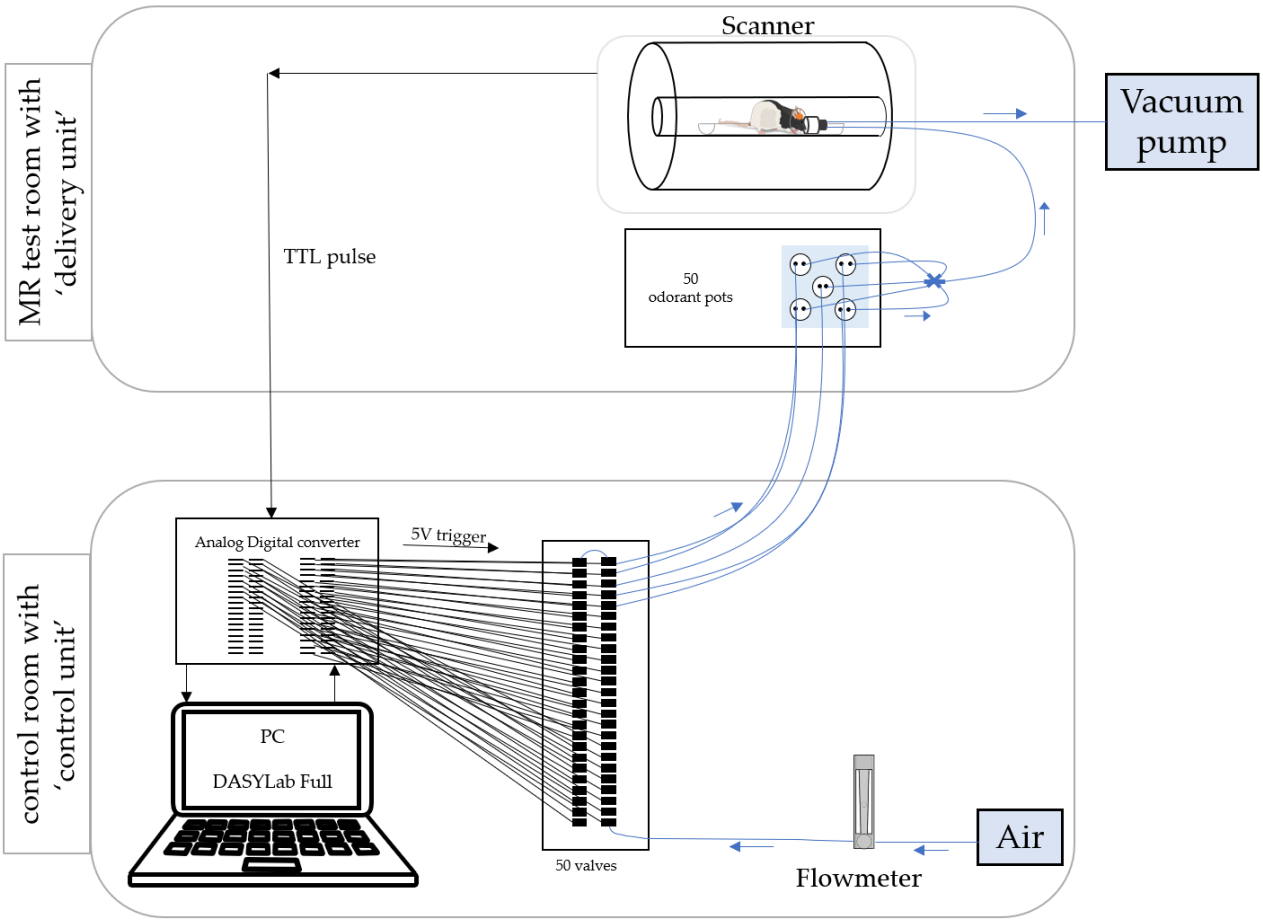

Figure 3: Basic scheme of the airflow and controlling parts for the odor delivery by the olfactometer. The olfactometer can be divided into two parts. First, the control unit, located outside the scanner room where the TTL pulse sent by the scanner is processed to open valves individually and allow the odors to be delivered. Secondly, the delivery unit is located close to the scanner. Here, the airflow is led through stimulus pots (odorant pots) containing either an or no odorant to be delivered to the animal's nose.

A detailed description of the individual components used to build the olfactometer can be found in Chwiesko (2017). In brief, the control unit is subdivided into the assembly of valves used to control the delivery of airflow to the odorant pots, the signal converter, and the stimulation program needed for the operation of the valves. As mentioned above, the components containing metal or electrical parts are located outside of the MR scanner room. These include the air supply (clinic air wall outlet), followed by a flowmeter controlling the flow rate (10L/min) throughout the

experiments. The flowmeter is connected to the valve assembly that contains 50 electromagnetic 2/2 way valves. These valves are operated by the computer software DASYLab Full (Data Acquisition System Laboratory, National Instruments), connected to the Analog-Digital converter that converts the scanner output trigger to be used for synchronized odor delivery with image acquisition. On the other end, the valves are connected via PFA tubing with the odorant pots containing the odors.

Further tubing from the odorant pots leads to the odor delivery mask placed in front of the rat's nose inside the scanner. The odor delivery unit (located inside the scanner room), including the odorant pots, one-way check valves used to avoid cross-contamination, odor delivery mask, and the tubing, were either made from PFA or Teflon due to its non-adhesive properties and MR safety. The adjusted and customized odor delivery mask is connected to one tube that delivers the odor stimulus (individual tubes from the pots were combined with 6- and 3-way Teflon connectors) and to one 'exhaust' tube to remove odor using a continuous vacuum system (vacuum pump located outside of the scanner room). Furthermore, pots exclusively used to deliver air (odorless) in between odor presentations (to flush lingering odors) are used as control pots (a total of 10 pots). Duplicating the system designed in Bochum, including the adaptation to 9.4T scanner and first functionality tests, required nearly 11 months.

Validation of odor delivery by the olfactometer

2.2.1 Animals

Male adult Long Evans rats weighing between 380 and 510 g and 6 to 8 months of age were used in this study. Rats were kept single-caged and under a reversed 12 h light/dark cycle (7 a.m. lights off; 7 p.m. lights on). Water and energy-reduced food were provided *ad libitum*. A total of 10 rats were used for the first experiment and 2 rats (different cohort) were used in Experiment 2. All procedures were approved by the animal care committee of the State of Saxony-Anhalt (42502-2-1489 LIN) and performed in compliance with the guidelines of the European Community.

2.2.2 Animal preparation

The animals were initially anesthetized with isoflurane (2 % lowered to 1.5 %, in 50:50 N2:O2; v:v) with a calibrated vaporizer. Following, a small cannular was inserted intravenously into the tail vein to inject medetomidine (continuous infusion during the scan; 60-80 µg/kg per h i.v.). Then the isoflurane concentration was reduced stepwise and stopped. Thereafter, the animal was placed and fixed using a cloth and tape into the animal bed with their nose placed within the odor delivery mask. The animal's normal body temperature was maintained with a heating mat and its eyes were coated with a moisturizing balm. Once the experiment was completed, the continuous medetomidine injection was stopped. The animals were placed in their homecage after receiving a subcutaneous injection of atipamezole (anti anesthetic; 60-80 µg/kg; Antisedan, Pfizer, Karlsruhe, Germany).

2.2.3 Odor stimuli

The odors used in this study consisted of 100 % pure essential oils (Dragonspice Naturwaren, Reutlingen, Germany) and common household spices. Neutral odors from different categories like fruity, flowery, or spicy were chosen. A total of 19 different odors were used for the experiments. Odors presented to at least 4 out of the 7 animals used in data analysis were banana, bay, chamomile, cherry, curcuma, cumin, orange, sunscreen, sweet woodruff, and pine. Presented to 3 or fewer animals were Aloe Vera, apple, cinnamon, fennel, galangal, mango, pine-needle, pistachio, and rose. The strength of the odors was kept comparable.

2.2.4 Stimulation paradigm

Two experiments were conducted using different cohorts of rats. A simple block design was used in this study for both experiments (see **Figure 4A** and **B**). As described in Chwiesko (2017) for Experiment 1, five different odors were presented from 5 distinct channels in a pseudo-random manner. Each odor was presented 7 times in

total. The odor stimulation lasted for 8 sec with an inter-stimulus interval of 32 sec (`no odor´; air), resulting in a total scanning time of approximately 26 minutes.

In Experiment 2, only the odor 'cherry' was presented in 8-sec stimulation blocks. The BOLD response upon 7 presentations of 'cherry' in Channel 1 was considered the 'control cherry map'. Preliminary data showed that the extraction of a specific odor map required a minimum of 7 presentations of the odor. The remaining 36 channels delivered the odor only once. A total of 3 channels were used as 'control' channels, i.e., did not deliver any odors, only air. This paradigm resulted in a total scanning time of approximately 40 minutes. Stimulus delivery followed the sequence of channels used in Experiment 1 (i.e., was pseudorandomized). The odor-specific map elicited by the 7 presentations of 'cherry' by Channel 1 was then compared to the ones elicited by different combinations of 7 other channels.

A **Experiment 1**

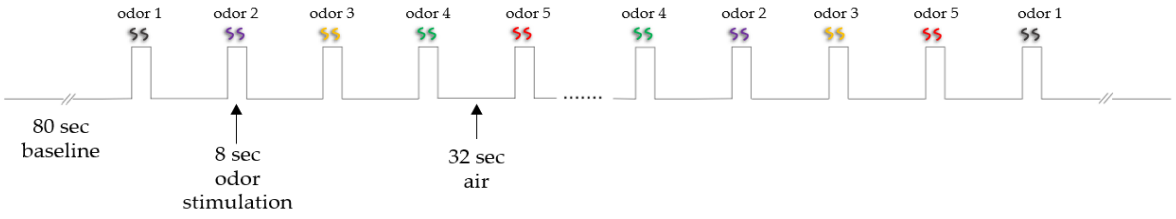

B **Experiment 2**

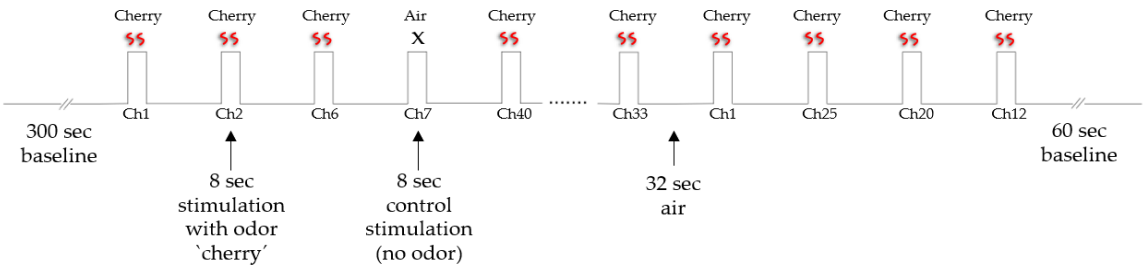

Figure 4: Olfactory stimulation protocols used for the fMRI scan. The paradigm consists in delivering short (8 sec each) odor stimuli over approximately 26 min (**A)** or 40 minutes (**B)** to investigate odor maps elicited by the odor delivery (Experiment 1) and to validate the possible delivery of a given odor from each of the 37 pots available (Experiment 2), respectively. Inter-stimulus intervals were 32 sec.

In **A**, 5 odors (e.g., sweet woodruff, cherry, curcuma, sunscreen, and banana) were presented 7 times each in a pseudo-random manner. In **B**, only the odor 'cherry' was presented. One channel was used to deliver 'cherry' 7 times to identify the odor map (Ch1). The remaining 36 channels presented the odor only once. Three channels were used as controls and delivered air.

2.2.5 fMRI image acquisition

Both experiments were conducted using a Bruker BioSpec 9.4T small animal scanner (Bruker Biospin, Ettlingen, Germany). An 86 mm volume coil was used for radiofrequency transmission. A 10 mm surface coil was placed and secured on the rat's head between its eyes to receive the MRI signal. After placing the animal in the scanner, a localizer scan was conducted. The parameters of the functional scan for both experiments using a single-shot gradient echo-planar imaging (EPI) sequence were: repetition time (TR) 2 s, echo time (TE) 16 ms, matrix size 128 x 68, field of view 25.6 x 13.6 mm^2. 14 slices were recorded with a slice thickness of 700 μm and an in-plane resolution of 200x200 μm^2. The acquisition time of 2 sec resulted in 791 recorded volumes for Experiment 1 (total scan time of ~26 min) and 1204 volumes for Experiment 2 (total scan time ~40 min). A T2 turbo RARE sequence (TR 3427 ms, TE 25.5 ms, matrix 256 x 132, number of slices 14 with a slice thickness of 700 μm and 200x200 μm^2 in-plane resolution) was used to acquire a high-resolution anatomical image for each animal using the identical slice geometry as the previously obtained gradient-echo EPI. A monitoring system (SA Instruments, Inc.), including a pneumatic pillow (Graseby respiration sensor), was used to monitor the temperature and respiratory rates of the animals.

2.2.6 Data processing and analysis

Processing of the functional and structural images was conducted using MATLAB and SPM12 (MATLAB Version R2016b, The MathWorks Inc., Natick, USA, and https://www.fil.ion.ucl.ac.uk/spm/). After converting the images using the build-in Dicom converter of SPM12, head motion correction and slice-timing correction were performed. Next, spatial smoothing using twice the voxel size was conducted. An olfactory bulb mask was manually built using ITK-SNAP (http://www.itksnap.org/) from the individual anatomical scans. For statistical analysis, a general linear model (GLM) was used on the single-subject level. A threshold of $p<0.001$ uncorrected and a cluster size >10 voxels was set for the activation clusters in the olfactory bulb to pass. For visualization, the individual anatomical scan conducted for each animal was used. The BOLD time series of the selected ROIs (regions of interest) were extracted from the individual animals using the SPM toolbox Marseille Boîte À Région d'Intérêt (MarsBaR; Brett et al., 2002). To compare across animals, each BOLD time series was normalized using the averaged BOLD signal intensity of 100%. To display significant BOLD signal intensity changes during the odor presentation, event-related BOLD responses were calculated. To do so, the following frames (time periods) were chosen: (1) four frames before odor presentation (-8 s until -2 s), (2) during odor presentation (between 0 and 8 s, corresponding to 5 frames), and (3) 5 frames following after the end of the odor presentation (10 to 18 s). In each animal, all event-related BOLD responses to a particular odor stimulus were averaged. This response was considered to represent the BOLD response elicited by that particular odor stimulus in one individual animal. Due to putative variations of baseline BOLD signal, a confounding effect on the calculated BOLD responses was avoided by relating each BOLD response to the BOLD signal intensities of the immediately preceding 8 s, which were set to 100 %. To detect significant differences in BOLD responses between the odor presentation and baseline, a one-sample t-test was performed. Differences were considered significant with a p-value <0.05.

2.3 Results

To test the functionality of the 40-channels fMRI-compatible olfactometer for the use of 9.4T scanning, two fMRI experiments with rats under medetomidine sedation were performed. First, to show the ability of the olfactometer to deliver different odors eliciting odor-specific BOLD activation patterns within one scanning session, short presentations of 5 distinct odors were used. Further, the global similarity of these odor maps across animals was assessed (Experiment 1). Second, to demonstrate the ability of each of the 40 olfactometer channels to deliver an odor stimulus, one single odor was delivered from each of the 40 channels of the olfactometer. Then, the odor maps obtained upon different randomized combinations of 7 presentations were compared.

2.3.1 Delivering different odors leads to distinct odor maps

Odor-elicited BOLD responses were observed in rats under medetomidine sedation. Using repeated 8-sec randomized presentations of 5 different odors within an fMRI scanning session led to distinct BOLD activation patterns (odor maps; **Figure 5**). Out of the 10 animals used in Experiment 1, 7 rats (i.e., 70%) showed distinct activation maps with clusters >10 voxels at $p < 0.001$ (uncorrected; this threshold corresponds to a t value greater than 3.10) for at least 4 (out of 5) odors. The 3 other animals had to be excluded from analyses due to a lack of BOLD response (n=1; a 'non-responder' also common in human studies) or breathing issues during the sedation causing strong motion artifacts (n=2; criteria of exclusion of half of a voxel (<100 μm in-plane)).

Odor-specific activation of the olfactory bulb (OB) can be detected upon visual inspection (see arrows in **Figure 5B**; for anatomical axes used for orientation see **Figure 5A**). In addition, partially overlapping activation could be found for some odors (white circles; **Figure 5B**), especially in the medial part of the OB, for example, for sweet woodruff, cumin, chamomile, or orange. Besides the large central activation of the OB, the superficial layers were dorsomedially activated when 'sweet woodruff'

was used as a stimulus (see arrow; Rat 1; **Figure 5B**). Also, an odor-specific activation located in the center of the half of the bulb could be found when 'cherry' was used as a stimulus (see arrow; **Figure 5B**). For 'curcuma', a large dorsolateral activation of the OB, including activation of the center of the halves, was found (see arrows; Rat 1; **Figure 5B**). Contrary, activation elicited by 'sunscreen' was more restricted to the superficial layers spreading along the dorsoventral axis, i.e., lacked further central activation (see arrow; Rat 1; **Figure 5B**). Further posterior, activation of the inner dorsal layers was present during the presentation of 'bay' (see arrow; Rat 2; **Figure 5B**). Besides a dorsomedial activation, a medioventral activation of the olfactory bulb could be found using 'pine' (see arrows; Rat 2; **Figure 5B**).

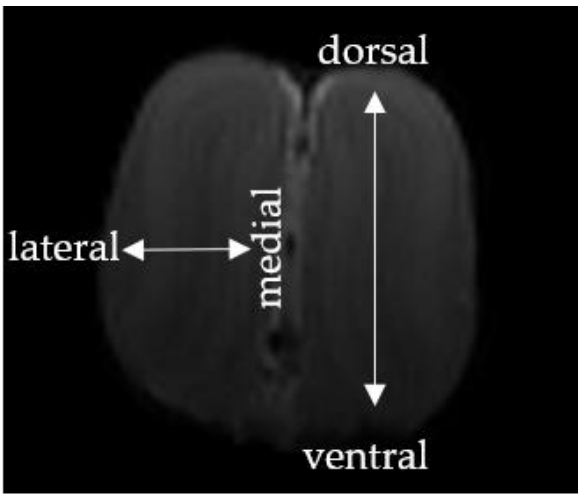

Figure 5A: Anatomical axes of the olfactory bulb used for orientation. The middle of the dorsoventral and lateromedial axis of one half was referred to as the center of the half in the results section. Contrary, the outer part of halves was labeled as superficial.

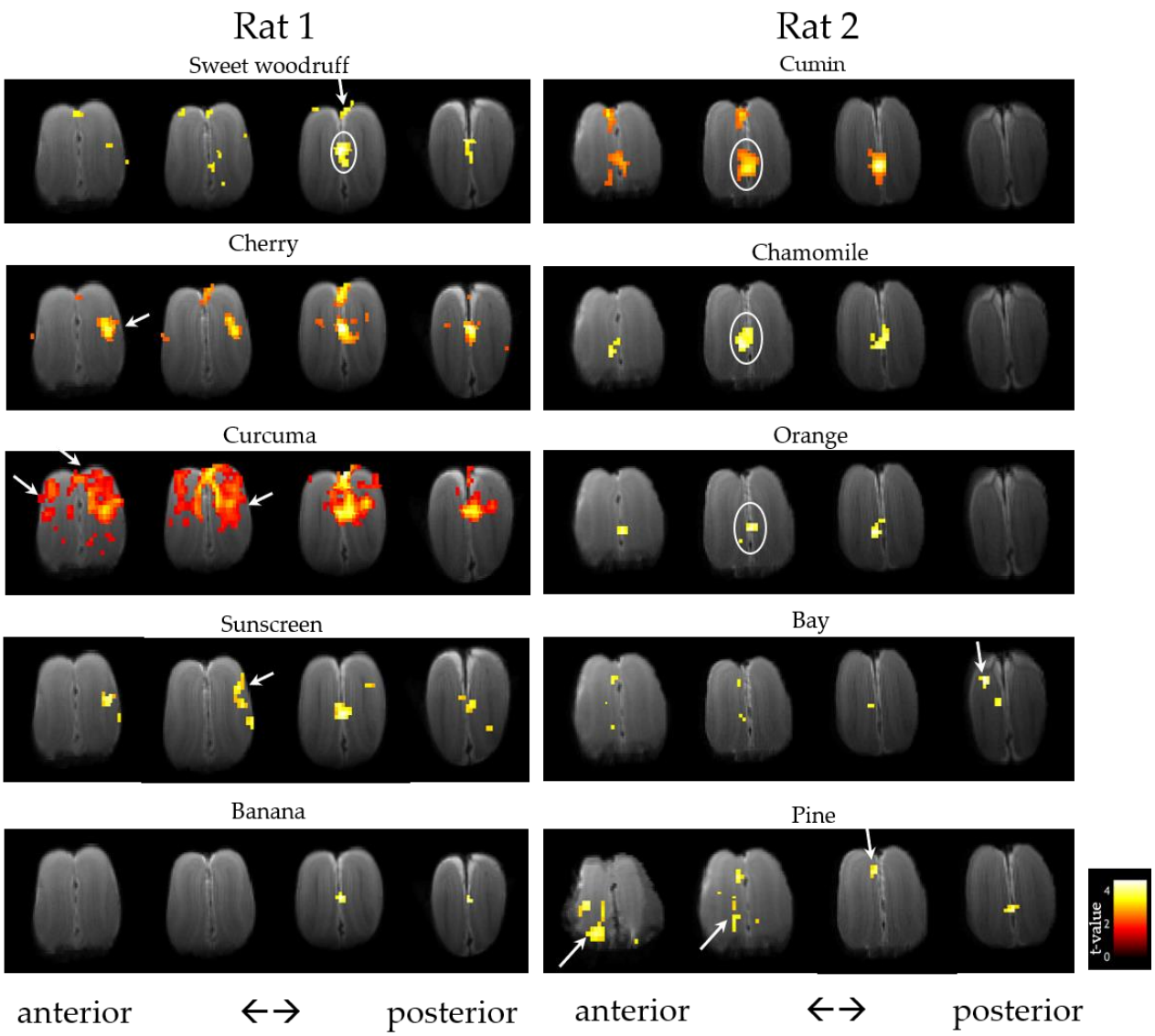

Figure 5B: Repeated short stimulations of 5 different odors lead to distinct odor maps in the olfactory bulb (contrast `odor>air´). Some odor-specific clusters (white arrows), as well as overlapping activation patterns (white circles), are evoked by different odors. The left and right columns show data from 2 different animals that showed odor-specific clusters for each odor ($p<0.001$, uncorrected; cluster size >10 voxels, corresponding to a t value greater than 3.10).

To visualize the temporal relationship between odor presentation and corresponding BOLD response, an event-related response was calculated for the odor-specific clusters and compared to baseline (`no odor´/`air´ delivery). Statistical analysis revealed a significant increase or a tendency of an increase in BOLD signal intensity compared to baseline for all odor-specific clusters (i.e., observable only for a specific odor). For 6 of

the 7 scanned rats (85% of the rats), at least a tendency of BOLD signal intensity increase could be found for a minimum of 4 (out of 5) odors. Two rats showed distinct odor maps for the 5 odors with clusters yielding significant differences between odor delivery and baseline (examples shown in **Figure 6A**). Two further animals showed 4 distinct odor maps with clusters above the threshold confirmed by a significant increase of BOLD response to baseline. For the 2 remaining animals showing 4 or 5 distinct odor maps, only a tendency of increase of BOLD signal intensity from baseline could be detected for all applied odors (examples shown in **Figure 6B**). The last of the 7 rats only showed a tendency of signal increase for 3 out of 5 odors.

In summary, for the majority of the odor stimuli, distinct odor maps were found in most rats, validating the use of the olfactometer for fMRI studies.

A

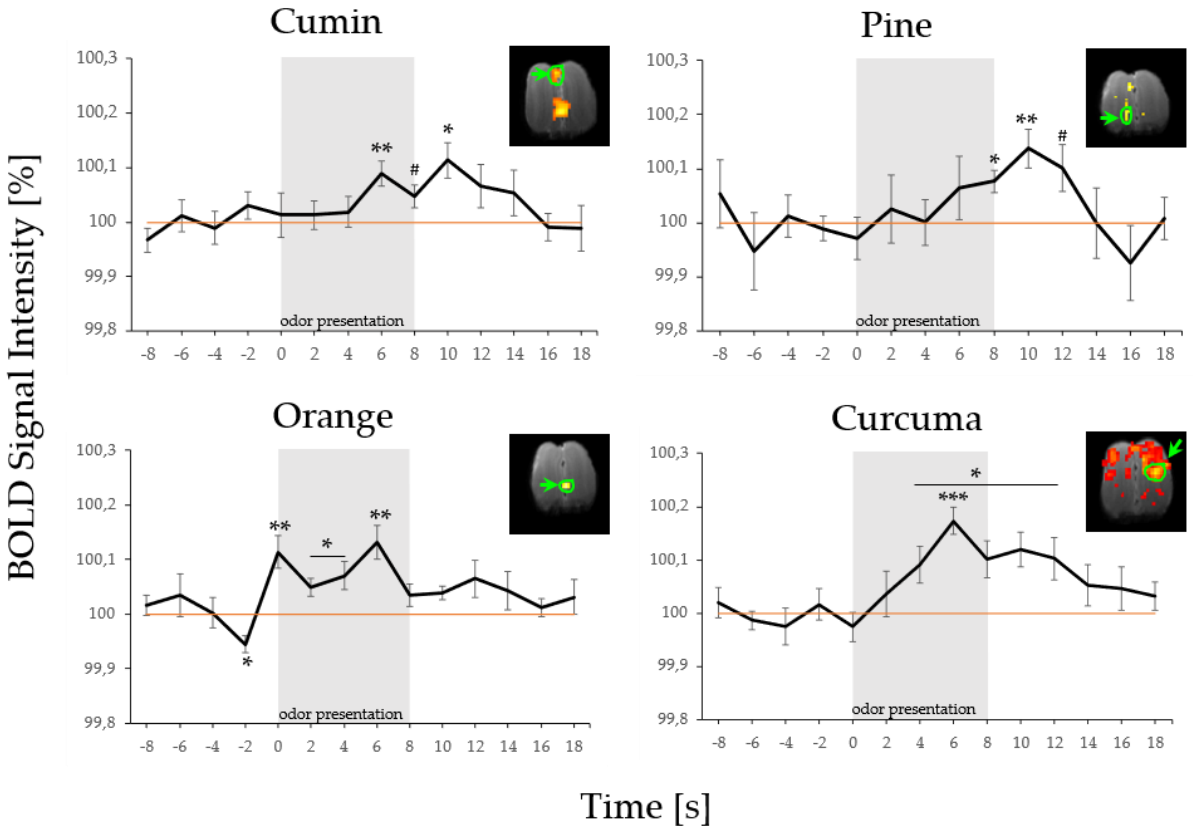

B

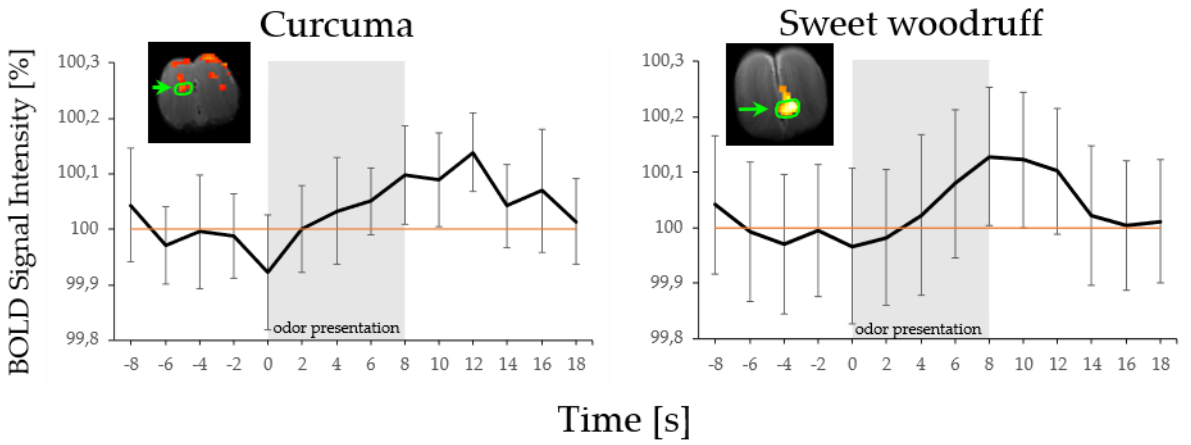

Figure 6: Representative averaged BOLD response of odor-specific cluster chosen as ROIs. ROIs in **A** show a significant increase in BOLD signal intensity upon odor presentation compared to baseline. Voxel size of clusters of depicted ROIs (shown with light green circles) range from 30 to 782 voxels (cumin: 50 voxels; pine: 46 voxels; orange: 30 voxels; curcuma: 782 voxels). Asterisks indicate a significant increase in BOLD signal intensity evoked by odor presentation. *p<0.05; **p<0.01; ***p<0.001; #p<0.06. **B** Averaged BOLD response of clusters only showing a tendency of BOLD signal intensity increase.

Furthermore, we were able to detect similar odor maps across animals that nevertheless differ in size. In Experiment 1, 10 of the odors delivered were used for over half of the rats (i.e., were common for 4 out of the 7 used rats). For most of these odors (8 out of 10), we detected similar odor maps across animals, despite some local variability. The odors 'cherry' and 'curcuma' showed a BOLD response above the threshold and presented similar global patterns in all rats exposed to these odors (see arrows for the 'curcuma clusters' (as an example) shown in **Figure 7**). This was not the case for the remaining 6 odors (banana, bay, chamomile, cumin, orange, and pine). While approximately 40% of the rats showed similarity in their 'orange' map, 80% showed it in their 'pine' odor map. The percentage of similar activation maps across animals in the remaining odors (banana, bay, chamomile, and cumin) was between 60 and 70% of the rats. For the rats not included above two possibilities are present:

(1) they did not elicit a BOLD response above the set threshold (i.e., no BOLD response in 40% of the rats for 'banana' and ca. 15% for bay, cumin, chamomile, and orange) or (2) the activated cluster location was not the same to the one above mentioned (e.g., for 'pine' the remaining 20% of animals showed an activation cluster in a different location of the OB).

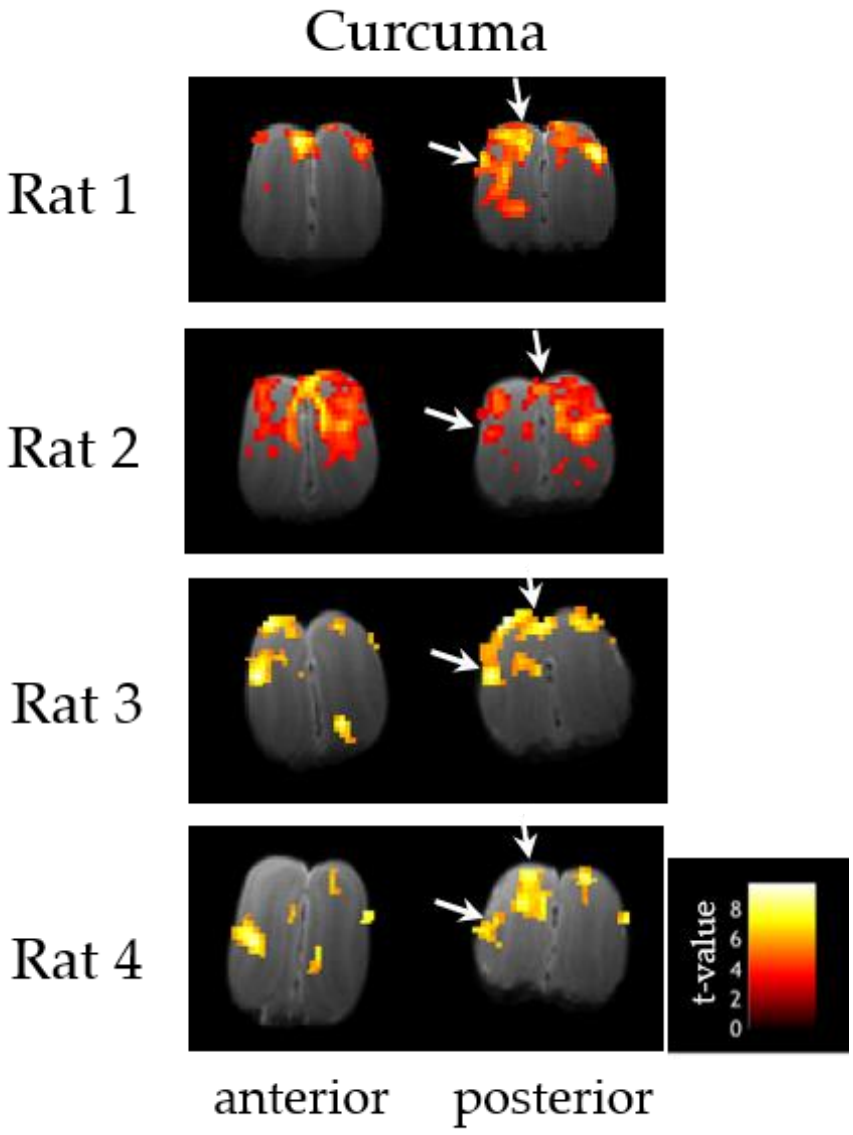

Figure 7: Repeated short stimulations with curcuma led to a similar odor map in the olfactory bulb across animals (contrast `curcuma>air´). Especially the dorsomedial and -lateral activation are present in all animals (see white arrows; $p<0.001$, uncorrected; cluster size >10 voxels).

These findings of global similarity, aside from a considerable local variability of odor maps across animals, is consistent with previously published studies using different chemical compounds instead of essential oils or household odorants (Schafer et al., 2006).

Summing up the results, our results demonstrate the elicitation of different odor maps in the olfactory bulb upon the delivery of distinct odors. Furthermore, they are in line with previous studies regarding global similarity of odor maps across animals, providing strong support for the proper functioning of this fMRI-compatible olfactometer during 9.4T fMRI scans.

2.3.2 A high throughput fMRI-compatible olfactometer

In Experiment 1, 'only' 6 of the 40 channels of the olfactometer were used to deliver the stimuli repeatedly (5 distinct odors and air 'only'). Experiment 2 focuses on demonstrating the ability of each of the 40 olfactometer channels to deliver a stimulus. Here, only the odor 'cherry' was used as a stimulus (7 times from Ch1) and 1 time by any of the other 36 odor channels. Then the odor map elicited by the 7 presentations by Ch1 was compared to the one by 7 other presentations of 'cherry' using other channels (different combinations are used of single presenting channels).

Odor maps elicited by 7 presentations of 'cherry' from channel 1 (**Figure 8A**) or by the single presentations of 'cherry' from different combinations of 7 other channels randomly chosen (see **Figure 8B-D**) were similar in the two rats scanned for Experiment 2, suggesting that any of the channels can be used to deliver an odor stimulus reliably. By calculating the averaged BOLD response of the ROI chosen from the activated cluster after 7 presentations from Channel 1, we detected a significant increase in the signal intensity for both animals. This increase demonstrates the relation to the delivery of the odor stimulus (see Rat 8: see right-hand side of **Figure 8A**). A similar result could be found for the 7 randomly chosen single-presenting channel combinations (see right-hand side of **Figure 8B-D**; of note: D shows

only a tendency). In contrast, averaged BOLD signal intensity performed for the same voxels (‘cherry sensitive voxels’), in the same animals, when only `air´ was delivered from the 3 ‘control’ channels, did not reveal any increase in BOLD signal intensity compared to baseline during this period (see **Figure 8E**).

The pattern of an increase in BOLD signal intensity with 'cherry' delivery was also reflected at the level of the individual channels. They showed a visual tendency of an increase during or immediately after odor presentation for all 37 individual channels presenting 'cherry' for both animals (**Supplementary Figure 1**).

Taken together, these results suggest that the olfactometer is capable of delivering odors via a high number of channels.

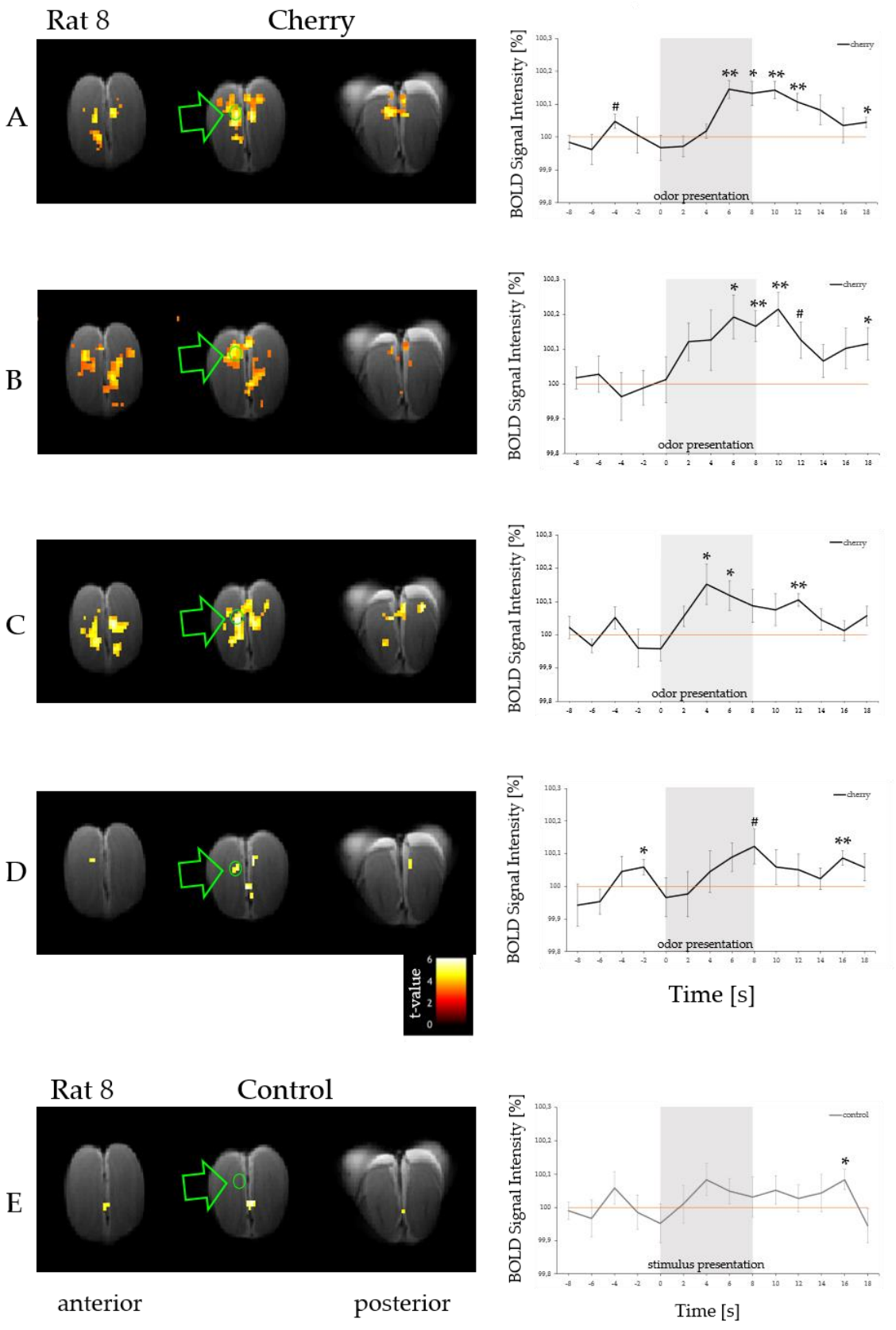

Figure 8: Repeated short stimulations using the odor 'cherry' led to a similar odor map in the olfactory bulb regardless of the chosen channels ($p<0.001$, uncorrected; cluster size >10 voxels).

A On the left, the BOLD activation for the contrast `cherry>air´ for the 7 presentations only from one channel (Channel 1) is displayed. **B – D** shows the BOLD response for the same contrast when different combinations of 7 other channels (delivering the odor only once each) were randomly chosen. On the right of each row, the averaged BOLD response of the ROIs chosen from the corresponding clusters (see green arrows and circles in the activation maps on the left) show a significant increase in BOLD signal intensity. For the cluster in **D**, only a tendency of BOLD signal increase could be detected. Voxel size of clusters of depicted ROIs range from 12 (**D**) to 191 (**C**) voxels. In **E**, the response of the 7 presentations of the control stimulus (`air´) is displayed. Asterisks indicate a significant difference in BOLD signal intensity evoked by stimulus presentation compared to baseline. *p<0.05; **p<0.01; #p<0.06.

2.4 Discussion

This study aimed at duplicating a high throughput fMRI-compatible olfactometer designed by C. Chwiesko (previous Ph.D. student in the lab) for 7T scanner use and testing its functionality for 9.4T scanner use. Two experiments were conducted to achieve the latter goal: in Experiment 1, repeated short stimulations of 5 distinct odors were used to evaluate the ability of this olfactometer to elicit distinct odor maps in the olfactory bulb within a single scan at 9.4T. In addition, Experiment 2 provided proof that the olfactometer could deliver odorants through each of its 40 channels.

2.4.1 Odor maps in the olfactory bulb of sedated rats

In the first part of the study, we were able to detect distinct odor-specific activation maps for multiple odors presented within one fMRI scanning session. To validate the ability of the olfactometer to elicit distinct odor-specific activation maps (odor maps) using a short stimulation duration (8 sec), the contrast `odor´ versus `air´ for each of the odor stimuli was performed. After that, the resulting BOLD activation patterns were compared. Focusing on the 10 odors common to all animals (4 out of the 7), 85%

of the animals showed a BOLD response above the threshold for each odor, except banana (57%). Suggesting the olfactometer reliably delivered the odors, and the olfactory stimulation was detectable in the olfactory bulb using a 9.4T scanner. Odor maps contained **odor-selective clusters as well as clusters that could be found for several odors**. The odor-selectivity of given clusters was confirmed by calculating the averaged BOLD signal intensity changes upon odor delivery. A significant increase was found for most clusters. The rest showed at least a tendency of BOLD signal increase (see for examples see **Figure 6A** and **B**, respectively).

The **partial overlapping of activation patterns** for different odorants is consistent with previously published fMRI studies (Schafer et al., 2006; Xu et al., 2000, 2003). Using the [^{14}C]2-deoxyglucose method Johnson and colleagues showed that besides a unique activation pattern in the glomerular layers for different odorants, some of the odorants lead to an overlapping activation pattern (Johnson et al., 2002; Johnson & Leon, 2000). While focusing in more detail on the similarity of the chemical structure of the odorant stimuli, Johnson et al. discovered a more alike activation pattern for odorants sharing a similar chemical structure (Johnson et al., 2002). This finding might explain some of the discovered overlaps of activation patterns in this study.

In addition to the distinct odor maps found for different odors within a scan within animals, we were able to detect a **global similarity in activated patterns** across animals, including some local variability. This finding is consistent with previously published reports using artificial odors (Johnson et al., 2002; Schafer et al., 2006) and provides further validation of the functionality of our olfactometer. On the other hand, local variability is believed to stem from various physiological parameters that influence the BOLD signal. In line with this assumption, anesthesia has to be named as one factor that can influence the outcome. Another reason could be that the bulb from different animals varies in shape and size, which could complicate the same placement of the slices in the bulb across animals.

Some studies focusing at least partly on comparing the odor-specific activation maps in the OB were conducted. Yet, those studies either used a long stimulation period, a smaller number of different odors, or scanned the rodents under different conditions than our study. Using urethane anesthetized rats, Schafer and colleagues presented 4 different odors within one scan, giving the possibility to assess the odor specificity of the odor maps. Yet, a long odor stimulation (2 min stimulation) was used to achieve this result at 7.0T and 9.4T (Schafer et al., 2006). Using short odor stimulations (2 sec each) followed by either a reward or not within one scan and in awake mice, Fonseca and colleagues presented 4 different odors (Fonseca et al., 2020) at 9.4T. Averaging the activation maps in the OB over trials of the same odor, they also found distinct odor-specific maps as presented in our study. Yet, they did not find a global similarity across animals for single odors like us. Of note, Martin et al., using short odor stimulus presentations in a 7T scanner, found an activation pattern in the olfactory bulb of sedated rats (C. Martin et al., 2007). However, in this study, only one odor was presented (including a long 2 min inter-stimulus interval). Although the BOLD response was similar to those elicited by a long stimulation, verifying the success of eliciting a BOLD response in the OB with a short odor stimulation, the question of odor specificity of the map could not be addressed by this study.

2.4.2 Odor stimuli and anesthesia

Importantly, studies published to date report odor maps in the olfactory bulb elicited by 'pure' artificial odors (e.g., amyl acetate, ethyl acetate, or isoamyl-acetate) while more '**naturalistic**' stimuli are used in the present study: 'pure' essential oils (like cherry, banana, or pine) or household scents (such as thyme, sage, etc.). This is relevant because this study's long-term goal is to develop an fMRI set-up allowing for memory function to be investigated in experimental conditions as close as those used in humans where common odors are used over chemical odorants. Based on our results, we would **recommend** the use of bay, cherry, curcuma, cumin, and pine as they all elicited a BOLD response above threshold ($p<0.001$ uncorrected and >10 voxels). Further, they

showed a significant increase (or a tendency) of BOLD signal intensity from baseline in all animals (odors common to 4 out of the 7 rats). 'Chamomile' elicited a BOLD response in about 85%; orange, sunscreen, sweet woodruff in more than 60%, and 'banana' in 60% of these animals. For odors presented to only 2 or 3 animals, apple, fennel, galangal, and pine-needle are the most efficient odors to evoke an activation. We do not recommend the following odors: Aloe Vera, cinnamon, mango, pistachio, and rose, as they either did not elicit a response or only in 1 out of the 3 rats.

Apart from using essential oils and household scents, this study is the first to describe distinct odor maps under **medetomidine sedation using a 9.4T scanner**. Prior fMRI studies investigating the olfactory bulb mainly used urethane-anesthetized rats (e.g., Schafer et al., 2006). Medetomidine is thought to be a good choice of sedation used in long-lasting fMRI experiments due to its temporal stable BOLD responses (Sirmpilatze et al., 2019). Furthermore, allowing the same animal to be repeatedly used (e.g., for longitudinal studies) is not possible with some other sedation types. In addition, a light sedative such as medetomidine is believed to induce a more "awake-like" BOLD response than using more deep anesthesia and could lead to a stronger BOLD response (see, for example, Kalthoff, 2012; Pawela et al., 2009). However, such a conclusion cannot be drawn from the present study as it would require direct comparisons between urethane and medetomidine anesthetized rats.

2.4.3 Bridging human and animal memory requires a high throughput olfactometer

For future use within the frame of memory-related fMRI studies, the ability of the olfactometer to **deliver a high number of distinct odorants within one scanning session** is essential. Our study showed that our olfactometer meets this requirement. This feature differentiates our olfactometer from the ones used in the literature so far, where at most 4 different odors were presented during a scan in rodent fMRI (Fonseca et al., 2020; Han et al., 2019). In human fMRI, one study describes a 24-channel MRI-compatible olfactometer (Bestgen et al., 2016), already quite a high number of different

odors, yet possibly not sufficient enough for a memory task, given a minimum of 30 to 40 stimuli are usually used in humans. In addition, as described in Chwiesko (2017), using DASYLab to control the odor stimulation paradigm to allow a synchronized odor delivery with image acquisition provides a simple programming tool. Due to its plain graphical interface, no programming skills are required, facilitating an easy overall use and simple adjustment of the paradigms.

The second part of the study focused on establishing the functionality of every single channel. Technical considerations limited the possibility of obtaining odor maps for 40 different odors at once. Short stimulation times require signal averaging over several stimulations to elicit an odor-specific activation pattern. Pilot studies done by Chwiesko (2017) revealed a minimum of 7 stimulus presentations to get the odor-specificity of a map under medetomidine. This would result in a long-lasting scanning time, which could increase the risk of more noise in the data or alternations in BOLD response due to the sedation. The approach used in this study provided a possibility to validate the functionality of the channels and keep the scanning conditions acceptable (including scanning duration: 40 min). In Experiment 2, we showed that similar patterns of activation (odor maps) were found upon the 7 odor stimulations delivered by Channel 1 than in any of the randomly chosen combinations of 7 other channels also delivering 'cherry', albeit only once. This result was observed in the two rats scanned for this purpose, and it was confirmed by the odor-selective clusters showing a significant BOLD signal increase upon delivery. The similarity indicated that no matter which channels were chosen, a comparable BOLD response is evoked. This was also reflected at the level of each single channel as an increase of signal elicited during or directly after the odor presentation could be found for all channels for both animals. Minor individual differences between the response intensity of the different channels, but also the animals were expected. Since an averaging of signals is required to evoke a reliable activation pattern, it cannot be concluded based on single BOLD responses whether every channel worked equally (e.g., the airflow and the resulting odor concentration are 100% similar). In contrast, focusing on the control

channels, where no odor was delivered, no significant increase of the BOLD signal intensity could be found during or immediately after the stimulus presentation period. Also, as a token of the reproducibility of such a study across experiments and animals, the 'cherry map' obtained in Experiment 2 using 7 stimulations delivered from Channel 1 was comparable to that obtained in Experiment 1, in which 'cherry' was also delivered by one single channel in another cohort of rats.

All in all, these findings help to demonstrate the **functionality of our high throughput olfactometer within a 9.4T fMRI setting**. Besides the ability to elicit distinct odor maps for distinct odors within animals, we could show that the olfactometer can deliver odorants from a high number of different channels. Furthermore, in line with the literature, a global similarity and a considerable amount of local variability of the activated clusters could be found across animals. To date, this type of study was conducted with chemical compounds, a lower number of stimuli, and mostly with animals anesthetized with urethane. Here, giving our framework of bridging further human and animal memory, we used naturalistic odors, a high number of stimuli, short stimulations, and medetomidine as an anesthetic.

Further improvement of the stimulus protocol should be considered (minimizing the signal-to-noise ratio etc.) to increase the ability to detect distinct odor maps within a scan with a higher spatial resolution. This should be the focus of future studies as the stimulation paradigm used in the present study was developed for a 7T scanner. Adjusting the stimulus paradigm could increase the odor-specific BOLD response. Plus, achieving a higher resolution could allow for the dissociation of individual cell layers in the olfactory bulb. However, this was not the focus of our study. Here, the overall functionality of our fMRI-compatible olfactometer was to be verified so that it can be used with memory-related tasks in the future.

Chapter 3

3. Hippocampal BOLD activation by familiar odors during a translational awake rat fMRI odor memory task

3.1 Introduction

Recognition memory, the ability to recognize previously experienced events, is an essential feature of everyday life. Therefore, understanding the involvement of different brain regions during recognition memory is an important and highly debated field of research in Neuroscience (Eichenbaum et al., 2007; Yonelinas et al., 2005). The high structural and functional conservation of the medial temporal lobe (MTL), a region heavily involved in memory function, allows for comparisons between humans and rodents using translational approaches (Manns & Eichenbaum, 2006; Sauvage et al., 2013). Within this structure, the hippocampus (HIP) and its specific contribution to recognition memory is of specific interest in this study. Functional magnetic resonance imaging (fMRI) is a widely-used imaging method to study memory function and brain areas in humans.

To date, no comparable fMRI study focusing on testing the memory function in rats is present. Testing memory function in rats under experimental conditions comparable to that of humans requires however 1) rats to be tested awake, 2) the possibility of presenting a high number of stimuli (like in human studies), and 3) using the same analyzing program and a similar analyzing pipeline as frequently used in humans. Overall, most fMRI studies made in rodents are performed under anesthesia. However, since anesthesia alters functional connectivity, brain metabolism, and neural activity (Gao et al., 2017; Paasonen et al., 2018), examining cognitive function with an fMRI scan is needed to be done under awake conditions.

Hence the aim of this study is two folds: developing an fMRI-compatible translational memory task for awake rats and shedding light on whether performing the long, yet required habituation procedure for scanning the rats awake is necessary or whether similar results could be found with the same fMRI protocol when the animals were scanned sedated.

Developing an fMRI-compatible translational memory task for awake rats requires habituating the animals to experimental conditions, including habituation to the body and head immobilization, the considerable MR sequence sound, and the odor presentation during the task. Furthermore, a stimulus comparable to the stimuli (words or pictures) presented in human studies should be used. Neutral odors, such as household scents, are thought to be the best choice. Given the innate ability of rats to discriminate odors is utilized, olfaction being a primary sense in rats, plus shown by a study by Nigrosh and colleagues, rats show preferential attention towards odors as stimuli (Nigrosh et al., 1975). Additionally, the possibility of presenting a high number of stimuli has to be developed to be able to compare the results of rats to humans, since here a high number of different stimuli are presented to investigate recognition memory (Shepard, 1967; Inoue & Bellezza, 1998; Stark & Squire, 2000; for review see Yonelinas, 2001). The experimental design should identify brain regions with a higher BOLD response for `old´ odors (for which memory could be formed) than for `new´ odors, as this is a standard contrast in human fMRI memory tasks. Finally, the data should be similarly analyzed as done in humans, using the same analyzing program (SPM) frequently used in human fMRI plus performing similar group analyses to compare the BOLD response to old versus new stimuli (here: odors). To validate our translational approach to be able to compare human and rat recognition memory tested using fMRI, we compared discovered activity patterns and discussed their similarity.

A second main aim of the study was to offer valuable clues to the necessity of scanning rats awake to test their cognitive function or whether similar results could be found when scanning the animals sedated. Here the time-consuming, yet required

habituation procedure would be unnecessary. After performing the same habituation procedure to the `old´ odors, using the same MR scanning protocol and analysis pipeline for both groups (awake and sedated scanned), activity patterns showing the BOLD signal changes were compared. Different comparisons were made between the same animals (i.e., first scanned awake and after a couple of days scanned sedated) or between different populations (i.e., the animals that were scanned awake versus different animals that were only scanned sedated).

3.2 Material and methods

3.2.1 Animals

Male adult Long Evans rats weighing between 300 and 420 g and 6 to 8 months old at the start of scanning were used in this study. Rats were kept single-caged and under a reversed 12 h light/dark cycle (7 a.m. lights off; 7 p.m. lights on). Water and energy-reduced food were provided *ad libitum*. A total of 9 rats were used to be scanned awake in this study. Plus 5 additional rats that were only scanned sedated. Two rats had to be excluded from the "awake group analysis"; one was a 'non-responder,' and the others' head motion was above the threshold of at most half of a voxel. All procedures were approved by the animal care committee of the State of Saxony-Anhalt (42502-2-1489 LIN) and performed in compliance with the guidelines of the European Community.

3.2.2 Habituation procedure

The performance of a recognition memory task in the awake condition leads to various stressors for the animals that have to be considered and minimized. Using a thorough habituation procedure can help reduce some of the main stressors, namely the required head and body immobilization, the considerable volume of the sequence

sound, and the presentation of the odor stimuli. As developed by Chwiesko and colleagues (2017), the habituation procedure consisted of several stages of habituation of the animals to these different stressors. A timeline of these stages is shown in **Figure 9**. As an indicator of comfort in the different stages, the amount of body struggle movements, respiration rate, and chromodacryorrhoea (Mason et al., 2004) were assessed. Higher rates indicating higher stress levels. During the whole habituation procedure and the MR scan, the animals were never anesthetized except throughout the head-fixation surgery.

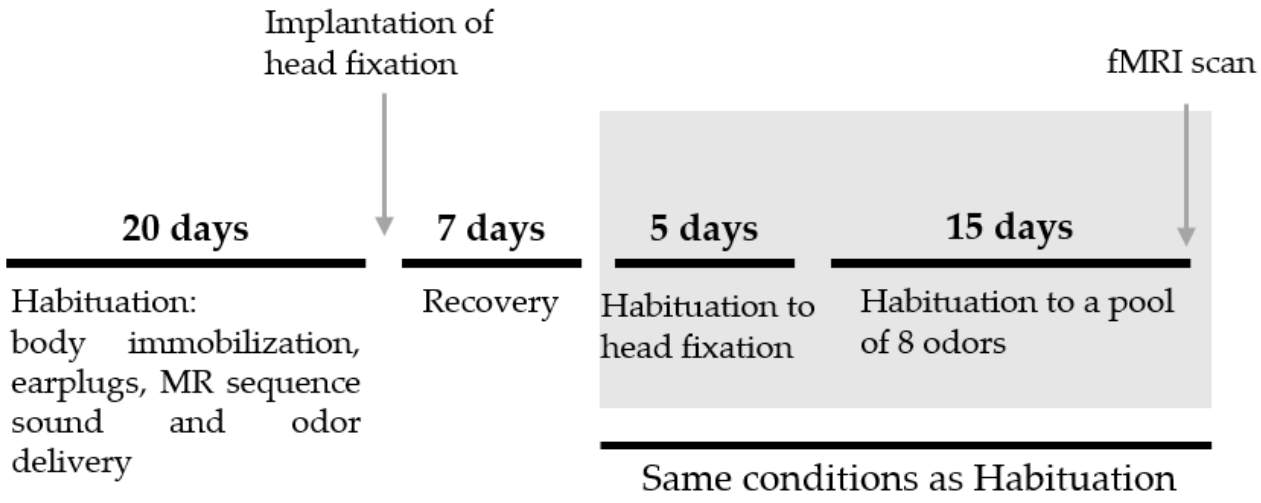

Figure 9: Timeline of the habituation schedule for the fMRI-compatible olfactory memory protocol for awake rats. After habituating the animals to the body immobilization, earplugs, the MR sequence sound, and delivery of odors, a head fixation was implanted. Following a recovery period, the animals were habituated to being head fixed and to a pool of 8 odors (`old´ odors).

Stage 1: Habituation to body immobilization

At first, the rats were habituated to body immobilization. The animals were wrapped into a felt cloth and fixed in a custom-made carrier with Velcro fasteners. The time spent immobilized was increased gradually over around 20 days from 3x1 min up to 1x45 min per day.

Stage 2: Habituation to earplugs and sequence sound

Once the animals showed no struggle movement during the 45 min immobilization period, the animals were accustomed to wearing earplugs to reduce the sequence sound volume the animals will be experiencing during the scan. At this stage of habituation, the animals were exposed to the exact sequence sound used during the MR scan later on (including scanner set up, gradient warm-up, functional and anatomical sequence sound). As soon as the animals remained calm during the sound presentation, single odor puffs (not used later in the experiment) were delivered using a syringe close to the animals' noses. This odor presentation was conducted during the functional sequence sound of the experiment (approximately 6 ½ min). Head fixation surgery was performed once the animals showed approaching the odors instead of a flight reaction.

Stage 3: Familiarization to head fixation

After recovery from surgery, rats were stepwise habituated to being head-fixed additionally to the body immobilization. First, the head of the animal was lightly fixed using tape to connect the head fixation implant and the custom-made rat carrier (see **Figure 11**). Fixed in the rat carrier, the rat was again exposed to the 45 min MR sequence sound wearing earplugs. After 3 days, the head fixation implant was fixed entirely to the head fixation holder during the 45 min MR sequence sound presentation.

Stage 4: Familiarization with one odor set plus habituation to odor stimulation timing

At the final stage of the habituation procedure, the animals were familiarized with a set of 8 odors (`old´ odors) and habituated to the odor stimulation timing during the recognition memory paradigm (see **Figure 10**). After the animals were fixed in the rat carrier like in stage 3 and the functional MR sequence started, single odors from the `old´ odor set were presented. On day 1 first only 3 out of the 8 odors were presented

with initially long delays. This number of odors increased, and the delays between the odor presentation decreased over the following days until the animal was familiar with all 8 odors. During the last 4 days, the odors were presented in the block design paradigm, as shown in **Figure 10**, with the appropriate delays to mimic the actual imaging condition. The presented odor order differed on each of these 4 last days, and the total amount an odor was presented during this stage was counterbalanced throughout the 8 odors.

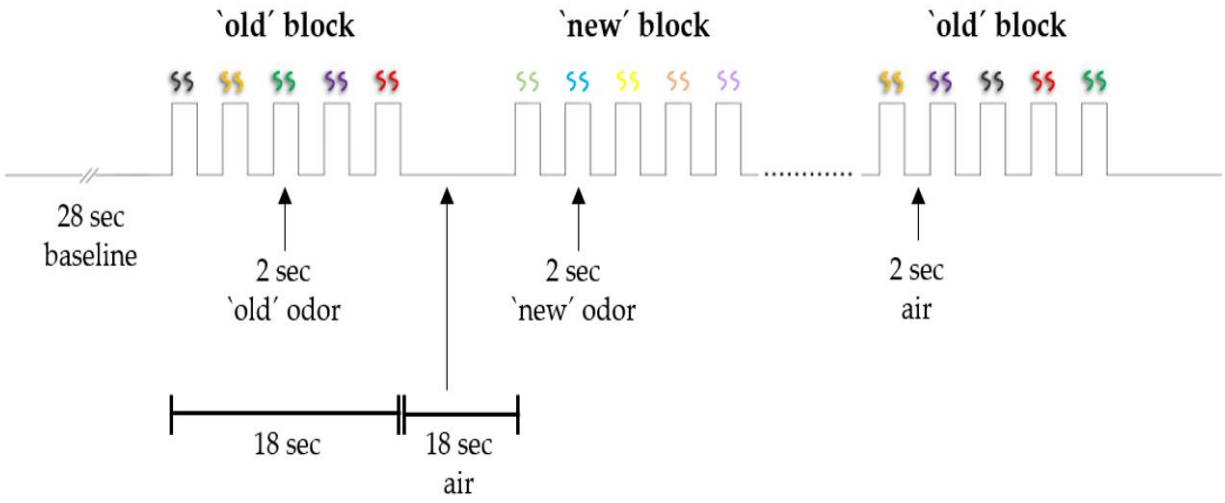

Figure 10: Olfactory memory protocol used for fMRI in awake rats. The memory paradigm consists of delivering odor blocks (5 containing `old´ odors and 5 containing `new´ odors, intermixed) over 6½ minutes. For each block, 5 different odors chosen pseudo-randomly were presented. For each `old´ block, 5 odors were selected from the 8 odors rats had been habituated with (an `old´ odor could be presented several times within a session). A `new´ block consisted of 5 odors the animals had never experienced (each odor was presented only once).

3.2.3 Head fixation implantation

To reduce head motion during the scan, the rats had to undergo a head fixation implantation surgery. All surgical procedures were under aseptic conditions, a normal body temperature was maintained with a heating mat and eyes were coated with a moisturizing balm. Anesthesia was first induced with 3 % isoflurane followed by an injection of ketamine/xylazine (100 mg and 5 mg per kg body weight, respectively) to position the animals in the stereotactic apparatus. During the whole surgery, anesthesia was maintained using 1-2 % isoflurane. After exposing the skull and all soft tissue and muscles carefully removed from the bone, the skull was thoroughly cleaned and dried. 10 micro screws made of Polyether ether ketone (PEEK; Solid Spot, California) were screwed into the bone to provide additional adhesion for the dental cement. The exposed skull was covered with dental cement (C&B Metabond® Quick Adhesive Cement, Parkell), and an in-house-made head-fixation implant composed of four interconnected 20 mm PEEK screws (head-down) was embedded in the cement. An additional layer of cement was applied around the head-fixation implant. Oral antibiotic (Baytril, Bayer Health Care) was provided to the animal for 5 days post-surgery (2.5 % in drinking water). As an analgesic, Carprofen (5 mg/kg) was injected right after surgery and every 12 hours for 3 days. After a 7 days recovery period, stage 4 of the habituation procedure started.

3.2.4 Head holding and body immobilization apparatus

To keep the motion of the rats as low as possible, a custom-made animal restrainer was used (see **Figure 11**). The restrainer consisted of a head and a body part interconnected tightly after the rat was positioned inside. The tubular shape of the body part secures a tight yet comfortable immobilization of the rat's body. An odor delivery mask was implemented in the head part right in front of the animals' noses. Through this mask, the individual odor could be delivered, and an attached vacuum pump removed the presented odor from the system afterward. The embedded PEEK screws of the head fixation implant were inserted through a small slat and fixed with PEEK nuts. This slat

was connected after that to the head part of the restrainer and fixed with nuts. A compound (Repair Stick Aqua, Weicon) was used to individually fit the position of the 20 mm surface loop coil properly onto each animal's head around the bottom of the head-fixation implant (see inserted box in **Figure 11**).

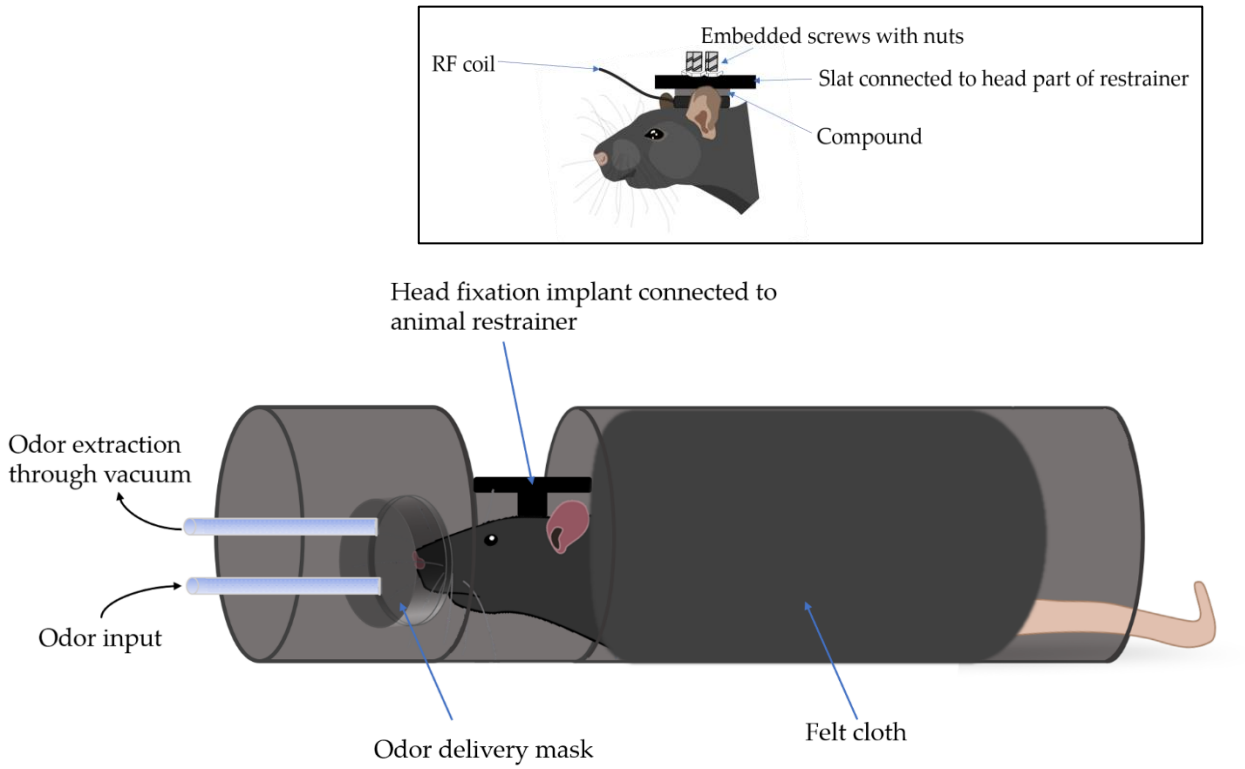

Figure 11: Schematic illustration of a body immobilized and head-fixed rat within the custom-made animal restrainer (plus a more detailed view of the head fixation implant connected to the animal restrainer). The body is immobilized by a felt cloth wrapped around the animal. Additionally, the head is fixed via the head fixation implant connected tightly to the animal restrainer. A more detailed buildup of the individual components of the headfixation can be found in the box above. First, the RF coil (surface loop coil) is placed above the head, and a hardening component is used to fit the coil individually. Afterward, the 4 embedded screws of the head fixation implant are inserted through a customized slat and fixed with nuts. This slat is subsequently connected to the head part of the animal restrainer. In front of the animal's nose, the odor delivery mask is placed.

3.2.5 Olfactory stimulation

Odor stimuli

The odorants used in this study consisted of 100 % pure essential oils (Dragonspice Naturwaren, Reutlingen, Germany) and common household spices. Two sets of odors were presented. One set containing the 8 odors the rats have been familiarized with during the habituation process: `old´ odor set. The other contained 25 odors that the rats never experienced beforehand (`new´ odors). The odors used were counterbalanced across different odor classes, e.g., fruity or flowery.

Olfactometer

A detailed description of the structure and operation of the olfactometer can be found in **Chapter 2.2**. In brief, the odors were individually stored in Teflon pots located in the scanner room. Additional Teflon pots that never contained any odor were used as a control pot to wash out the odor from the tubing. PFA tubing (Fluidflon, Pro liquid) was used to connect the odor pots with the odor delivery mask on the one side and with valves that regulated the airflow controlled by DASYLab Full on the other. The odor delivery was synchronized with the fMRI data acquisition using TTL triggers from the scanner (see **Figure 3**). The scanner output was delivered via an Analog-Digital converter to a computer and using a custom-written script in DASYLab Full, the odor stimulation was controlled accordingly to the stimulation paradigm.

Stimulation paradigm

A simple block design was used in this study (see **Figure 10**). As specified in Chwiesko (2017), a total of 10 blocks (5 `old´, 5 `new´) were presented pseudo-randomized over 6 minutes and 30 sec. 5 different odor stimulations were presented during each block, each 2 s long with a 2 s inter-trial interval. For the `old´ odor blocks, 5 odors were chosen from the pool of 8 odors the animals have been familiarized with during the

habituation procedure. Each `old´ block consisted of a different set of old odors from this pool, leading to a repetition of these odors within the experiment. Contrary, the `new´ blocks contained novel odors that the rats had never experienced before (in total, 25 different `new´ odors per experiment). The block length was 18 s with 18 s of constant odorless airflow in between each block.

3.2.6 fMRI image acquisition

Magnetic resonance imaging data were acquired using a Bruker BioSpec 9.4T small animal scanner. An 86 mm volume coil was used for radiofrequency transmission. For receiving the MRI signal, a 20 mm surface loop coil was placed above the HIP of the rat (position set through the head-fixation implant). After placing the surface loop coil, the rat was head-fixed and immobilized as previously described and positioned in the scanner. For animal positioning, a localizer scan was performed. The functional scans were acquired with single-shot gradient echo-planar imaging (EPI) sequence with the following parameters: repetition time (TR) 2 s, echo time (TE) 12 ms, matrix size 77 x 50, field of view 30.8 x 20 mm^2. 40 slices were recorded with a slice thickness of 1 mm and an in-plane resolution of 400x400 μm^2. Each functional scan lasted 6 min and 30 s containing 195 repetitions. For coregistration, high-resolution anatomical scans were performed using a T2 turbo RARE sequence (TR 3427 ms, TE 24 ms, matrix 256 x 256, number of slices 40 with a slice thickness of 1 mm and 100x100 μm^2 in-plane resolution). The slice geometry, i.e., 40 axial slices, was identical to the previously obtained gradient-echo EPI. Respiratory rates of the animals were recorded using a pneumatic pillow (Graseby respiration sensor) and a monitoring system (SA Instruments, Inc.). The overall duration of animal fixation lasted at most 45 min including around 35 minutes in the scanner.

3.2.7 Data processing and analysis

A summary of the data analysis is shown in **Figure 12**. Functional images were processed in MATLAB and SPM12 (MATLAB Version R2016b, The MathWorks Inc., Natick, USA, and https://www.fil.ion.ucl.ac.uk/spm/). First, data were converted from Dicom to NifTI using the build-in Dicom converter of SPM12 ("Dicom Import"). ITK-SNAP (http://www.itksnap.org/) was used to manually build a rat brain mask from the individual anatomical scans. This step was performed to be able to extract the brain from the anatomical scans using ImCalc. To perform a group analysis, all functional and anatomical scans were reoriented to the same voxel orientation. Next, head motion correction and slice-timing correction were performed. Six motion parameters (3 translations and 3 rotations) were obtained and used to calculate the averaged and the maximum displacement of the raw data for each functional scan. A motion threshold of at most half of a voxel (<200 μm in-plane) was applied. After, spatial smoothing with twice the voxel size was conducted. On the single-subject level, a general linear model (GLM) was used for statistical analysis. To account best for the different hemodynamic delay of awake rats compared to humans, the stimulus representing block was modified by a double-gamma hemodynamic response function (HRF) using the following parameters: onset 0s, time-to-response-peak 4s, time-to-undershoot peak 8s. An adapted MATLAB script previously published by Lambers et al., 2020, was used to be able to modify the HRF accordingly. The six motion regressors were included as covariates into the GLM to reduce motion artifacts. To generate the group activation maps at the 2nd level analysis, a one-sample t-test was conducted with $p < 0.01$ uncorrected and cluster size >3 voxels (corresponding to a t value greater than 3.14). For visualization, an anatomical scan conducted in the experiment was used (location of the activated voxel cluster remained the same regardless of which anatomical scan was used). Significant voxel of activation represents different signal intensity between the `old´ and `new´ odor sets. Based on the 2nd level activation maps, regions of interest (ROIs) were selected and defined using the Paxinos and Watson rat brain atlas (6th edition, 2007). The BOLD time series of the

selected ROIs were extracted from the individual animals using the SPM toolbox Marseille Boîte À Région d'Intérêt (MarsBaR; Brett et al., 2002). To compare across animals, each BOLD time series was normalized using the averaged BOLD signal intensity of 100%. To detect significant BOLD signal intensity change during the odor presentation, event-related BOLD responses were calculated. To do so, the following frames (time periods) were chosen: (1) four frames before odor presentation (-8 s until -2 s), (2) during odor presentation (between 0 and 18 s, corresponding to 10 frames), and four frames following after the end of the odor presentation (20 to 26 s). In each individual animal, all event-related BOLD responses to a particular odor stimulus were averaged, and this response was considered to represent the BOLD response elicited by that particular odor stimulus in one individual animal. Due to putative variations of baseline BOLD signal, a confounding effect on the calculated BOLD responses was avoided by relating each BOLD response to the BOLD signal intensities of the immediately preceding 8 s, which were set to 100 %. The event-related BOLD responses of all animals were then averaged to calculate the averaged BOLD response of all animals to a specific stimulus. To detect significant differences in BOLD responses between the presentation of the `old´ and the `new´ odors, a two-tailed unpaired Student´s t-test was performed. Differences were considered significant with a p-value <0.05.

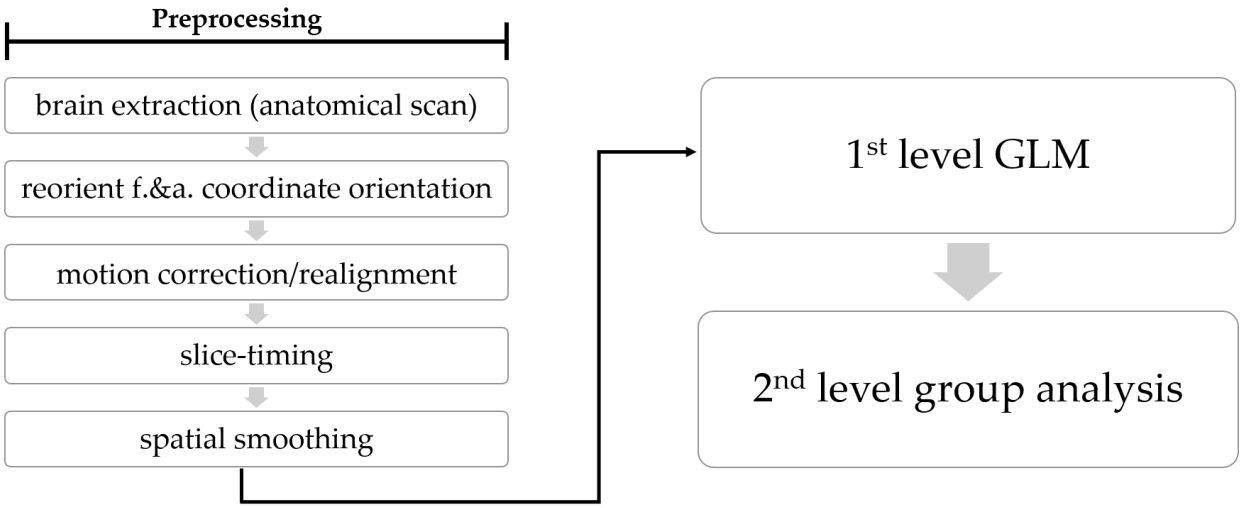

Figure 12: Flowchart of the data analysis pipeline. f.: functional scan; a.: anatomical scan.

3.2.8 Sedated animals

Next to scanning the rats awake, a scan under sedation was performed using 1) the same rats that were previously scanned awake (n=5) and 2) a different group of rats that were only scanned anesthetized (n=5). The second group underwent the same habituation procedure described above, lacking the head fixation surgery and body immobilization. For the anesthetized scan, all animals were initially anesthetized with isoflurane (2 % reduced to 1.5 %, in 50:50 N_2:O_2; v:v) with a calibrated vaporizer. A small cannular was inserted intravenously into the tail vein to inject medetomidine (continuous injection during the scan; 60-80 µg/kg per h, i.v.). After starting the continuous injection of medetomidine, the isoflurane concentration was reduced stepwise to zero. Following this, the animal was placed and fixated into the animal bed with its nose placed within the odor delivery mask. Once the sedated animal was placed inside the scanner, the same order of MR scans, including the same parameters as described for the awake scans, was conducted.

Furthermore, the data analysis followed the same pipeline as used for the awake scans. The only difference was the use of adapted HRF parameters (onset 0s, time-to-

response-peak 2s, time-to-undershoot peak 10s). After the experiment was completed, the continuous medetomidine injection was stopped. The animals were placed in their homecage after receiving a subcutaneous injection of atipamezole (60-80 µg/kg; Antisedan, Pfizer, Karlsruhe, Germany).

3.3 Results

The goal of this study is two folds. The first goal aims at developing an fMRI-compatible experimental protocol that allows for fMRI memory studies in humans and rats to be more readily comparable. We propose to achieve this first goal by 1) developing a protocol allowing for rats to be scanned awake, 2) implementing a new set-up allowing for the presentation of a large number of stimuli, as is the case in humans and 3) studying contrasts usually investigated in humans using SPM (for example: `old>new´ contrast to identify brain areas displaying higher activation for pre-experienced stimuli (`old´) as opposed to `new´ stimuli). The second goal of this study is to establish whether scanning animals awake is necessary when it comes down to investigating cognitive function or if imaging sedated rats under the same experimental conditions yields comparable results.

3.3.1 Imaging brain activation in awake rats exposed to a large number of stimuli

A customized head holder designed to be used with a 20 mm surface loop coil was developed for scanning rats awake during an odor memory paradigm. After habituation to experimental conditions (including body immobilization, MR sequence sound, odor delivery, head fixation, repeated exposure to the pool of `old´ odors; **Figure 9**), rats were scanned awake using the olfactory memory protocol illustrated in

Figure 10. A total of 10 odor blocks were delivered: 5 `old´ blocks intermixed with 5 `new´ blocks.

The 'realignment parameters' (see Material and Methods) were used for evaluating the head motion. Translational and rotational head movements are displayed in **Figure 13**. Overall, the head motion was low. The average translational motion of individual scans for the n=7 rats included in the study was below 60 µm, and the rotational motion ranged from 0.12 to 0.27 degrees. The maximal displacement of individual scans ranged from 11.5 to 175 µm in translation (i.e., was below the criteria of exclusion of half of a voxel (<200 µm in-plane) as described in the Material and Method section) and from 0.17 to 1.8 degrees in rotation (**Figure 13A** and **B**, respectively).

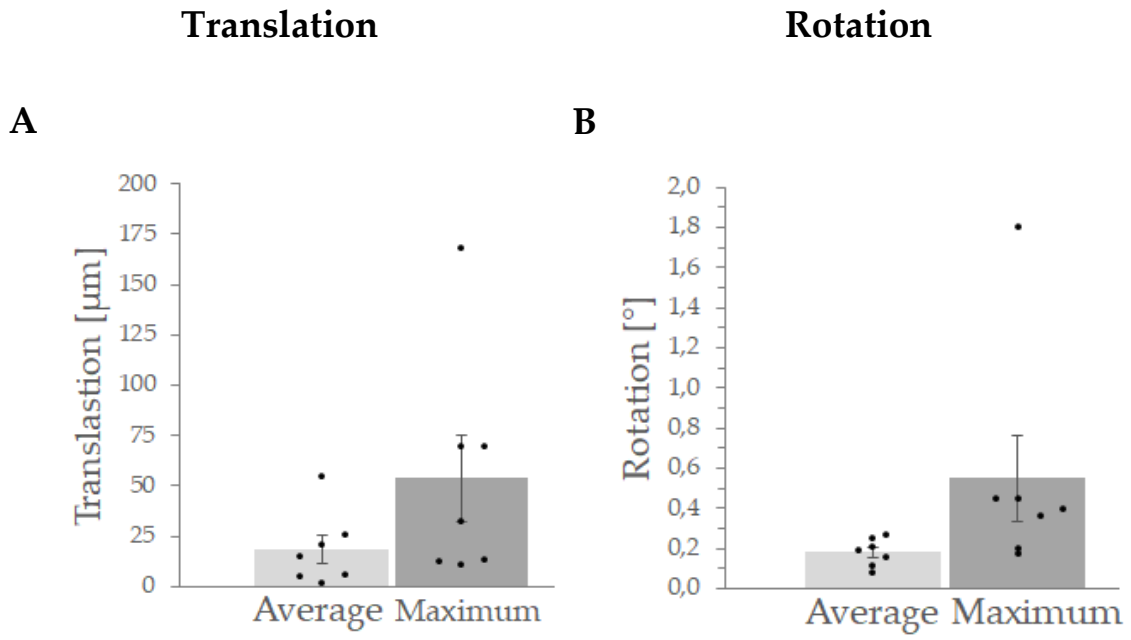

Figure 13: Characterization of head movement of the awake scanned animals in terms of **A**) translation (in mm) and **B**) rotation (in degrees). Displayed are the averaged and the maximum displacement of the raw data used in the group analysis. Each dot represents a single functional scan. The average displacement of individual scans included in the analysis was below 60 µm and varied between 0.12 to 0.27 degrees, and the maximum displacement from 11.5 to 175 µm and 0.17 to 1.8 degrees (bars representing mean ± SEM).

Respiration rate throughout the fMRI sessions did not significantly differ from that of the normal breathing rate for rats (85 breaths per minute based on the Animal Care and Use Committee of the John Hopkins University, USA), suggesting a low-stress level. Averaged breathing rates during `new´ odor block presentations (90±3 breaths/min) or `old´ odor blocks (92±3 breaths/min) were similar to that during baseline (90±3 breath/min; **Supplementary Figure 2 and Table 2**).

To map odor-related BOLD signal changes, an HRF that best matched the BOLD responses in awake animals was used for GLM analysis (see Materials and Methods).

All regions in which significantly stronger BOLD responses were induced by `old´ compared to `new´ odors appear as activation clusters in a second-level analysis (`old>new´). A significantly stronger activation for blocks of `old´ odors (i.e., odors for which memory could be formed) in comparison to blocks of `new´ odors was found in parts of the hippocampus (HIP) along the anterior-posterior axis. Similar to the hippocampus, activation clusters were also detected in the cingulate cortex (CgCx), the globus pallidus (GP), and the ventral posterolateral/-medial thalamic nucleus (VPL/VPM), indicating that in all of these structures, the `old´ odors triggered stronger BOLD responses than the `new´ odors (**Figure 14**).

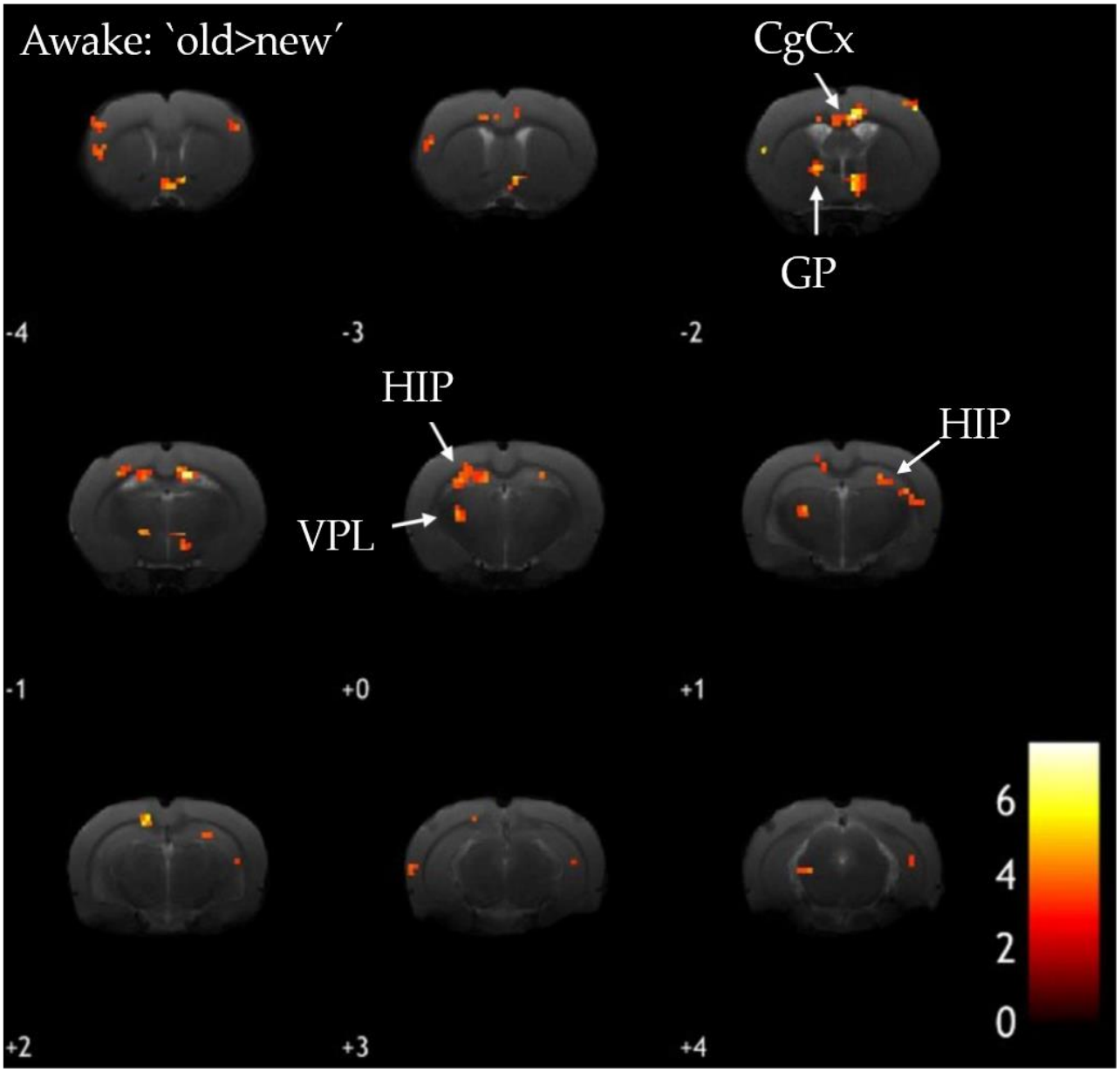

Figure 14: 2nd level group activation for the contrast `old>new´ in awake rat fMRI (n=7). White arrows indicate clusters from which the signal was extracted (see **Figure 15**). CgCx: cingulate cortex; GP: globus pallidus; HIP: hippocampus; VPL: ventral posterolateral thalamic nucleus. Data shown with a p value of <0.01 uncorrected and cluster size >3 voxels. Significant clusters for `old>new´ contrast were only found in parts of the HIP, CgCx, GP, and VPL.

To visualize time-dependent differences in hemodynamic responses, we calculated the average BOLD response (event-related average) to `old´ and `new´ odors for all significant clusters (**Figure 15** and **Supplementary Figure 3**). In some clusters, we did not find a significant difference in the averaged magnitude of the BOLD response between the `old´ and `new´ blocks during or immediately after the odor presentation period, so we consider these clusters to be inconclusive. When we calculated the contrast `new>old´, we did not detect one cluster showing a significant difference between `new´ and `old´ blocks that could be confirmed by significant differences of the BOLD response during the odor presentation period nor subsequently (**Figure 16** and **Supplementary Figure 4**).

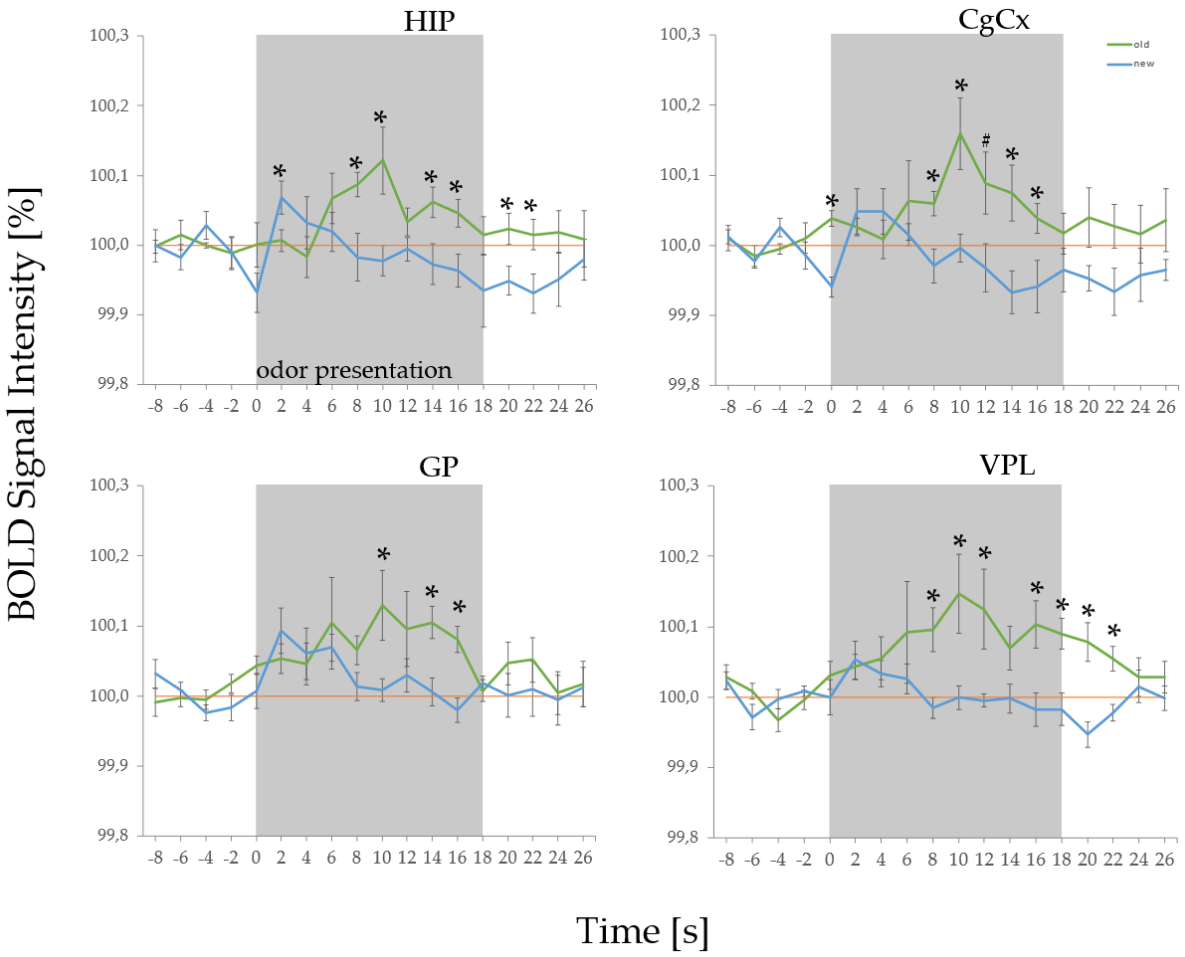

Figure 15: Averaged BOLD response of chosen ROIs (see white arrows in Figure 14). Voxel size of clusters of depicted ROIs range from 7 to 37 voxels (GP: 7 voxels; VPL: 9 voxels; CgCx: 24 voxels; HIP: 37 voxels). Grey background indicates the stimulus presentation. Asterisks indicate a significant difference in BOLD signal intensity between `old´ and `new´ odor presentation. *$p<0.05$; #$p = 0.051$.

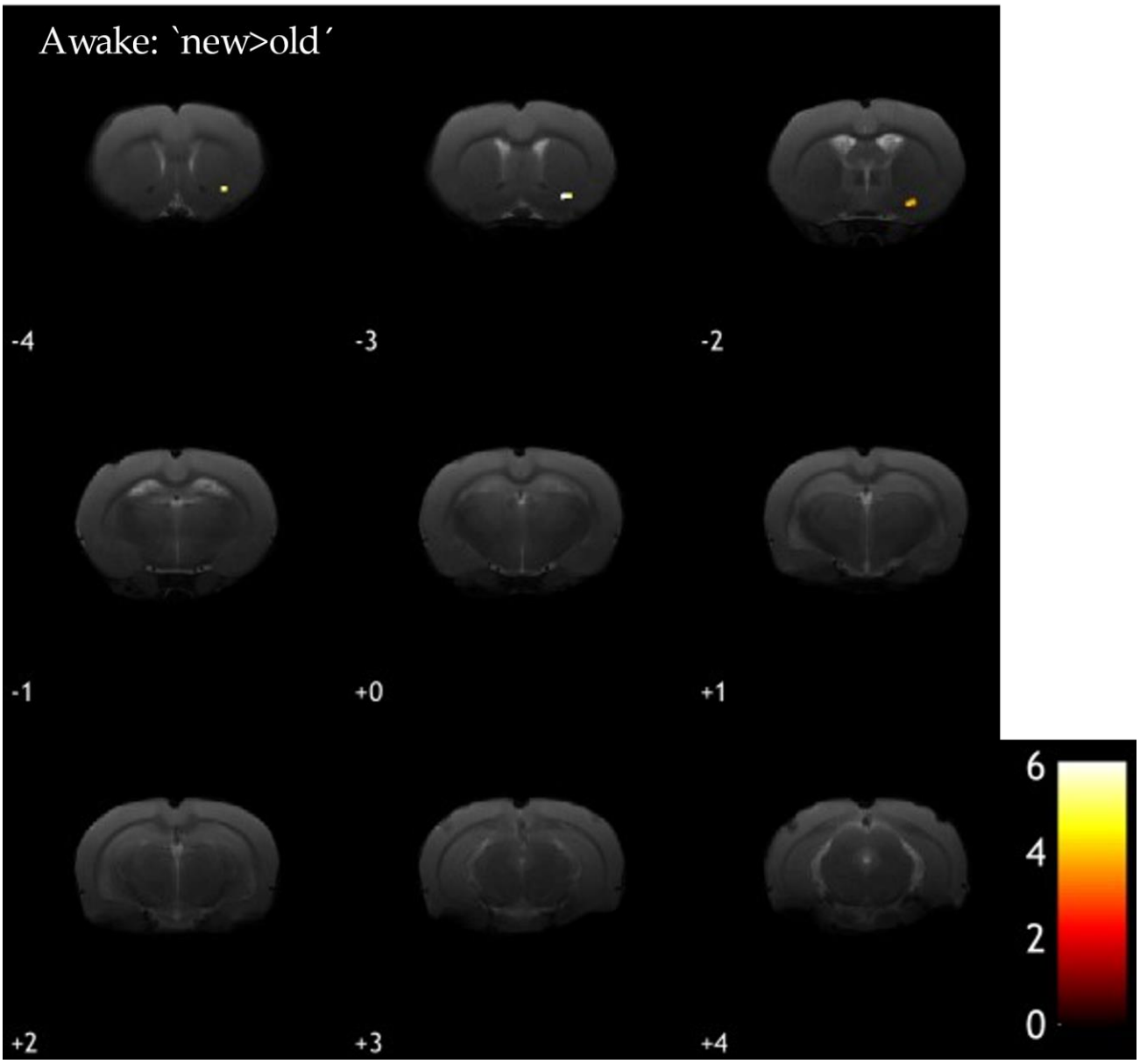

**Figure 16: 2nd level group activation for the contrast `new>old´ in awake rat fMRI** (n=7). Data shown with a p value of <0.01 uncorrected and cluster size >3 voxels. No significant cluster showing a difference between the `new´ and `old´ odor presentation could be found.

To confirm that all odor presentations elicited BOLD responses, we also performed a first level analysis, i.e., calculated the contrast `old´ odors versus `air´ (i.e., no odor) and `new´ odors versus `air´ (i.e., no odor). As expected, both `old>air´ and `new>air´ contrasts revealed clusters of activation in brain areas involved in processing olfactory and somatosensory information (**Supplementary Figure 5**). Indeed, when compared to `air', both `old´ and `new´ odor blocks induced a significantly larger activation in parts of the laterodorsal thalamic nucleus, the piriform cortex, olfactory tubercle, and parts of the ventral pallidum. Large activation clusters were only detectable in the HIP and the VPL/VPM for the `old>air´ contrast (**Supplementary Figure 5A**). For the `new>air´ contrast, this was only the case for the anteromedial/mediodorsal thalamic nucleus and retrosplenial granular cortex (**Supplementary Figure 5B**). In summary, these control analyses show that both contrasts `old>air´ and `new>air´ revealed BOLD clusters of activation in regions processing the type of stimuli used in the study (i.e., odors). However, clusters specific to areas related to cognition were detectable only in the contrast `old>air´, bringing further support to the validity of the pattern of activation reported in the previous paragraph for the `old>new´ contrast.

Altogether, these results show that, in awake rats, a stronger BOLD response is detected for blocks of odors for which memory could be formed (i.e., `old´ odors) than for blocks of `new´ odors in regions tightly or more loosely related to memory function (the HIP and the CgCx or the VPL/M and the GP, respectively).

3.3.2 Imaging brain activation in the same rats under sedation

Given the laborious character of the habituation protocol, we tested in the follow–up experiment whether scanning rats awake was necessary to detect the pattern of activation described above or whether scanning rats under sedation using the same MR scanning protocol would suffice. For this purpose, rats previously scanned awake were subsequently scanned under sedation.

As was the case for the previous experiment, the best parameters for rat HRF under sedation were defined (time-to-peak 2 s and time-to-undershoot 10 s). Under this experimental condition, we did not detect any significant cluster of BOLD activation for the `old>new´ contrast that could be confirmed by calculating the average BOLD response (**Figure 17**). Of note, 3 out of the 7 rats scanned awake lost their head fixation and could not be scanned sedated as they were already sacrificed. Also, 1 rat excluded from the analysis of the experiment with awake animals (due to a head motion >200 μm in-plane) was included in the analysis of rats under sedation as the head motion was then <200 μm in-plane. This yielded a total sample size of n=5 for the experiment under sedation.

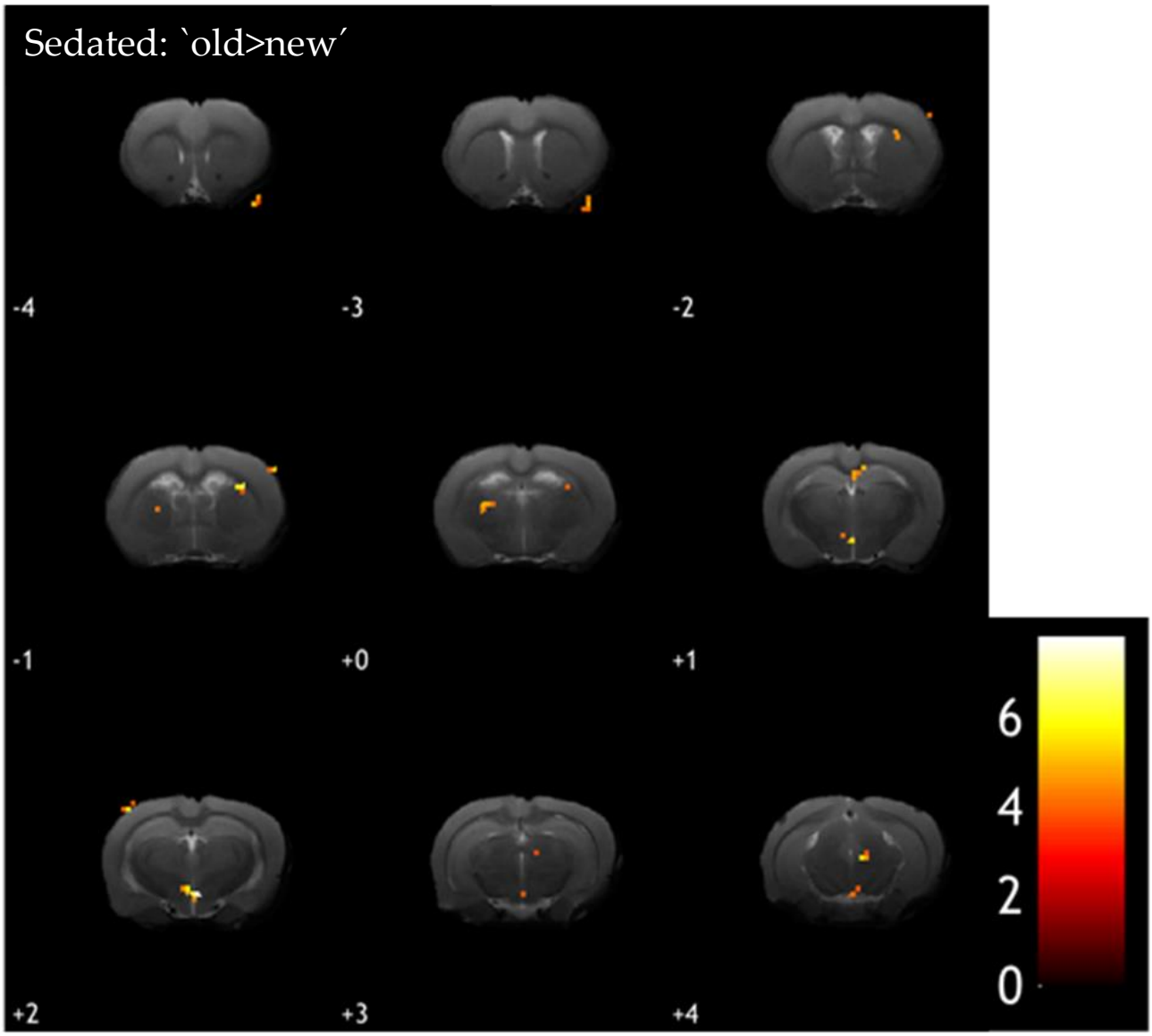

Figure 17: 2nd level group activation for the contrast `old>new´ in sedated rats fMRI (n=5). Data shown with a p value of <0.01 uncorrected and cluster size >3 voxels. No significant difference was found in any of these clusters in a particular time period of the BOLD response

To further establish that sedating animals dramatically reduces the likelihood of detecting an increased activation for `old´ versus `new´ odor blocks upon testing, an additional group of rats (n=5) was trained, scanned using the odor memory protocol, and brain activity imaged under sedation (i.e., these rats were not scanned awake first). Results were comparable to those obtained with the previous sedated group: no clusters yielding a significant difference in BOLD signal intensity between `old´ and `new´ odor blocks could be confirmed by calculating the average BOLD response (event-related average) (data not shown).

In addition, similar to the analysis performed for the "awake animal scans", we performed a first level analysis, i.e., calculated the contrast `old´ odors versus `air´ (i.e., no odor) and `new´ odors versus `air´ (i.e., no odor). Contrary to the results found for the awake studies, no areas showing a significant difference in BOLD signal intensity could be found for either the `old>air´ or `new>air´ contrast.

Altogether, these results show that scanning animals while awake dramatically increase the likelihood of detecting significant BOLD responses related to the presentation of odor stimuli for which memory could be formed.

3.4 Discussion

There are two main achievements in this study. First, we developed a cognitive task suitable for awake rat fMRI, enabling the comparison to human fMRI recognition memory tasks. Performing group analysis, we found higher BOLD signal changes for odors where memory could have been formed versus new odors, in regions tightly or more loosely related to memory function (the hippocampus and the cingulate cortex or the globus pallidus and the ventral posterolateral/-medial thalamic nucleus, respectively). Similar activation in the hippocampus and cingulate cortex was found

in human fMRI studies focusing on comparing old versus new stimuli, validating our approach. Second, we were able to shed light on the importance of scanning rats awake when the focus of the study is testing cognitive functions.

3.4.1 Imaging brain activity in awake rats under comparable conditions to human studies

To provide such a translational rat fMRI cognition memory task, several challenges had to be resolved. For the sake of adequate comparison of humans and rodents, and because anesthesia is known to alternate neuronal processes, the animals need to be scanned awake. Even though scanning the animals awake has a lot of advantages, various stressors challenge the whole process.

Habituation procedure

The considerable MR sequence sound, the immobilization, and rapid odor presentation could influence the scanning outcome, and therefore, a habituation procedure has to be performed. To reduce the scanner noise, the animals were accustomed to wearing earplugs early in the process of being habituated to the immobilization. A customized head and body immobilization system and an extensive habituation procedure adapted from Chwiesko and colleagues (2017) were successfully used to **reduce the animal's motion** to a minimum. Additionally, the 'realignment parameters' provided by SPM were used to minimize possible motion artifacts in the scans further. Exposing them to the odor delivery procedure at an early stage (habituation stage 2) noticeably reduced the stress for the animals. This **reduction of stress** could be observed as the rats did not show a 'flight' response during the odor presentation throughout the habituation procedure.

Furthermore, monitoring the respiration rate during the scan revealed an average breathing rate comparable to the normal breathing rate of rats (according to the Animal Care and Use Committee of the John Hopkins University, USA). This further

indicates the success of the extensive habituation process, specifically regarding the odor presentation. Another evidence that the odor presentation does not vigorously stress the animals is the fact that there is no significant difference in respiration rate between the `old´ and `new´ odor presentation.

The high number of different odor presentations

Another parameter that had to be considered while developing the translational rat task was the **presentation of a high number of different stimuli** (in our case, different odors). In many standardized human memory studies, a high number of stimuli (e.g., words, pictures, or faces) were presented to the participant during the task to examine recognition memory (Shepard, 1967; Inoue & Bellezza, 1998; Stark & Squire, 2000; for review see Yonelinas, 2001). Up to date, for awake studies, only studies repeatedly presenting an electrical paw stimulation (Peeters et al., 2001), whisker stimulation (Chen et al., 2020), or odor presentation of at most 4 different odors during the fMRI scan are available (Fonseca et al., 2020; Han et al., 2019) and did not focus on cognition memory. To study cognition in rats, we used the innate ability of rats to discriminate odors (Eichenbaum et al., 1988). Additionally, it has been shown that rats show preferential attention towards odor stimuli (Nigrosh et al., 1975). A custom-built MR-compatible olfactory setup [for details, see **Chapter 2**] enables the presentation of up to 40 different odors during one scan. Using odors in cognition fMRI in rodents provides a stimulus that is similar in valence and intensity compared to a list of, e.g., neutral words used in human studies. Presenting common household scents with no meaning to the animals provides a mild and neutral stimulus in contrast to the stimuli (fear or electrical) usually used in the literature (Brydges et al., 2013). As mentioned above, recognition memory was not in the scope of the present studies so far. Although the olfactometer provides the possibility of presenting up to 40 different odors, the stimulus paradigm chosen in this study involved a total of 33 odors (8 `old´ and 25 `new´ presented in overall 10 blocks of odor presentation). This provided a good

balance between the time the rat was immobilized awake and the number of odor blocks sufficient for statistical power. Using block design was chosen, as here the BOLD signal adds up from multiple repetitions, a feature that is good for detecting small changes in BOLD signal intensity.

Data analysis and state of the art in literature

A final aspect of achieving this translational memory task in rats was using the **same analyzing program (SPM) frequently used in human** fMRI. In addition, applying a **similar analyzing pipeline including contrasts** used to detect brain areas stronger activated for `old´ than for `new´ stimuli as investigated in human memory fMRI tasks. This contrast used together with the high number of stimuli presentations is a standard procedure used in human fMRI. However, this specific contrast investigating cognitive-related BOLD signal change between `old´ and `new´ stimuli was not studied in the rodent literature to this day.

To our knowledge, only one study so far addresses the issue of performing a behavioral memory task while being scanned awake in mice (Han et al., 2019). In this study, the authors imaged the large-scale networks of awake mice during an odor-based Go/No-Go task. Contrary to our study, Han and colleagues used mice instead of rats, their habituation procedure was not to a comparable level as ours, and only 2 different odors were used. Furthermore, only the different brain activation patterns during the "hit" or the "correct rejection" trials were presented, showing the activated brain regions due to, e.g., olfaction, motor processing, and reward processing. Pointing in the same direction, we performed the contrast looking at `old>air´ and `new>air´ to validate the activation of non-cognitive regions involved in the processing of olfactory information or somatosensory cues besides the cognition related regions. Han et al. however, did not report brain areas that are stronger activated for the "hit" than the "miss" or "correct rejection" than "false alarm" trials. One reason not to show this result might have been that no significant difference could be found for these contrasts.

However, finding a difference in BOLD activation could reflect the memory component of this task. In particular, finding a higher BOLD activation for "hit" than for "miss" trials would provide an idea about the regions specifically involved with the correct memory performance during the task. Another difference that is present is the different analyzing approach performed in this study. While we focused on including only one functional scan per animal in the group analysis, Han et al. included all functional scans below their exclusion criteria, including more than one scan per animal.

Various studies showed a difference in the hemodynamic response function (HRF) between humans and rodents and additionally between scanning conditions (awake or anesthetized). Therefore, selecting an appropriate hemodynamic response function to model the signal in rodent fMRI will improve signal detection. Peng and colleagues showed that using the canonical HRF, characterized by two gamma functions, is a good choice for rat fMRI (Peng et al., 2019). Furthermore, since anesthesia also influences the BOLD response, Lambers and colleagues investigated to which extent common experimental conditions influence the analysis outcome based on the HRF used (Lambers et al., 2020). Doing so, they determined that the use of a condition-specific HRF (i.e., scanned under anesthesia or not, stimulus duration, region of interest, and stimulation type) should be considered while analyzing rat fMRI data to achieve the best possible result of detecting the BOLD signal. As a result of this suggestion, and to improve detection performance for our data, we identified a time-to-peak of 4 s and a time-to-undershoot of 8 s for our awake data with the help of ANOVA comparisons. The same was done for our anesthetized fMRI data leading to a 'parameter pair' of 2 and 10 s (time-to-peak and -undershoot, respectively). These chosen parameters were the best fit overall for the cognitive regions within the focus of this paper; however, they also improved the detection performance for other regions compared to the default (human HRF) of SPM. The detection might improve even further if the focus is laid onto the remaining brain regions, but this was not the goal of our study.

3.4.2 Specific activation of cognition related brain areas in awake rats

The present finding in awake rats further supports the hippocampus (HIP) involvement among other regions in recognizing memory of odors for which memory could have been formed. **Stronger BOLD activity for these `old´ odors in contrast to `new´, unexperienced odors** was detected in parts of the **HIP**, **cingulate cortex** (CgCx), **globus pallidus** (GP), and **ventral posterolateral/medial thalamic nucleus** (VPL/M). These regions are suggested to be tightly or at least loosely related to cognitive functions.

Several different techniques were used to evaluate the involvement of the HIP in recognition memory. Using event-related fMRI in humans, Donaldson and colleagues discovered a higher hippocampal activation for `old´ than for `new´ items presented (Donaldson et al., 2001). Another human fMRI study detecting a higher BOLD signal change in the HIP for `old´ (studied) items than `new´ items was published by Stark and Squire (Stark & Squire, 2000). Other imaging techniques performed in rodents, such as evaluating the expression of Immediate Early Genes like *Arc* showed activated neurons in the HIP during recognition memory tasks (Beer et al., 2013, 2014; Kubik et al., 2007; Nakamura et al., 2013; Nakamura & Sauvage, 2016). Another approach defining the involvement of the HIP in recognition memory was the use of hippocampal lesion studies. Either by investigating the change of the curvilinear and asymmetrical components in receiver operating characteristic (ROC) curves after the lesion (Fortin et al., 2004) or the effect on a Delayed Nonmatching to Sample task (Clark et al., 2001). An extensive review about the HIP and object-in-place memory with the help of electrophysiological studies but also lesion studies was published by O'Keefe and Nadel (O'Keefe & Nadel, 1978). The studies mentioned above and others provide evidence for the involvement of the HIP in recognition memory, e.g., for binding representations of items to contextual information (for an animal and human review, see Bird, 2017). Furthermore, in our study, an overall engagement of the HIP (both subareas and parts of the rostral and the caudal HIP) could be observed, suggesting

that no specific pattern within the HIP is present during this type of olfactory cognition experiment.

Additionally to the HIP, activation in parts of the CgCx, an area highly connected with the HIP, was found. The CgCx is thought to play a determinant role in memory due to its connection within the Papez circuit. The Papez circuit describes the connection of the HIP via the fornix with the mammillary bodies, which project to the anterior thalamic nuclei. The anterior thalamic nuclei are connected to the cingulate cortex and the cingulate cortex to the entorhinal cortex, which itself is bi-directionally connected to the HIP. This extended ”hippocampal-diencephalic” system is proposed to be required for encoding the episodic memory in humans and animals (Aggleton & Brown, 1999; Aggleton & Pearce, 2001; Rolls, 2019). Furthermore, direct connections between the HIP and the CgCx, mainly through the presubiculum, were found in rats (Meibach & Siegel, 1977), providing further support for the involvement of the CgCx in memory. To our knowledge, no study has been published so far reporting the involvement of the CgCx in rodents during recognition memory. In humans, BOLD activation in the CgCx was found for recognizing familiar words, objects, or places (Heun et al., 2006; Sugiura et al., 2005). Kozlovskiy and colleagues suggested that the role of the CgCx in memory function could be to filter irrelevant information during the memory recall process in which denying false and uncertain memory is required (Kozlovskiy et al., 2012). This function could explain the activation of the CgCx in various other memory studies (e.g., investigating working, episodic, emotional, or spatial memory) and support our finding of stronger activation in the CgCx for `old´ than for `new´ odors induced by memory for the `old´ odors.

The consistent finding of stronger activation for `old´ than `new´ stimuli in the HIP and the CgCx between human studies (Donaldson et al., 2001; Heun et al., 2006; Stark & Squire, 2000; Sugiura et al., 2005; Yonelinas et al., 2005) and our study supports the validity of the approach of a translational rat fMRI cognition memory task.

Another brain region that was stronger activated for `old´ than for `new´ odors is the globus pallidus (GP). This region is a core structure of the basal ganglia, a region on

their part connected with the HIP and thought to be involved in cognitive functions in mammals (Packard & Knowlton, 2002). Based on the affiliation of the GP with the basal ganglia, we suggest that the GP might also be involved in cognitive functions. Only very few studies so far focus on determining the function of the GP within memory function, e.g., the review by Packard & Knowlton only mentions the involvement of the GP within the motor or response element of habit memory. Another paper showed the role of the GP in passive avoidance responding memorization using tetrodotoxin blockade in rats (Lorenzini et al., 1995). Up to our knowledge, no one has yet focused on recognition memory. Of note, using electrophysiology, a study performed in cats showed a connection between the HIP and the globus pallidus (Sabatino et al., 1986). This connection could further support our suggestion that the GP might also be involved in cognitive functions. For a solid declaration about the involvement of the GP in cognitive functions, especially regarding the experimental design used within the present study, further studies specifically focusing on this structure have to be performed.

The ventral posterolateral/medial thalamic nucleus showed a significant difference of BOLD signal intensity change for `old´ compared to `new´ odors. Following our previous assumption that a significantly stronger BOLD activation for `old´ in contrast to `new´ odor presentations suggests an involvement of this region in cognitive functions, it could be assumed that the VPL/M might be at least loosely related to cognitive functions. So far, only studies have been published showing the connection to the somatosensory cortex and their involvement in processing nociceptive and tactile/ kinesthetic information from the body and the head, respectively (for a review, see Groenewegen & Witter, 2004). These results do not exclude the possibility of the involvement, at least loosely, of the VPL/M with cognitive functions. Another indicator that the VPL/M might be related to cognitive function could be the exclusive significant activation of this region for the contrast `old>air´, but not for `new>air´ (`air´ representing the air presentation between the blocks). This finding could provide further evidence for the VPL/M involvement during cognition memory. In addition, it

has to be mentioned that apart from the VPL/M, only the HIP, a region extensively proven to be involved in cognition memory, was activated exclusively for the `old>air´ contrast. However, further recognition memory studies focusing specifically on the VPL/M are needed to validate our suggestion.

3.4.3 Contrary results for novelty detection

Opposing to the results for the `old>new´ contrast, **no significantly activated clusters** could be found while looking for brain regions that are more activated during the `new´ odor presentation compared to `old´ odors (`**new>old´**). This result is contrary to some of the present literature showing activation of the HIP, perirhinal cortex, and prefrontal cortex in humans during novelty detection (for reviews see (Kafkas & Montaldi, 2018; Ranganath & Rainer, 2003)). Regarding the HIP, it is necessary to mention that besides the studies referenced in the reviews above, some studies are reporting no BOLD response for the `new´ stimulus in contrast to the `old´. For the HIP, one of our main focuses, it has been proposed that this inconsistency might be due to dependency on the demands present in the tasks. As in our study and, e.g., Donaldson et al. (Donaldson et al., 2001), explicit memory demands lead to higher activation of the HIP for `old´ than `new´ stimuli. In contrast, when, e.g., associative novelty was investigated, a higher HIP BOLD signal chance was found for `new´ than `old´ stimuli (Kumaran & Maguire, 2007). In addition to the human studies, using lesion studies, it has been shown that the rat prefrontal cortex is involved in novelty detection (Dias & Honey, 2002). Various factors could explain the discrepancy of our results to the literature. Overall, it might be that the activation due to the `new´ odors is not as strong as the activation induced by the `old´ odors. Using a mild stimulus, i.e., odors, instead of a more intense one, i.e., emotional, electrical, or mechanical is expected only to induce a smaller BOLD signal change overall. This assumption could partly be supported by the fact that only with our quite liberal threshold we could detect BOLD clusters that were significantly activated due to our stimulus. Furthermore, to enhance the signal specificity more towards the HIP and adjacent

regions, a local shimming was performed focusing on these regions rather than the anterior part of the brain, which includes the prefrontal cortex.

3.4.4 Specific activation of olfactory and cognitive-related regions

As already mentioned as a control to confirm whether the odor presentations per se yielded a BOLD response, the responses of `old´ and `new´ odors versus the `air´ presentation between the stimuli blocks were examined. As expected, an **activation in non-cognitive regions** that are involved in the **processing of olfactory information or somatosensory cues**, namely in parts of the **olfactory tubercle, piriform cortex, laterodorsal thalamic nucleus, and ventral pallidum**, were found for `old´ and `new´ odor blocks vs. `air´ blocks. Contrary, only for the `old´ odor blocks, an extended activation of the HIP and the VPL/M, both regions believed to be cognitively related, could be found. Larger clusters of activation in the anteromedial/mediodorsal thalamic nucleus and retrosplenial granular cortex were only detectable for the `new>air´ contrast. One study examining the change of activity of the Immediate Early Gene c-*fos* discovered, among other regions, a higher c-*fos* activation in the anteromedial thalamic nucleus and retrosplenial granular cortex when comparing the c-*fos* count of animals in a novel and a familiar experimental room (Jenkins et al., 2002). Leading to the suggestion that these two regions might be stronger involved in detecting novel than familiar input. Additionally, a review published by Courtiol and Wilson suggests an involvement of the mediodorsal thalamic nucleus in olfactory perception (Courtiol & Wilson, 2015). This could provide a possible explanation for the large BOLD activation for the `new>air´ contrast and the at least partly activation for the `old>air´ contrast of the mediodorsal thalamic nucleus.

Awake rats, all results taken together, show a significant increase in brain regions related to cognitive functions for odors where memory could have been formed in contrast to new, never experienced odors. Additionally, given comparable conditions

during the scan (e.g., a high number of stimuli and awake scanning) and using a similar analyzing pipeline as used in human fMRI, similar results were found as in human studies.

3.4.5 Comparison of BOLD activation between awake and sedated condition

A second aim of the current study was to provide further input to the question of whether it is necessary to perform an awake rat fMRI scan due to the time-consuming yet required habituation procedure. For comparison, the rats previously scanned awake were subsequently scanned sedated using the same experimental setup, including the same MR scanning protocol. Based on previously published fMRI studies investigating the BOLD response comparing awake versus anesthetized rodents, we expected to see a difference in activation patterns between both groups. Contrary to the awake results, no cluster that showed a significant difference between the presentation of `old´ versus `new´ odors could be detected in our sedated group. A similar result, contrary to the awake result, was found with an additional group of animals scanned under sedation. This latter group experienced the same odor habituation procedure as the awake animals lacking the head-fixation surgery and was never scanned awake beforehand. Beyond the result for the `old>new´ contrast, in both sedated groups also no clusters showing a significant difference between the presentation of `new´ versus `old´ odors could be detected. Furthermore, no activated areas could be found by examining the responses of `old´ and `new´ odors versus the air presentation between the stimuli blocks. This result could lead to the suggestion that using an odor stimulation in an fMRI scan performed under sedation might not be sufficient to trigger a BOLD response in the examined brain regions. Sedated fMRI studies focusing on the primary olfactory regions, such as the olfactory bulb, do show significant BOLD activation [see, e.g., **Chapter 2**; (C. Martin et al., 2007; Schafer et al., 2006; Xu et al., 2000)].

The discrepancy in BOLD activation found between the groups is somehow in line with previous studies comparing the outcome of MRI scans under sedation or in awake rodents. Important to mention that the present studies only focused either on functional connectivity (Paasonen et al., 2018), resting-state (Liang, Liu, et al., 2015), electrical forepaw stimulation (Peeters et al., 2001), or visual stimulation (Dinh et al., 2021). Nevertheless, all studies mentioned above discovered a difference in BOLD activation between animals scanned awake versus sedated. The studies showed a larger BOLD response in the awake scanned animals in most regions that were examined. Additionally, a human fMRI study investigating the BOLD response patterns under awake and sedated conditions also shows a reduction in BOLD activation during the presentation of auditory or noxious thermal stimulation for the sedated subjects (Mhuircheartaigh et al., 2010). To our knowledge, comparing studies using milder stimuli in humans were not conducted yet, but taking into account the similarity of published data for stronger/aversive stimuli in humans and animals as mentioned above, we suggest it might provide a similar result as our study in rats.

Taken together, these results shed light on the **importance of awake scanning not only when the task involves cognitive function**s. If the cognitive function is tested using a mild/neutral stimulus as in our study to provide a translational task comparable to human recognition memory fMRI tasks, the importance is even further shown.

3.4.6 Comparison awake and sedated results within the same animals

The fact that the sample size for the experiment under sedation was smaller than that for the awake experiment (n=5 vs. n=7, respectively) is unlikely to have affected the output of the experiment under sedation. Reanalyzing the data for the awake experiment while limiting the sample size to n=4 (the number of rats common to the awake and the sedated experiment), still revealed BOLD activation clusters for the `old>new´ contrast in brain areas related the most to memory function, the HIP and CgCx, even though clusters lost in size. Clusters in the GP and VPL/M, more loosely

related to cognition, were no longer detectable with this sample of n=4, which is likely to be due to a decrease in statistical power. In addition, for the same 4 rats when tested under sedation, a similar pattern of decrease in cluster size and number was observed for the `old>new' contrast in the inconclusive clusters previously present.

For future MR experiments, the current study provides a foundation to assess recognition memory performance when adding an operant task, requiring the rats to respond based on their memory for previously habituated odors.

In addition, the possibility to combine it with invasive approaches, e.g., lesion, electrophysiology, or optogenetics while scanned awake, yields excellent potential for neuroscience and neuroimaging research.

Chapter 4

This chapter is published in Scientific Reports as:

Lesion of the hippocampus selectively enhances LEC's activity during recognition memory based on familiarity

Author names and affiliations

Liv Mahnke[1], Erika Atucha[1], Eneko Pina-Fernàndez[1], Takashi Kitsukawa[4] & Magdalena M. Sauvage[1,2,3]

[1]Leibniz-Institute for Neurobiology, Functional Architecture of Memory Dept., 39118, Magdeburg, Germany

[2]Otto von Guericke University, Medical Faculty, Functional Neuroplasticity Dept., 39120, Magdeburg Germany

[3]Otto von Guericke University, Center for Behavioral Brain Sciences, 39106, Magdeburg Germany

[4]KOKORO-biology group, Osaka University, 565-0871, Osaka, Japan.

4. Lesion of the hippocampus selectively enhances LEC's activity during recognition memory based on familiarity

4.1 Abstract

The sense of familiarity for events is crucial for successful recognition memory. However, the neural substrate and mechanisms supporting familiarity remain unclear. A major controversy in memory research is whether the parahippocampal areas, especially the lateral entorhinal (LEC) and the perirhinal (PER) cortices, support familiarity or whether the hippocampus (HIP) does. In addition, it is unclear if LEC, PER, and HIP interact within this frame. Here, we especially investigate if LEC and PER's contribution to familiarity depends on hippocampal integrity. To do so, we compare LEC and PER neural activity between rats with intact hippocampus performing on a human to rat translational task relying on both recollection and familiarity and rats with hippocampal lesions that have been shown to then rely on familiarity to perform the same task. Using high resolution Immediate Early Gene imaging, we report that hippocampal lesions enhance activity in LEC during familiarity judgments but not PER's. These findings suggest that different mechanisms support familiarity in LEC and PER and led to the hypothesis that HIP might exert a tonic inhibition on LEC during recognition memory that is released when HIP is compromised, possibly constituting a compensatory mechanism in aging and amnesic patients.

4.2 Introduction

The medial temporal lobe (MTL) includes the hippocampus as well as brain areas surrounding the hippocampus that are crucial for memory function: the parahippocampal areas (Eichenbaum, 2006; Squire et al., 2007). The lateral (LEC) and medial entorhinal (MEC) cortices, as well as the peri- and postrhinal cortices (PER and POR, respectively), are part of the parahippocampal areas. Whereas decades of studies have investigated the role of the hippocampus (HIP) in memory function in humans and animals while empirical data on the parahippocampal regions, especially on LEC and MEC, have started accumulating only recently with the discovery of the grid cells in rats (Fyhn et al., 2004; Hafting et al., 2005) and the functional dissociation of LEC and MEC in humans (Maass et al., 2015; Navarroo Schröder et al., 2015). Some early studies have however predicted an important role of the LEC in supporting the recognition of familiar items (i.e., single objects, odors, etc.) mainly based on its strong anatomical ties with PER (Brown & Aggleton, 2001; see Eichenbaum et al., 2007 for a review) while others have attributed this function to HIP in addition to its well-established role in the recollection of episodic events (Squire, 1992; Squire & Zola, 1998; Wixted & Squire, 2011). Plethora of studies have reported a specific involvement of PER in the familiarity process, especially during spontaneous object recognition memory in rodents and word recognition memory in humans (Atucha et al., 2017; Bowles et al., 2007, 2010; Farovik et al., 2011; Haskins et al., 2008; Köhler & Martin, 2020; Murray et al., 2007; see for reviews Brown & Aggleton, 2001; Eichenbaum et al., 2007). In contrast, clear empirical evidence for a selective involvement of LEC in familiarity judgments is lacking. In humans, this is essential because human studies typically investigate BOLD signals in the anterior parahippocampal gyrus, reflecting the activation of both PER and LEC (Eichenbaum et al., 2007). Likewise, in animals, evidence for a role of the LEC in familiarity is very scarce with, to date, only one study using a response deadline design yielding familiarity judgments has reported a clear contribution of this area (Atucha et al., 2017). This is a clear shortcoming as conflicting

reports suggest that LEC and PER might not constitute a single functional entity (Burwell, 2000; Burwell & Amaral, 1998; Kajiwara et al., 2003). Thus, the extent to which familiarity truly relies on the LEC function remains unclear.

LEC shares major direct bidirectional projections with the HIP (Basu et al., 2016; Insausti et al., 1997; Leitner et al., 2016; Steward & Scoville, 1976; Witter et al., 2021), while PER and HIP are much less anatomically connected (Agster et al., 2016; Tomás Pereira et al., 2016; Van Strien et al., 2009). In addition, the extent to which HIP affects PER function has been extensively investigated, especially during object recognition memory in animals (see for reviews Aggleton & Brown, 2005; see also Aggleton et al., 2005 for human data). However, no study has yet investigated whether hippocampal function might influence LEC's contribution to familiarity judgments. Hence, the extent to which the familiarity signal in LEC might be tied to hippocampal activity and if this relationship is comparable to that between PER and HIP is not known.

While recognition memory relies typically on both recollection and familiarity in young adults, familiarity is spared and recollection dramatically impaired when hippocampal function is compromised, as seen for example in aging (Daselaar et al., 2006; Duverne et al., 2008; Howard et al., 2006; Prull et al., 2006). Likewise, rats with hippocampal lesions have been reported to rely on familiarity to solve odor recognition memory tasks, while rats with intact hippocampal function rely on both familiarity and recollection to perform the same tasks (Eichenbaum et al., 2012; Fortin et al., 2004; Sauvage, Beer, & Eichenbaum, 2010; Sauvage, Beer, Ekovich, et al., 2010). To evaluate if LEC and PER familiarity signals depend on hippocampal integrity, we studied changes in neural activity in LEC and PER in these rat models yielding either familiarity and recollection judgments (HIP intact group) or only familiarity judgments (HIP lesion group). Changes in neural activity in LEC and PER upon HIP lesion would be symptomatic of a contribution of the HIP to the LEC and PER familiarity signals. No changes indicating the absence thereof. To do so, we imaged brain activity during the retrieval phase of the human to rat translational delayed-non match to odor recognition memory task. To validate this brain activity, an imaging

technique yielding cellular resolution based on the detection of the Immediate Early Gene (IEG) *Arc* RNA was used. This technique is commonly used to map MTL activity and allows for the assessment of the percentage of cells recruited during cognitive tasks (Bramham et al., 2008; Guzowski et al., 2005; Guzowski, McNaughton, et al., 2001; Guzowski, Setlow, et al., 2001; Kubik et al., 2007; Nakamura et al., 2013; Sauvage et al., 2019; Shepherd & Bear, 2011). These comparisons revealed a robust and comparable recruitment of LEC and PER during familiarity judgments as well as a selective increase of activation of LEC following HIP lesions within this frame (i.e., not of PER), suggesting that distinct mechanisms might support familiarity in these areas.

4.3 Material and Methods

4.3.1 Subjects and stimuli

Adults male Long Evans rats (350-430g) were maintained under reverse light/dark cycle (7:00 A.M. light off/7:00 P.M. light on), food deprived up to 85% of their body weight and received water *ad libitum*. The size of the groups was based on previous studies (Atucha et al., 2017; Nakamura et al., 2013; Sauvage et al., 2008). The animals (n=23) were handled a week before the experiment and testing was performed in their home cage. Rats were randomly divided into a `Home cage control´ group, a `Sham´ group, and a `Lesion´ group. A total of 4 rats were excluded from the analyses. n=2 rats did not reach the criteria fixed for the behavioral performance of 80% over 3 consecutive days criteria. In situ hybridization failed on n=1 rat (ish signal 2*SD lower than the group mean in a control area) and n=1 rat did not survive the surgery. This yielded the final group sizes of (n=6) for the `Sham´ group, (n=7) for the `Lesion´ group, and (n=6) for the `Home cage control´ group. The stimulus odors were common household scents (anise, rosemary, fennel, etc.) mixed with playground sand, and this scented sand (one odor per cup) was held in glass cups (HHIndustries). A pool of 40 scents was available, and 20 pseudo-randomly chosen odors were used each day. All

procedures were approved by the animal care committee of the State of Saxony-Anhalt (42502-2-1555 LIN) and performed in compliance with the guidelines of the European Community and ARRIVE guidelines.

4.3.2 Behavioral paradigm

Behavioral training followed the training protocol previously described in Sauvage et al. (Sauvage et al., 2008; Sauvage, Beer, & Eichenbaum, 2010). In brief, to study recognition memory, we used the innate ability of rats to dig and to discriminate between odors. Each training session contained a study phase, a delay, and a recognition phase (**Figure 18a**). On each daily training session rats were presented with a unique study list of 10 odors, i.e., the list changed for each session. Following a 30-min retention delay, memory was tested using a list of odors that included the 10 odor stimuli (`old´ odors) used during the study phase intermixed with 10 additional odors that were pseudo-randomly chosen from a pool of forty odors but were not presented during the study phase (`new´ odors; **Figure 18a**). During the recognition phase of the task, animals were tested for their ability to distinguish between the 10 odors that were presented during the study phase (`old´ odors) and the 10 additional odors (`new´ odors). Animals were first trained to dig in the stimulus cup with unscented sand to retrieve one ¼ of a piece of Honey loops (Kellogg´s) and were subsequently trained on a delay non-matching-to-sample (DNMS) rule. During the recognition phase, when rats were presented with an odor that was part of the study list (an `old´ odor), rats were required to refrain from digging, turn around, and go to the back of the cage to receive a food reward: a correct response for an `old´ odor (**Figure 18b**; an incorrect response would be digging in the stimulus cup). Conversely, when the odor was not part of the study list (a `new´ odor), animals could retrieve a buried reward by digging in the test cup: a correct response for a `new´ odor (**Figure 18c;** an incorrect response would be going to the back of the cage to receive the reward). To ensure that the task could not be solved by smelling the reward buried in the sand, all cups were baited, but the reward was not accessible to the animal for the `old´ odors. In addition, no

spatial information useful to solve the task was available to rats, given that testing cups for `new´ and `old´ odors were presented at the exact same location. Reward locations differed for the `new´ and `old´ odors (front and back of the cage, respectively), but were only experienced by the animals once a decision had been made (i.e., when the trial was over), hence could not contribute to behavioral performance. The training lasted ~3½ months, including surgery recovery time and post-surgery training. Pre-surgery training consisted of several steps during which the number of studied odors increased from one to 10, the delay increased from one to 30 minutes, and the number of odors during the recognition phase increased from two to 20 (half `old´, half `new´). The post-surgery training mirrored the final stage of the pre-surgery training (10 odors study list, a 30 min delay, and a 20 odors testing list). Animals transitioned between successive training stages when performance reached a minimum of 80% correct for three consecutive days. After reaching the final training stage (10 study odors, 30 min delay, and 20 test odors) and performing at least 80% correct for three consecutive days, the animals were split into two groups of equivalent memory performance. Subsequently, animals underwent surgery and received either a selective lesion to the hippocampus (the HIP lesion group) or a sham-surgery (the HIP intact group). After 2 weeks of recovery, rats were trained until a plateau performance was reached over 3 consecutive days and sacrificed immediately after completion of the last recognition phase, which lasted ~8 min. Throughout the training, each HIP lesion rat was paired with an intact HIP rat of comparable pre-surgery performance, and both animals were sacrificed on the same day.

Also, as *Arc* premRNA expression has been shown to reflect memory demands (Atucha et al., 2017; Flasbeck et al., 2018; Guzowski et al., 1999; Nakamura et al., 2013; Vazdarjanova et al., 2006), brain activity was imaged in an additional home-caged control group that was placed in the same testing room as the performing animals throughout the training but to which no memory demands was applied (i.e., animals remained in their home-cage) to ensure that *Arc* premRNA expression was low in rats that did not perform a memory task. In addition, we further established that LEC

activity reflects the extent of the contribution of familiarity to memory performance by bringing evidence that retrieving memories under the same experimental conditions but based on a different cognitive process than familiarity (i.e., based on recollection, the second process contributing the recognition memory) leads to a different pattern of activity in the LEC than when memory performance relies on familiarity. For this purpose, an additional experiment was performed with a different cohort of rats following the exact same protocol as described above but using household odors (thyme, sage, etc.) paired with media (plastic beads, sand, etc.) as stimuli as this specific associative recognition memory task was found to rely on recollection (Sauvage et al., 2008).

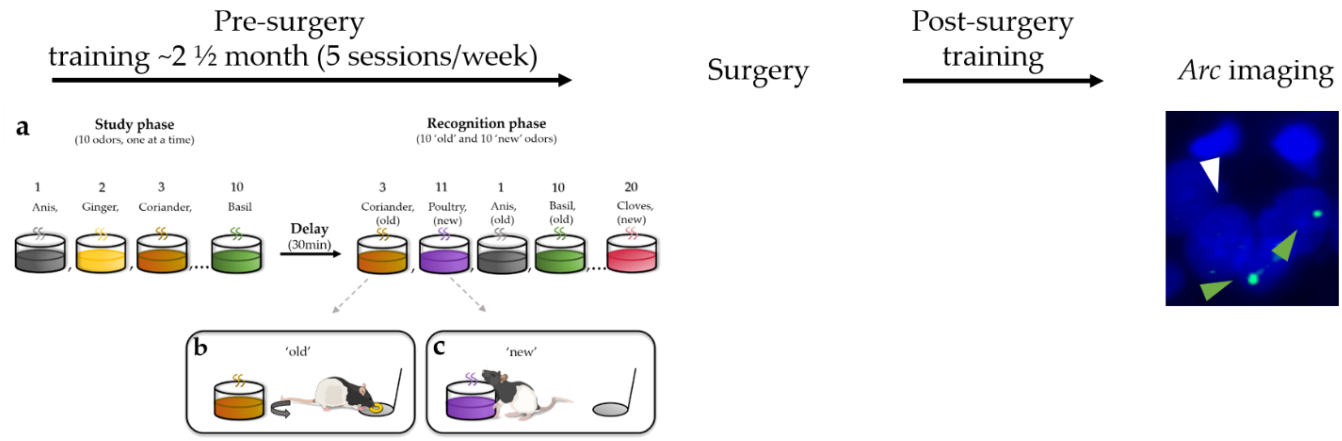

Figure 18: Overview of the experimental design. ***Left***: Pre-surgery training. (**a**) Ten odors are presented to the animal during the study phase (one at a time). After a 30 min delay, the memory for the studied odors is tested by presenting the same odors intermixed with 10 `new´ odors to the animals (also one at a time). **b, c**: Delayed nonmatching-to-sample rule. If the odor belonged to the study list (`old´ odor), the rat was expected to refrain from digging and turn around to get a food reward at the back of the cage (**b**). If the odor did not belong to the study list (`new´ odor), the rat could dig in the stimulus cup to retrieve a buried reward (**c**). ***Right***: After reaching the criterion, HIP and sham-surgeries were performed. After recovery, post-surgery training lasted until rats reached a plateau performance on 3 consecutive days subsequently to which rats were sacrificed and their brain processed for *Arc* imaging (green arrowheads: examples of *Arc* positive cells, white arrowhead: *Arc* negative cell, nuclei are counterstained with DAPI). [Adapted from Nakamura et al., 2013]

4.3.3 Surgery

Rats were anesthetized by using 0,5% pentobarbital (diluted in 1,2-Propanediol) and placed into a stereotactic frame (Kopf Instruments, Tujunga, CA, USA). A heating pad was used to control body temperature, and eyes were coated with a moisturizing balm. Additional pentobarbital was applied to maintain anesthesia when necessary. The lesions were made by injecting N-Methyl-D-aspartic acid (10 µg/µL NMDA in 0.9% saline; Sigma, Germany) into the dorsoventral and mediolateral hippocampus at 8 sites bilaterally at a flow rate of 0.15 µL/min (see **Table 1** for coordinates). The injection needle was left in place for an additional 2.5 minutes following the injection to

facilitate diffusion and then slowly withdrawn. The sham-surgery rats (HIP intact group) underwent the same surgical procedure (craniotomy and placement of the needle), but no NMDA was injected. All animals were allowed to recover for two weeks before the post-surgery training took place. Upon lesion assessment using Nissl staining (**Figure 19A and B**), one HIP lesion rat was placed in the HIP intact group as hippocampal damage was minimal (ca. 17%), no change between pre-and post-surgery memory performance was observed, and adding this animal in the HIP intact did not alter differences found in memory performance nor in IEG patterns of activity in LEC and PER between HIP intact and HIP lesioned groups. Thus, the final group size for the HIP lesion group was n= 6 and n=7 for the HIP intact group.

A

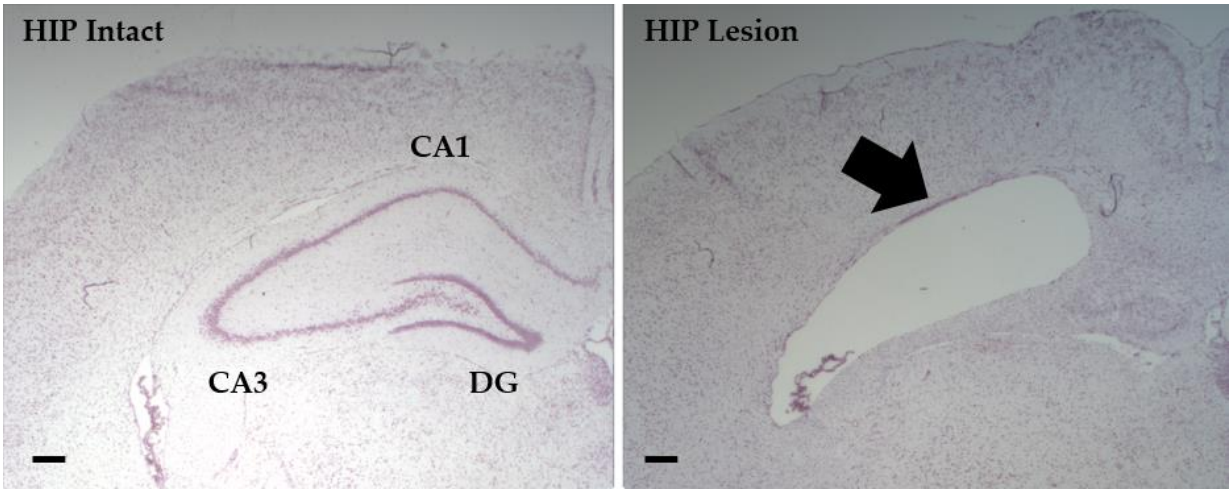

B

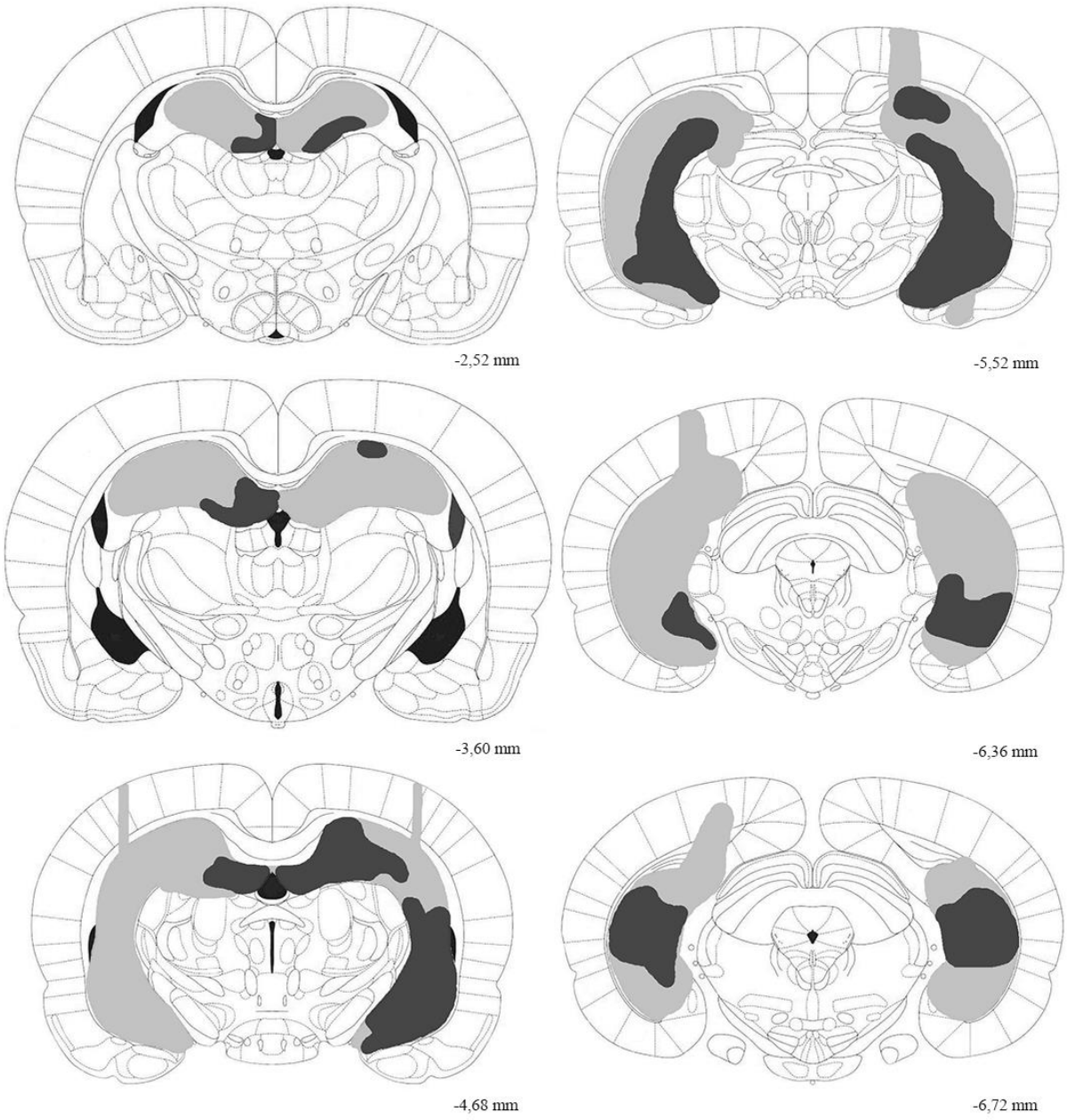

Figure 19: Extent of the HIP lesion. **A)** Photomicrographs of Nissl-stained coronal sections of HIP intact (left) and HIP lesion (right; black arrow points to the damaged area.) rats. Scale bar 200 μm. **B)** Representation of the HIP lesion. Light grey: largest lesions. Dark grey: smallest lesions. Approximately 76% of the HIP was lesioned on average.

Table 1: Coordinates relative to Bregma (in mm) and corresponding volumes (in µl) for NMDA injections in the hippocampus

Anterior-posterior (AP)	Medio-lateral (ML)	Dorso-ventral (DV)	Volume per site (µL)
-3.6	± 1.0	-3.6	0.2
-3.6	± 2.0	-3.6	0.2
-4.6	± 2.0	-4.0	0.2
-4.6	± 3.5	-4.0	0.2
-5.5	± 3.0	-4.1	0.15
-5.5	± 5.2	-6.3	0.15
-5.5	± 5.2	-4.0	0.15
-6.3	± 4.4	-4.4	0.15
-6.3	± 5.1	-6.5	0.15
-6.3	± 5.1	-5.5	0.15

4.3.4 Brain collection

Animals were deeply anesthetized with isoflurane and decapitated. Brains were immediately collected, frozen in isopentane cooled in dry ice, and subsequently stored at −80°C. Brains were then coronally sectioned on a cryostat (8 µm sections; Leica CM 3050S, Leica Microsystems), collected on polylysine-coated slides, and stored at −80°C.

4.3.5 Fluorescent in situ hybridization histochemistry

The *Arc* DNA template was designed to amplify a fragment containing two intron sequences from bases 1934–2722 of the rat *Arc* gene (NCBI Reference Seq: NC_005106.2). DIG-labeled *Arc* RNA probes were synthesized with a mixture of digoxigenin-labeled UTP (DIG RNA Labeling Mix, Roche Diagnostics) and purified using Probe quant G-50 Micro columns (GE Healthcare). Fluorescent *in-situ* hybridization histochemistry was performed as previously described in the study of Nakamura et al. (2013) with modifications. In brief, slides were fixed with 4% buffered paraformaldehyde and rinsed several times with 0.1 M PBS. After washing, the slides were treated with an acetic anhydride/triethanolamine/hydrochloric acid mix

(0.25% acetic anhydride in 0.1 M triethanolamine/HCl), rinsed with 0.1 M PBS, and briefly soaked with a prehybridization buffer. The prehybridization buffer contained 50% formamide, 5×SSC, 2.5×Denhardt´s solution, 250 µg/ml yeast tRNA, and 500 µg/ml denatured salmon sperm DNA. For the hybridization step, a 0.05 ng/µl digoxigenin-labeled *Arc* RNA probe was applied to each slide, and after adding a coverslip, the slides were incubated in a humidified environment at 65°C for 17 h. After the hybridization, sections were first rinsed at 65°C in 5×SSC and then in 0.2×SSC for 1 h. Subsequently, the slides were rinsed in 0.2×SSC at room temperature before the sections were incubated with 1% bovine serum albumin (BSA) in TBST buffer (0.1 M Tris-HCl pH 7.4, 0.15 M NaCl, 0.05% Tween 20) for 15 min. The incubation with the anti-digoxigenin-POD took place afterwards (1/2000 dilution in BSA/TBST, Roche Diagnostics) at room temperature for 3 h. Sections were then rinsed with TBST and the signal amplified using the Tyramide Signal Amplification (TSA) Cy5 System. DAPI (4',6'-diamidino-2-phenylindole, 1/100.000) was used to counterstain nuclei. Slides were then coverslipped and stored at +4°C. Additional slides without *Arc* pre-mRNA probe were used as a negative control. In these slides, no *Arc* labeling was detected.

4.3.6 Image acquisition

To image *Arc*, one slide per animal was processed. Slides contained 4 nonconsecutive brain sections, and images from nonadjacent sections distant approximately 200 microns were acquired. The number of activated neurons was evaluated on approximately 55 neurons per area on 3 nonadjacent sections (i.e., on a total of approximately 165 neurons per area covering approximately 400 microns). Images were captured with a Keyence Fluorescence microscope (BZ-X710; Japan). Images were taken with a 40× objective (Nikon) for PER and LEC and a 20×objective for CA1 and CA3 in z-stacks of 0.7-µm–thick images containing 12 to 16 images (see example **Figure 20**). The exposure time, light intensity, contrast, and gain settings were kept constant between image-stacks. As first described in the seminal work of Guzowski and colleagues (Guzowski et al., 1999), contrasts were set to optimize the appearance

of intranuclear foci (Ennaceur & Delacour, 1988; Guzowski et al., 2005; Vazdarjanova et al., 2002; Vazdarjanova & Guzowski, 2004). LEC, PER, CA1, and CA3 images were captured at the anteroposterior (AP) levels: −5.1 to −5.3 mm defined from Bregma ((Palkovits, 1983); **Figure 21**). To prevent an underestimation of the engagement of the hippocampus during the retrieval phase of the task, hippocampal ROIs (only in HIP intact rats) were defined based on HIP areas showing maximal *Arc* expression in the same task (Atucha et al., 2017).

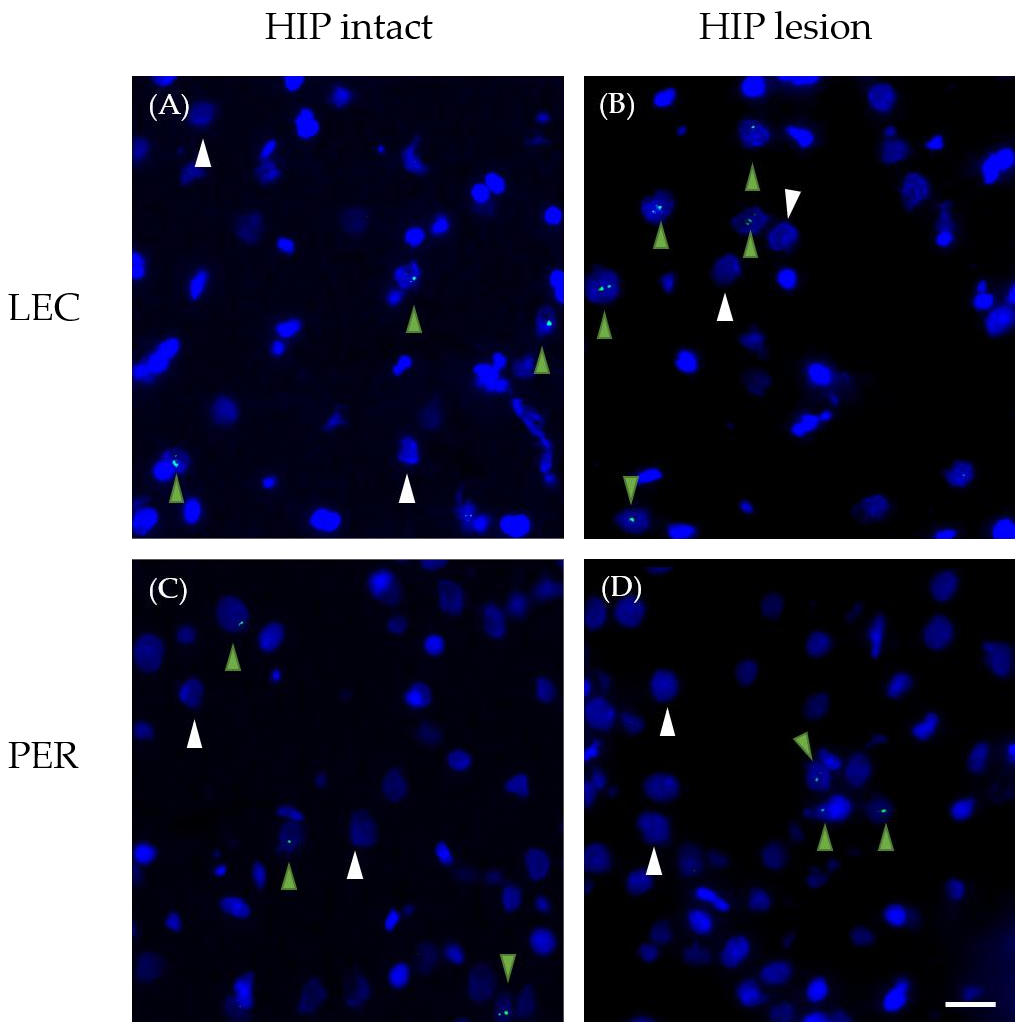

Figure 20*:* Representative images of *Arc* RNA expression in LEC and PER during memory retrieval in HIP intact and HIP lesioned groups. Lesioning HIP enhances the percentage of *Arc* positive cells in LEC (A vs. B), while it has no significant effect in PER (C vs. D). DAPI-stained nuclei are shown in blue. *Arc* intranuclear signal in green. Green arrowheads show *Arc* positive cells. White arrowheads show *Arc* negative cells. Scale bar 20 μm.

A

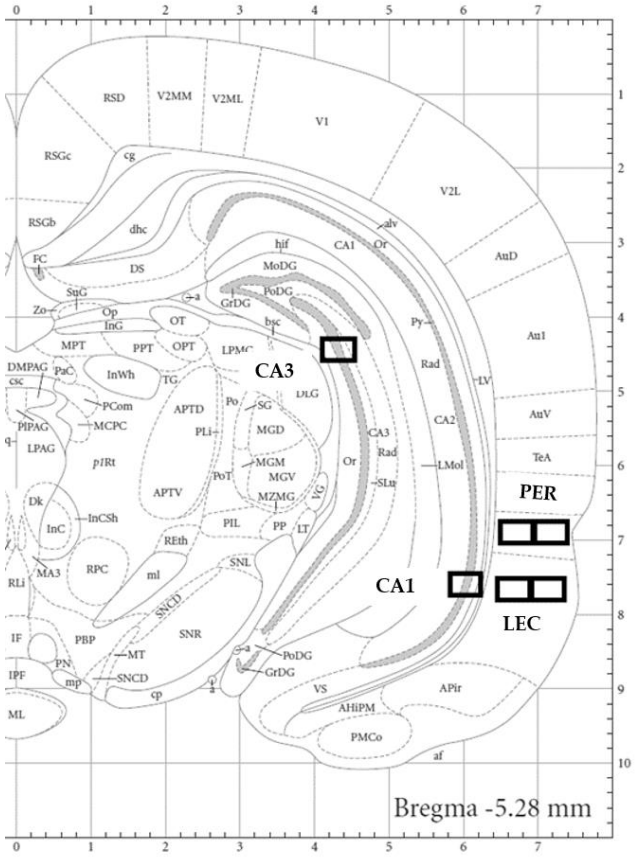

B

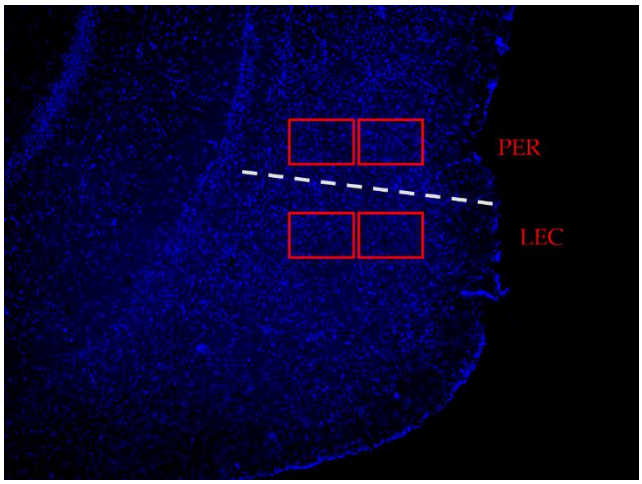

Figure 21: A) Location of the imaging frames for the regions of interest. CA1: cornu ammonis field 1; CA3: cornu ammonis field 3; PER: perirhinal cortex; LEC: lateral entorhinal cortex. **B) Example of a DAPI counterstained rat coronal section** with PER and LEC imaging frames (red) and the PER/LEC border (dashed line). Calbindin staining was used to define the border between the PER and the LEC in prior experiments. LEC imaging frames were one frame distant from PER frames to ensure that LEC activity was imaged.

4.3.7 Counting of Arc-positive cells

To account for stereological considerations, neurons were counted on 8-µm–thick sections that contained one layer of cells, and only cells containing whole nuclei were included in the analysis (West, 1999). The quantification of *Arc* expression was performed in the median 60% of the stack in our analysis because this method minimizes the likelihood of taking into consideration partial nuclei and decreases the

occurrence of false negatives. This method is comparable to an optical dissector technique that reduces sampling errors linked to the inclusion of partial cells into the counts and stereological concerns because variations in cell volumes no longer affect sampling frequencies (West, 1993). Also, as performed in a standard manner in *Arc* imaging studies, counting was performed on cells (>5µm) thought to be principal cells because small non-neuronal cells such as astrocytes or inhibitory neurons do not express *Arc* following behavioral stimulation (Vazdarjanova et al., 2006). The designation "intranuclear-foci–positive neurons" (*Arc*-positive neurons) was given when the DAPI-labeled nucleus of the presumptive neurons showed 1 or 2 characteristic intense intranuclear areas of fluorescence. DAPI-labeled nuclei that did not contain fluorescent intranuclear foci were counted as "negative" (*Arc*-negative neurons) (Guzowski et al., 1999; see **Figure 20** for examples of *Arc*-positive and *Arc*-negative images). Cell counting was performed manually by experimenters blind to experimental conditions. Percentage of *Arc*-positive neurons was calculated as follows: *Arc*-positive neurons / (*Arc*-positive neurons + *Arc*-negative neurons) × 100.

4.3.8 Histological analysis

For each rat, a set of coronal sections covering the entirety of the hippocampus along its rostrocaudal axis was stained with cresyl violet (Nissl staining). Lesions were represented on six equally spaced sections (see **Figure 19B** for the largest and smallest lesions). Estimates of the percent damage to the hippocampus were calculated from these sections using the software 'Analysis' (Soft Imaging Systems, Olympus, UK). Besides the cortical damage reported in **Figure 19B**, no additional obvious extra-hippocampal damages could be observed.

4.3.9 Statistics

Data are expressed as mean ± SEM. Given the a priori hypotheses, one-tailed t-tests were performed. Bonferroni corrections for multiple comparisons were applied to reduce the likelihood of false positives. Unpaired t-tests were used to compare

memory performance between the HIP lesion and HIP intact groups and paired t-tests to compare pre- and post-surgery performance. One-sample t-tests were used for comparison to chance level (50%). To compare *Arc* expression two-tailed unpaired t-tests were used for between-groups comparisons (lesion vs. intact) and two-tailed paired t-tests for within-group comparisons LEC and PER). Given the a priori hypothesis, a one-tailed paired t-test was used to compare *Arc* expression in CA1 and CA3 in the HIP intact group. To estimate whether a brain region was engaged during memory retrieval one-sample t-test comparisons to zero were performed. Finally, a One-way ANOVA was used to compare baseline *Arc* expression between MTL areas in home caged control rats. All statistical analyses were performed using the software IBM SPSS Statistics version 23.

4.4 Results

4.4.1 Memory performance and assessment of hippocampal lesions

Animals learned to discriminate `old´ from `new´ odors over 49 ± 1 training sessions. Once the criterion was reached (at least 80% correct responses for 3 consecutive days), two groups of comparable memory performance were formed: one hippocampus (HIP) lesioned group and one HIP intact group (performance pre-surgery: HIP lesion: 85.8% ± 1.5, HIP intact: 84.3% ± 1.3, $t_{(11)} = 0.77$, $p = 0.23$ see **Figure 22**). Subsequently, a hippocampal lesion was performed on the lesioned group and a sham surgery on the intact group (i.e., the hippocampus was not lesioned in the latter group). After two weeks of recovery, both groups were trained until the HIP intact group reached again the criterion, which took 9±1 training sessions. Memory performance of the HIP intact group following surgery was comparable to performance prior to surgery (HIP intact pre- vs. post-surgery: 84.3% ± 1.3 vs. 85% ± 2.9, $t_{(6)} = -0.20$, $p = 0.42$). Conversely, as reported in the study of Fortin and colleagues (2004), a significant drop in performance was observable in the lesioned group (HIP lesion pre-vs post-surgery: 85.8% ± 1.5 vs.

68.3% ± 3.6, $t_{(5)} = 4.13$, $p = 0.005$ at α=0.05) which was also observable when compared to the HIP intact group post-surgery performance (HIP lesion: 68.3% ± 3.6; HIP intact: 85% ± 2.9; $t_{(11)} = -3.67$, $p = 0.002$ at α=0.05). Importantly, performance in both groups was higher than chance level, indicating that the HIP lesion group was still successfully retrieving memories (comparisons to chance level (50% correct): HIP lesion: $t_{(5)} = 5.13$, $p = 0.004$; HIP intact: $t_{(6)} = 12.12$, $p < 0.001$), albeit with lower accuracy than the HIP intact group. Lesion assessment revealed that on average 75% ± 9.9 of the hippocampus was damaged in the HIP lesion group (see **Figure 19A and B**).

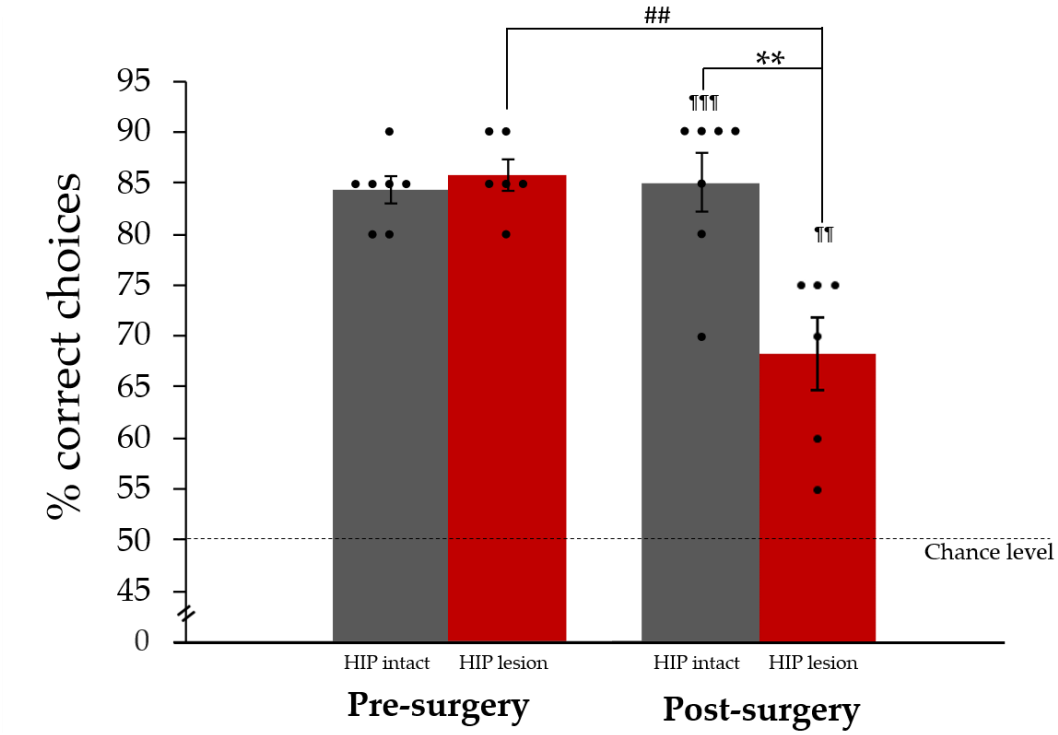

Figure 22: Pre- and post-surgery memory performance. Pre-surgery performance is comparable between HIP intact and lesioned groups. Likewise, pre- and post-surgery performance did not differ for the intact HIP group. Lesion of HIP significantly altered memory performance as shown by a lower performance post- than pre-surgery in the HIP lesion group ($^{\#\#}p < 0.01$, at α=0.05 Bonferroni corrected) and when compared to HIP intact performance post-surgery ($^{**}p < 0.01$, at α=0.05 Bonferroni corrected). Importantly, post-surgery, HIP lesion rats could still successfully perform the task, albeit with lower accuracy than HIP intact rats (comparison to chance level: $^{¶¶}p < 0.01$, $^{¶¶¶}p < 0.001$).

4.4.2 Hippocampal lesion affects familiarity signals in LEC, but not in PER

LEC and PER were engaged during the retrieval phase of the DNMS task in both the HIP intact and HIP lesion groups (comparisons to 0: HIP intact: LEC $t_{(6)} = 8.87$, $p < 0.001$; PER $t_{(6)} = 9.15$, $p < 0.001$; HIP lesion: LEC $t_{(5)} = 9.93$, $p < 0.001$; PER $t_{(5)} = 8.06$, $p < 0.001$; Fig. 6). In the HIP intact group, LEC and PER were recruited to a comparable level (LEC vs. PER: $t_{(6)} = 1.28$, $p = 0.25$). In addition, further statistical comparisons showed for the first time that impaired hippocampal function led to an increase in LEC activity (HIP lesion vs. intact: $t_{(11)} = -2.53$, $p = 0.014$; **Figure 23**), revealing that LEC activity is sensitive to the HIP lesion and that LEC is more recruited in rats relying primarily on familiarity (the HIP lesion group) than in rats relying on both familiarity and recollection (the HIP intact group). In sharp contrast, activity levels in PER remained comparable independently of whether the hippocampal function was compromised or not (HIP lesion vs. intact: PER: $t_{(11)} = -1.15$, $= 0.14$; **Figure 23**), indicating that PER activity is independent of hippocampal function within this framework. This differential effect of hippocampal lesion on LEC and PER activity was further supported by a direct comparison between LEC and PER showing a higher engagement of LEC than PER following hippocampal lesion during retrieval of odor memories (HIP lesion LEC vs. PER: $t_{(5)} = 3.67$, $p = 0.014$), despite a comparable level of engagement in rats with intact hippocampus (HIP intact LEC vs. PER: $t_{(6)} = 1.28$, $p = 0.25$). Importantly, the fact that LEC activity is tied to the contribution of familiarity to memory performance and not to the contribution of non-cognitive processes occurring during memory retrieval was investigated in a previous study by our group involving the same task and the implementation of a response deadline known to orient judgments towards familiarity (Atucha et al., 2017). In this study, LEC was also recruited in rats relying on familiarity, whereas it was not engaged when no demands were imposed on the familiarity process in a control group that was exposed to the same experimental conditions but randomly-rewarded instead of following a delayed-non-match to sample rule (DNMS) (Atucha et al., 2017; see **Supplementary Figure 6**). Of note, both experimental manipulations leading to familiarity judgments in this

DNMS task (implementing a response deadline in Atucha et al., 2017 or lesioning the hippocampus in the present study) yield similar levels of activation in the LEC (response deadline vs. HIP lesion: $t_{(10)} = 0.724$; $p = 0.486$). Moreover, an additional control experiment using a version of the DNMS task orienting judgments towards recollection this time (using pairs of stimuli instead of single stimulus) further indicated that LEC changes in neural activity are likely to reflect changes in the contribution of familiarity to solving the task as opposed to changes in other cognitive processes. Indeed, activity in the LEC in the group relying on recollection was low and significantly reduced compared to that of the HIP lesioned group that relies on familiarity (comparisons to 0: Recollection: $t_{(5)} = 16{,}41$, $p < 0.001$; Familiarity: $t_{(5)} = 7.19$, $p < 0.001$; Recollection vs Familiarity: $t_{(10)} = 4.29$, $p < 0.01$; **Supplementary Figure 7**). In summary, the present results suggest an inverse functional relationship between HIP and LEC during familiarity judgments and the absence of strong ties between PER and HIP function within this frame.

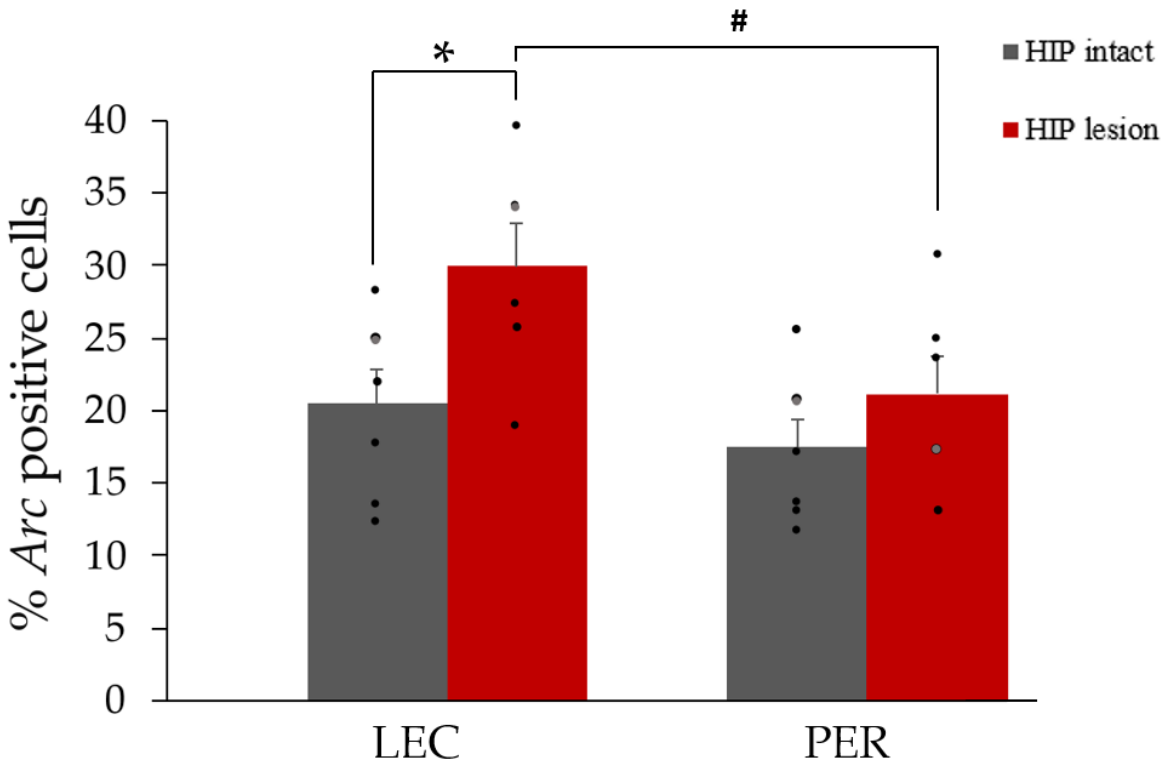

Figure 23: Percentage of *Arc* positive cells in LEC and PER in HIP intact and lesioned rats performing the memory task (bars represent means ± SEM). LEC and PER are recruited during the task in both groups (comparisons to 0: $p < 0.001$). Importantly, *Arc* RNA expression is increased only in LEC and not in PER following HIP lesion (* $p < 0.025$, at α=0.025 Bonferroni corrected), suggesting a distinct functional relationship between LEC and HIP, and PER and HIP. In addition, LEC is more recruited than PER during the task in rats with compromised hippocampal function ($^{\#}p < 0.05$, at α=0.05 Bonferroni corrected) while they are recruited to a similar extent in rats with intact hippocampus, suggesting a potential compensatory mechanism.

4.4.3 Besides LEC and PER, HIP is also engaged during the task in rats with intact hippocampus

In addition to relying on familiarity, rats with intact functional hippocampus were shown to also rely on recollection (supported by the hippocampus) to solve the task used in the present study (Fortin et al., 2004). Thus, we tested that the hippocampus was engaged during the task in rats with intact functional hippocampus (understandingly, such an assessment could not be performed in the HIP lesion group as HIP has been lesioned). High resolution imaging of CA1 and CA3 revealed a strong recruitment of these areas at retrieval, with a higher recruitment of CA3 than CA1, indicating that the hippocampus was indeed engaged in addition to LEC and PER in intact HIP rats (comparison to 0: CA3: $t_{(3)} = 15.45$, $p = 0.001$, CA1: 0: $t_{(3)} = 6.68$, $p = 0.007$; CA3 vs. CA1: $t_{(3)} = 2.76$, $p = 0.035$; **Figure 24**; see previous paragraph for LEC and PER statistical comparisons;).

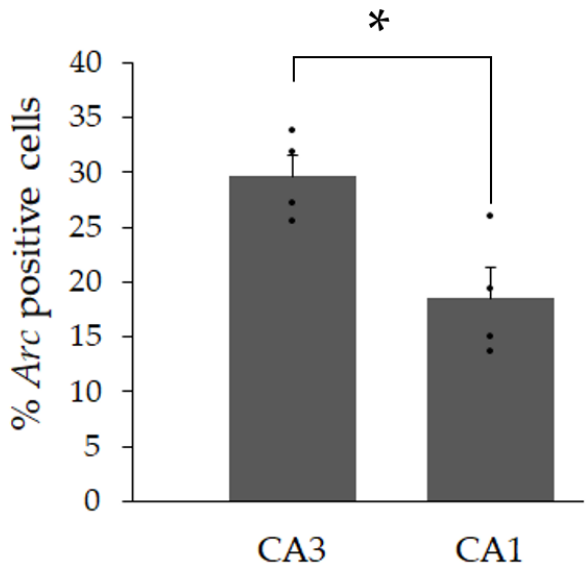

Figure 24: Percentage of *Arc* positive cells in CA3 and CA1 hippocampal subfields in HIP intact rats performing the memory task (means ± SEM). In addition to LEC and PER, CA3 and CA1 are highly recruited during memory retrieval in rats with intact hippocampus that rely on recollection and familiarity to solve this task (comparisons to 0: $p < 0.01$; CA3 more than CA1: *p: < 0.05).

4.4.4 LEC, PER, CA1, and CA3 are only mildly engaged in rats that do not perform the task

As expected, baseline *Arc* RNA expression in LEC, PER, CA1, and CA3 of home-caged controls was low (LEC: 8.27% ± 2.5; PER: 6.54% ± 2.27, CA1: 5.37% ± 0.6, CA3: 12.63% ± 2.74; comparisons to 0: LEC $t_{(5)} = 3.31$, $p = 0.021$; PER $t_{(5)} = 2.88$, $p = 0.035$; CA1: $t_{(3)} = 8.92$, $p = 0.003$; CA3: $t_{(3)} = 4.61$, $p = 0.019$: **Figure 25**) and comparable across areas ($F_{(3,16)} = 1.55$, $p = 0.24$; **Figure 25**). These rats did not perform the task but were exposed to the testing room according to the same experimental scheme as rats performing the task. Also, as expected, *Arc* RNA expression in animals performing the task was overwhelmingly higher than in home-caged controls (HIP intact vs. controls: LEC $t_{(11)} = 3.59$, $p = 0.004$; PER $t_{(11)} = 3.72$, $p = 0.003$; CA1: $t_{(6)} = 4.64$, $p = 0.004$; CA3: $t_{(6)} = 5.08$, $p = 0.002$; HIP lesion vs. controls: LEC $t_{(10)} = 5.54$, $p < 0.001$; PER $t_{(10)} = 4.21$, $p = 0.002$), indicating that cognitive demands likely contribute to the differences in *Arc* expression observed between experimental and home-caged groups (Guzowski et al., 1999).

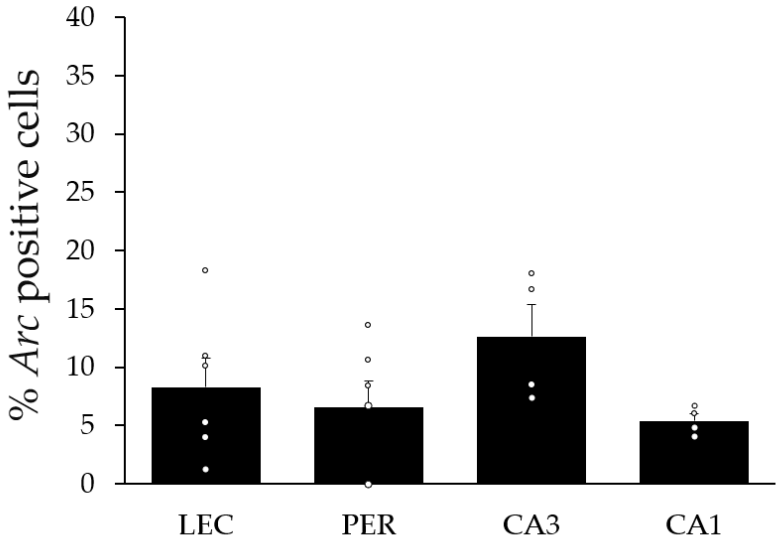

Figure 25: Percentage of *Arc* positive cells in LEC, PER, and CA3 and CA1 hippocampal subfields of rats that did not perform the task. (means ± SEM). Baseline *Arc* RNA expression in MTL areas was low (all comparisons to 0: $p < 0.05$) and comparable between areas in the home-caged controls.

4.5 Discussion

In this study, we have combined a human to rat translational memory task with hippocampal lesions and high-resolution imaging that allows for LEC's activity during recognition memory based on familiarity to be dissociated from PER's activity. We show that **LEC and PER are recruited to a comparable extent when the hippocampal function is spared**. In addition, we report for the first time that **LEC activation is inversely related to hippocampal function**, while activation of **PER is independent** of hippocampal integrity. These results indicate that both LEC and PER contribute to the familiarity process and that their contribution, although quantitatively similar, might rely on different mechanisms.

The fact that **LEC is recruited during recognition memory based on familiarity** in the present study supports the findings of the only study to date reporting a specific activation of LEC during familiarity judgments in a recognition memory task with high memory load, albeit using different experimental conditions (Atucha et al., 2017). In addition, it complements the results of previous studies with lower memory demands involving DNM to odor or spontaneous object recognition memory tasks (Albasser et al., 2013; Kinnavane et al., 2014; Ramus & Eichenbaum, 2000; Young et al., 1997).

Altogether these results indicate, by extension, that familiarity-induced signals observed in humans in the rhinal cortices do truly involve LEC and not only PER. In addition, we showed for the first time that **lesioning the hippocampus enhances selectively LEC's activity**. Importantly though, despite the fact that rats with hippocampal damage performed worse on the DNMS task than rats with intact hippocampus, they were still successful in retrieving memories. This suggests that the increase in LEC recruitment in rats with hippocampal lesions might reflect an attempt at compensating for hippocampal dysfunction. Such a compensatory mechanism in the form of increased reliance on familiarity associated with an increased activity in

rhinal cortices has been reported in a 3T fMRI study in older subjects with reduced hippocampal function but performance comparable to that of young adults (Daselaar et al., 2006). This latter study did however not focus on dissociating LEC's contribution from that of other parts of the rhinal cortex. The technical approach adopted in our study does not enable us to investigate the specific mechanism that leads to the increased activity in LEC. However, it is known that EC and the hippocampus share heavy bidirectional connections, principally excitatory projections (for a review, see Agster et al., 2016; Tomás Pereira et al., 2016; Van Strien et al., 2009) but also some long-range- projecting inhibitory (GABAergic) neurons believed to play an important role in memory by modulating EC's function (Melzer et al., 2012). Of particular interest for the present study, some long-range-projecting hippocampal neurons (somatostatin and GABAergic) target principally the superficial layers (I/II) in the EC (Melzer et al., 2012). Hence, it might be reasonable to speculate that the hippocampus could exert a tonic inhibition on LEC in subjects with healthy hippocampus, thereby possibly minimizing the contribution of familiarity to recognition memory and maximizing that of recollection. In turn, damage to the hippocampus might release this inhibition, promoting the use of familiarity judgments and yielding successful memory retrieval, albeit with a reduced performance. Evidence for such a shift in strategy, i.e., from a reliance on recollection to a reliance on familiarity, has been reported in young adult rats following hippocampal lesions and in aged rats in the DNMS task used in the present study (Robitsek et al., 2008; Sauvage et al., 2008). Likewise, patients with MTL damage, including the hippocampus, have been shown to perform better on associative word recognition memory tasks when compound words are used as stimuli, i.e., when patients are given the opportunity to unitize the two elements of a pair of unrelated words (for example as in 'motherboard') which relies on the familiarity process, instead of retrieving them independently (as in 'mother' and 'board'; Giovanello et al., 2006). In summary, our results show that LEC plays a crucial role in familiarity and suggest that the HIP to LEC projections might be modulating the extent to which familiarity contributes to recognition memory.

Conversely, damaging the hippocampus did not affect PER activity during familiarity judgments demonstrating that PER activity is not tied to hippocampal function within this frame. As a cautionary note, the fact that the overall activity in PER is not affected by hippocampal lesion does not exclude the possibility that coding properties of individual cells in the PER might be altered by the lesion, as PER (and LEC) cells properties have been shown to vary during a continuous DNMS task relying on both recollection and familiarity (Ramus & Eichenbaum, 2000; Young et al., 1997). Elucidating the latter question is however not within the scope of the present study, centered on network level mechanisms supporting familiarity with the LEC as a focus and will require further investigations focused on the cellular level to be thoroughly addressed. Similarly, it cannot be ruled out that the reliance of PER familiarity signals on hippocampal function might vary if stimuli differ even more in the degree of familiarity than it is the case in the present study as PER's contribution to familiarity itself has been recently reported to slightly vary under this condition (Ameen-Ali et al., 2021). Addressing this question is however not the focus of the present study and will also require further investigations.

The fact that **PER and HIP can work independently to detect the familiarity/novelty for items is a well-accepted concept**, especially in rodents as shown in lesion and IEG studies using spontaneous object recognition memory tasks with low memory demands (Aggleton et al., 2005; Aggleton & Brown, 1999, 2005; Brown et al., 2010). The present study builds upon this existing knowledge and shows evidence that PER and HIP function can also be independent in memory tasks requiring high memory demands (i.e., with a long study list of items, a large delay between study and retrieval phases, etc.) and different types of stimuli (i.e., here odors). This underlines the robustness of the findings and the fact that this result is independent of experimental conditions. Also, as mentioned previously, even though the role of PER in familiarity has been extensively studied in humans and rodents (Atucha et al., 2017; Bowles et al., 2007, 2010; Haskins et al., 2008; Köhler & Martin, 2020; Murray et al., 2007; Farovik et al., 2011; see for reviews Brown & Aggleton, 2001; Eichenbaum et al., 2012), evidence

for a specific involvement of LEC has been scarce in animals (Atucha et al., 2017) and inexistent in humans. Hence, the extent to which the engagement of LEC and PER during judgments based on familiarity is comparable in healthy subjects or when hippocampal function is compromised was not known. Our results address the latter question by showing that LEC and PER's contribution to familiarity is quantitatively comparable but that they might belong to distinct neuroanatomical subnetworks supporting familiarity judgments as lesions of the hippocampus increased only LEC's activity within this frame.

Furthermore, as a **token of the reproducibility of *Arc* IEG imaging data**, LEC and PER's activity in the group with intact hippocampus were comparable between the present study and the study of Atucha and colleagues, in which the intact hippocampus group was tested under the exact same experimental conditions. Likewise, activity in CA1 and CA3 in the group without hippocampal lesions was also comparable between studies and in line with the findings that rats rely on recollection, supported by the hippocampus (Eichenbaum et al., 2007; Fortin et al., 2004; Sauvage et al., 2008; Stark & Squire, 2000) in addition to relying on familiarity to solve the present DNMS task. Notably, in Atucha's and the current studies, CA3 was more recruited than CA1, possibly reflecting the engagement of CA3 in pattern completion, a mechanism thought to rely on recollection (Horner et al., 2015) and taking advantage of CA3's recurrent collaterals believed to be crucial for autoassociative networks (Kesner, 2013; Kesner & Rolls, 2015). Also, in the present study, MTL activity levels in rats with or without lesions were found to be tied to the memory demands of the tasks as MTL activity levels of home-cage controls, brought to the experimental room together with the trained animals but remaining undisturbed in their home caged, were very low in comparison. This point was also addressed in the study of Atucha and colleagues with two control groups: one subjected to a response deadline used as a control group for the DNMS rats relying on the familiarity process, and the other without response deadline used as a control group for the DNMS rats relying on both familiarity and recollection. These two control groups were exposed to the same

experimental conditions as the DNMS rats but were randomly rewarded instead of following a DNMS rule so that no memory demands would apply (i.e., the familiarity process or the familiarity and recollection processes were not involved, respectively). LEC level of activity in the randomly rewarded groups was very low and significantly lower than in groups relying on familiarity or on both familiarity and recollection. These findings indicate that activity changes in the LEC observed in Atucha et al.'s study unlikely stemmed from changes in non-cognitive processes occurring during memory retrieval. In addition, in the present study, LEC was significantly less recruited in rats that were tested in a version of the DNMS task in which rats did not rely on familiarity but on recollection, further supporting the claim that changes in LEC activity are tied to the contribution of familiarity to memory performance rather than to the contribution to other cognitive processes to the performance.

This, together with the fact that *Arc* RNA expression is closely tied to synaptic plasticity (Bramham et al., 2008; Guzowski, McNaughton, et al., 2001; Guzowski, Setlow, et al., 2001; Shepherd & Bear, 2011), is reported to better reflect task demands than other IEGs, such as *c-fos* and *zif268*, and not stress levels or motor activity (Flasbeck et al., 2018; Guzowski et al., 1999; Guzowski, Setlow, et al., 2001; Nakamura et al., 2013) and is commonly used as a marker of cell activation to map activity in the medial temporal lobe (Kubik et al., 2007; Sauvage et al., 2013, 2019) bring further support to the claim that activity levels in the MTL areas in this study are likely to reflect the memory demands of the task.

Altogether, our results provide clear empirical evidence for the long-standing, yet theoretical, claim of a **crucial role of LEC in familiarity**. Our findings also reveal that LEC's contribution is comparable to that of PER, making LEC a main contributor to this process, thus giving further support to the dual process theory predicting that familiarity is supported by LEC and PER (Diana et al., 2010; Eichenbaum et al., 2007; Sauvage, 2010). Our data also support to some extent the one process theory (Squire,

1992; Squire & Zola, 1998; Wixted & Squire, 2011), according to which the hippocampus contributes to familiarity, but is not rigorously in line with this classical model that predicts that hippocampus might enable familiarity. On the contrary, our results show that LEC's activity during familiarity judgments is inversely correlated with hippocampal function. Our results complement earlier findings showing that MEC specifically supports recollection in a rat lesion study (Sauvage, Beer, Ekovich, et al., 2010) and the report that the thinning of EC in elderly affects more familiarity but also recollection judgments in humans (Yonelinas et al., 2007). Taken together, these findings bring further evidence for a functional dissociation between LEC and MEC in recognition memory. The present experimental approach does not allow for a direct study of the mechanisms underlying LEC and PER's contribution to familiarity, but a well-accepted view in memory research is that representations of distinct items are formed at the level of LEC and PER, which, along with back projections to the neocortex, would support familiarity judgments (Eichenbaum et al., 2007). Our present results allow us to expand on this knowledge and to add that only LEC's contribution to familiarity is under the modulation of the hippocampus (and not PER's).

In summary, we report that **both LEC and PER function are crucial for familiarity judgment**s and showed that **familiarity signals in LEC are inversely correlated to hippocampal function (but not PER's)**, suggesting that brain networks supporting the contribution of LEC and PER to familiarity might be different.

Chapter 5

5. General Discussion

5.1 Summary of results

5.1.1 Testing the 40-channels fMRI-compatible olfactometer with a 9.4T scanner in sedated rats

The first study (**Chapter 2**) showed that using distinct odors and short stimulus durations elicited distinct odor maps within animals in the olfactory bulb (OB) in single fMRI scanning sessions. In addition, we could find a global similarity in odor-specific clusters across animals for the majority of the odors, in addition to a reasonable amount of local variability. This result was in line with previous studies using longer stimulation durations, awake animals, other types of sedation, or other technical approaches. In addition, we ensured that each of the 40 channels of the olfactometer could successfully deliver an odor stimulus detectable at the level of the olfactory bulb, thereby **bringing proof of principle for the use of our high throughput olfactometer in a 9.4T fMRI setting in sedated rats**. Further, this study shows that in primary olfactory processing brain regions (such as the OB), a BOLD response can be evoked under medetomidine sedation while using essential oils/household odorants.

5.1.2 Hippocampus activation patterns during an fMRI-compatible recognition memory task in awake rats are comparable to those obtained in humans

Using the olfactometer tested in **Chapter 2** and habituating the rats to being scanned while awake, we conducted an fMRI recognition memory task for rats that allows for data analyses comparable to those performed in humans (i.e., contrasts). In this fMRI experiment conducted in awake animals, a stronger BOLD activation was found in the hippocampus (HIP) for `old´ odors (odors that the animals had experienced prior scanning, i.e., for which memory could be formed) in comparison to `new´, unexperienced odors (`old>new´ contrast). Besides, in line with human studies, other

brain regions tightly related to cognitive function, such as the cingulate cortex, displayed a similar pattern. Yet, it was **not the case in sedated rats**. Hence, for the first time, using **fMRI in awake rats**, we could **show similar activation patterns during recognition memory in humans and awake rats**. This result is a major achievement for bridging further human to animal memory research and developing more human to rat translational projects. Because of imaging artifacts, especially present at the vicinity of the ear canals in rats, the contribution of the LEC and PER to recognition memory and its reliance on hippocampal function could not be assessed using an fMRI approach.

5.1.3 LEC and PER's contribution to recognition memory does not depend on hippocampal function

In **Chapter 4**, the focus was on investigating **the contribution of the lateral entorhinal and perirhinal cortices** (LEC and PER, respectively) **to familiarity**, one of the two processes supporting recognition memory, in relation to hippocampal integrity. Using high resolution Immediate Early Gene (IEG) imaging, we reported a **robust and comparable contribution of the LEC and PER during familiarity judgments**. Furthermore, following a hippocampal lesion, a selective increase of neural activity could be found in the LEC but not in the PER. These results confirmed the involvement of both regions in the familiarity process yet suggest their contribution rely on different mechanisms. As indicated by the change in neural activity after HIP lesion, familiarity signals in the PER appear to be independent of hippocampal function. At the same time, LECs' are inversely correlated to its function. The latter suggests the existence of a **tonic inhibition of the hippocampus on the LEC during familiarity judgments in rats with intact hippocampal function**.

5.2 Integration of the studies

Using the olfactometer setup tested in **Chapter 2**, we report in **Chapter 3** the involvement of the hippocampus (HIP) among other regions in recognition memory. The fact that similar results were observed in humans (Donaldson et al., 2001; Heun et al., 2006; Stark & Squire, 2000; Sugiura et al., 2005; Yonelinas et al., 2005) underline the validity of the translational approach intended to develop: using fMRI paradigms in awake animals to further bridge human and animal memory research. Importantly, we were able to demonstrate the importance of awake scanning when the focus is laid on cognitive functions and related brain regions.

To date, the detection of the activated brain areas in recognition memory in rodents was usually performed using imaging techniques based on the detection of Immediate Early Genes (Albasser et al., 2013; Kinnavane et al., 2014; Sauvage et al., 2013). This technique allows for cellular resolution yet requires animals to be sacrificed immediately upon completion. Hence it is not an '*in vivo*' technique and is not suited for longitudinal studies. In contrast, the 'nonlethal' character of fMRI studies allows for these types of within-subject studies often performed in humans.
However, an ongoing major challenge to readily compare studies between rodents and humans is that rats were scanned sedated, which is suboptimal when the memory function is investigated. Further, virtually no fMRI-compatible memory paradigms were available. With **Chapters 2 and 3**, we contributed to filling this gap.

Much remains to be done to achieve a spatial resolution with fMRI in awake animals as high as that achieved with IEG imaging. And additionally, circumvent MR 'bound' artifacts, such as signal distortions related to structure inhomogeneity (e.g., air in the ear canal) which can preclude the investigation of specific targets of interest with an fMRI approach, for example, the LEC and the PER. In the latter case, using an IEG imaging approach as done in **Chapter 4** can be an appropriate complementary

approach to allow for more thorough investigations than that made possible with fMRI even in awake animals.

5.2.1 Influence of anesthesia/sedation on the fMRI BOLD response

As previously mentioned in this thesis, it has been shown in the literature that anesthesia can significantly alter the BOLD response during an fMRI scan. A review published by Gao et al. reported that a profound influence of anesthesia can be found in cerebral hemodynamics, brain metabolism, neural activity, neurovascular coupling, and functional connectivity (Gao et al., 2017). To date, only studies focusing on either functional connectivity (Paasonen et al., 2018), resting-state (Liang, Liu, et al., 2015; Smith et al., 2017), electrical forepaw stimulation (Peeters et al., 2001), or visual stimulation (Dinh et al., 2021) have investigated the differences in BOLD response between animals scanned under sedated or awake conditions.

Our study is the first to focus on cognitive functions and brain regions within this frame. Our results bring clear evidence that despite the cost of a lengthy habituation procedure, there is a definite (and high) benefit in scanning animals under awake conditions, especially regarding studies focusing on cognition. As a reminder, no BOLD signal could be detected in sedated animals trained and scanned under the same conditions as the animals scanned awake. For the latter, a BOLD response could be detected in brain regions related to cognition. Similar findings were observed in humans, for example, in a study by Mhuircheartaigh and colleagues showing a reduction of BOLD responses to auditory and noxious stimuli in cortical and subcortical regions in sedated and unresponsive subjects compared to awake (Mhuircheartaigh et al., 2010). In addition, a review by Bonhomme and colleagues described the influence of anesthesia on cerebral blood flow, metabolic rate, and functional connectivity. A decrease in cerebral blood flow and metabolic rate can be found for the most commonly used anesthetics (Bonhomme et al., 2011). Notably, the functional connectivity first decreases in the higher-order cortical networks due to the anesthetic agents.

In conclusion, it appears to be a consensus that optimal BOLD detection might occur under awake conditions instead of sedation. Our data demonstrates this is especially the case when the focus of the investigation is laid on cognitive functions.

5.3 Challenges/limitations and outlook

5.3.1 Challenges and limitations

A few obstacles had to be overcome to perform this thesis's translational fMRI recognition memory task. As mentioned prior in **Chapter 3**, to scan rats under awake conditions, rats had to be *habituated* to the surrounding conditions of an fMRI scanning session, *movement artifacts* reduced to a minimum by using a head fixation and a *stimulus paradigm* equivalent to the one used in human memory tasks had to be used. Besides this, the *hardware* had to be put together and tested beforehand (see **Figure 3** for a graphical abstract). In addition, *analysis pipelines* had to be adapted from humans to rats to facilitate comparisons between species. To achieve this, as standard in human fMRI, a *group analysis* of the rat data and the *contrast `old´ versus `new´* stimuli had to be performed. Moreover, as mentioned in the literature, a *hemodynamic response function (HRF) adapted to rats* (instead of the human HRF) had to be identified to improve the detection performance and tailored to the regions of interest (HIP and cognitive regions).

Furthermore, since the HIP and its role in recognition memory was the main focus in the awake fMRI study, we used a *20 mm surface loop coil* placed right above the HIP to ensure a high sensitivity for BOLD detection. For the first study (see **Chapter 2**), the focus was set to an even smaller region of interest (ROI), therefore we chose the *10 mm surface loop coil*. If a different, more dorsally located ROI is chosen during the awake fMRI scan, the placement of the whole head fixation construct has to be adapted (placement more anterior or posterior). If the focus is more on the ventral part of the

brain, e.g., the subregions of the parahippocampal areas, a different receiver coil should be considered (including an adaptation of the head fixation implant). Because of the air present in the ear canal, a significant dropout of the EPI signal can be detected in the deep/ventral brain. Therefore, to improve the EPI signal of the ventral part of the brain, a different coil, for example, a volume coil, suggested by, e.g., Ferris, Febo, and Kulkarni (Ferris et al., 2013), should be used.

Lastly, aspects that have to be named that could be a limiting factor for longitudinal studies are the growth of the brain over time and possible image intensity changes. To account for these changes, various attempts were already made in human fMRI. Csapo and colleagues proposed a *model-based image similarity measure* for longitudinal image registration using MR images of monkeys (Csapo et al., 2012, 2013). Using the MRI images of Multiple Sclerosis (MS) patients, Diez and colleagues (2014) compared different registration methods to find the best fitting to be used for longitudinal studies, including studies where lesions are present (as in MS patients) (Diez et al., 2014). For rodent data, here focusing mainly on mice MR data processing, a preprocessing pipeline/toolbox was developed by the lab of Mallar Chakravarty in the Douglas Mental Health University Institute, Canada, to, e.g., improve the registration of the MR images and the BOLD detection ("RABIES" software can be found on GitHub).
Considering mentioned options, the limiting factor of brain growth over time and/or intensity change should be manageable and the registration of the longitudinal MR images successful.

5.3.2 Outlook

Despite what has already been achieved for translational approaches between human and rodent data for recognition memory, future technical optimizations might contribute to achieving the necessary steps towards analyses at a higher spatial resolution, e.g., allow for subregional investigations (for example, CA subfields, etc.).

In humans, Berron and colleagues (2017) were able to establish a segmentation protocol to manually delineate subregions in the parahippocampal gyrus and the hippocampal subfields at 7T. However, this segmentation protocol so far only includes the segmentation into the entorhinal cortex, perirhinal cortex (distinguishing areas 35 and 36), and parahippocampal cortex. A reliable subdivision of the entorhinal cortex into the medial and lateral part could not yet be achieved with it. Similar to this segmentation protocol, a protocol for segmentation of the individual MTL subregions (i.e., the parahippocampal region and the subfields of the HIP) in rodents needs to be implemented to dissociate the source of activity at the subregional level. Segmenting MTL subregions in rats would constitute one more step towards bridging further human and animal memory function by facilitating the comparison between fMRI and IEG imaging data. Here, especially the subfields of the HIP (CA1, CA2, CA3, subiculum, and dentate gyrus) are of interest as previous studies report different roles within the memory function (Beer et al., 2013; Hitti & Siegelbaum, 2014; Kesner et al., 2004; O'Mara, 2005). Notably, recent technical developments allowing for a 3D display of IEG imaging data and their implementation at the whole-brain level using a technique that produces structurally intact yet optically transparent tissue is also a further step towards this goal (Chung & Deisseroth, 2013; Epp et al., 2015). Indeed using this type of methods (CLARITY-like methods) in combination with IEG detection could allow a 3D display of the whole brain's activation similar to that obtained with fMRI, yet with a cellular resolution (for a review, see Sauvage et al., 2019).

One promising future approach for the use of fMRI in awake rats is the advantage of the possibility of combining the fMRI scan with a lesion of a specific brain region. As lesion studies in humans only are feasible to the extent of patients suffering damage in this specific area, artificially inflicted lesions can be done in laboratory rodents. These lesions can be locally very precise in only one region of interest (in humans, often more than one region is battered), allowing an accurate conclusion of the effects of this single region. Given our framework to study mnemonic deficits in models of amnesia, i.e., in

rats with damage to medial temporal lobe areas, the advantage is that the damage in the rats´ brain can be assessed post mortem and specific areas targeted. As presented in this thesis (**Chapter 4**), lesion studies are commonly used in rodent memory tasks (for example, see Clark et al., 2001; Faraji et al., 2008; Farovik et al., 2011; Fortin et al., 2004). To our knowledge, lesion studies in rodents used in combination with fMRI in awake or sedated rats focusing on cognitive functions have not yet been conducted. However, combining these two techniques would, in particular, allow us to look at possible compensatory effects due to hippocampal lesion and possibly reveal network changes in cognitive functions within this frame. For the latter, the use of an intra-subject experiment, i.e., conducting an fMRI scan before and after lesioning the region of interest, would be compelling. So far, an inter-subject comparison, i.e., comparing the brain activity of controls to the lesioned animals using a molecular imaging technique, is most commonly used. Combining awake fMRI in rats with a lesion approach will require some adjustments, such as adjusting the head fixation of the rats to be able to perform the lesion in between scans.

Combined fMRI applications in awake rodents with electrophysiology or optogenetics were already done (Aksenov et al., 2016; Liang, Watson, et al., 2015; C. J. Martin et al., 2006). Yet, no focus was laid on investigating the cognitive functions within this context. Instead, the studies focused on, e.g., investigating the thalamocortical sensory pathway during somatosensory stimulations or the network activated by medial prefrontal cortex outputs. Since all the `elements´ of this `construct´ are on hand, investigating the recruited brain regions and their network during recognition memory, as responses to these manipulations can be done in the future.

Also, in our present fMRI study, memory performance is not behaviorally evaluated as also done partly in human studies. Studies in humans using passive viewing paradigms showed no obligatory behavioral response to the stimuli to evoke a BOLD response in the MTL. For example, Holt et al. (2006) showed a higher hippocampal activation compared to baseline after passively viewing facial expressions in controls and patients with schizophrenia in a study investigating the involvement of the HIP

in emotional memory (Holt et al., 2006). In another study, (Kelley et al., 1998) discovered similar activation patterns between a passive viewing task of words, objects, or faces and an intentional encoding task (i.e., the subjects were told to remember the items for a later memory test). However, assessing memory performance as animals are scanned would further bridge our results with other studies in humans assessing memory performance upon scanning. To do so, we are currently establishing a new fMRI paradigm in awake rats. Here, the rats will be required to respond in two distinct ways when they are presented with `old´ or `new´, as done in a Non-matching to sample tasks that do not involve fMRI in our lab (see, e.g., **Chapter 4** or (Nakamura et al., 2013)). To date, two studies trained mice to show a licking response during awake fMRI (Fonseca et al., 2020; Han et al., 2019). Additionally, Fonseca and colleagues succeeded in training mice to press a lever during the fMRI scan. We plan on adapting this modus operandi to rats to include a `response feature´ to our fMRI-compatible memory task.

In conclusion, it should be kept in mind, while comparing the results, that both of the techniques (fMRI and molecular imaging) rely on vastly different parameters to visualize brain activity during recognition memory tasks. Hence, even if the experimental paradigms (i.e., stimulus protocol and behavioral training) are kept similar, differences are still expected to emerge and should be further investigated. Furthermore, it has to be acknowledged that the BOLD signal during an fMRI scan is an indirect measurement of neural activity, and its relationship is not fully understood yet. A detailed review of how the BOLD signal can be interpreted and the complex interaction to changes in cerebral blood volume and flow and oxygen consumption was done by Logothetis and Wandell (Logothetis & Wandell, 2004).
Nevertheless, comparing both techniques and their results still constitute a promising attempt at bridging human and rodent data in various fields.

Chapter 6

6. References

Aggleton, J. P., & Brown, M. W. (1999). Episodic memory, amnesia, and the hippocampal-anterior thalamic axis. *Behavioral and Brain Sciences*, *22*(3), 425–444.

Aggleton, J. P., & Brown, M. W. (2005). Contrasting Hippocampal and Perirhinalcortex Function using Immediate Early Gene Imaging. *The Quarterly Journal of Experimental Psychology Section B*, *58*(3-4b), 218–233.

Aggleton, J. P., & Pearce, J. M. (2001). Neural systems underlying episodic memory: Insights from animal research. *Philosophical Transactions of the Royal Society B: Biological Sciences*, *356*(1413), 1467–1482.

Aggleton, J. P., Vann, S. D., Denby, C., Dix, S., Mayes, A. R., Roberts, N., & Yonelinas, A. P. (2005). Sparing of the familiarity component of recognition memory in a patient with hippocampal pathology. *Neuropsychologia*, *43*(12), 1810–1823.

Agster, K. L., Tomás Pereira, I., Saddoris, M. P., & Burwell, R. D. (2016). Subcortical connections of the perirhinal, postrhinal, and entorhinal cortices of the rat. II. efferents. *Hippocampus*, *26*(9), 1213–1230.

Aksenov, D. P., Li, L., Miller, M. J., & Wyrwicz, A. M. (2016). Blood oxygenation level dependent signal and neuronal adaptation to optogenetic and sensory stimulation in somatosensory cortex in awake animals. *European Journal of Neuroscience*, *44*(9), 2722–2729.

Albasser, M. M., Olarte-Sánchez, C. M., Amin, E., Horne, M. R., Newton, M. J., Warburton, E. C., & Aggleton, J. P. (2013). The neural basis of nonvisual object recognition memory in the rat. *Behavioral Neuroscience*, *127*(1), 70–85.

Ameen-Ali, K. E., Sivakumaran, M. H., Eacott, M. J., O'Connor, A. R., Ainge, J. A., & Easton, A. (2021). Perirhinal cortex and the recognition of relative familiarity. *Neurobiology of Learning and Memory*, *182*(June 2020), 107439.

Andersen, P., Morris, R., Amaral, D. G., Bliss, T., & O'Keefe, J. (2007). the Hippocampus Book. In *Oxford University Press, Inc.*

Atucha, E., Karew, A., Kitsukawa, T., & Sauvage, M. M. (2017). Recognition memory: Cellular evidence of a massive contribution of the LEC to familiarity and a lack of involvement of the hippocampal subfields CA1 and CA3. *Hippocampus*, *27*(10), 1083–1092.

Babb, S. J., & Crystal, J. D. (2006). Episodic-like Memory in the Rat. *Current Biology*, *16*(13), 1317–1321.

Bäckman, L., Small, B. J., & Fratiglioni, L. (2001). Stability of the preclinical episodic memory deficit in Alzheimer's disease. In *Brain* (Vol. 124).

Basu, J., Zaremba, J. D., Cheung, S. K., Hitti, F. L., Zemelman, B. V., Losonczy, A., & Siegelbaum, S. A. (2016). Gating of hippocampal activity, plasticity, and memory by entorhinal cortex long-range inhibition. *Science*, *351*(6269), aaa5694–aaa5694.

Beer, Z., Chwiesko, C., Kitsukawa, T., & Sauvage, M. M. (2013). Spatial and stimulus-type tuning in the LEC, MEC, POR, PrC, CA1, and CA3 during spontaneous item recognition memory. *Hippocampus*, *23*(12), 1425–1438.

Beer, Z., Chwiesko, C., & Sauvage, M. M. (2014). Processing of spatial and non-spatial information reveals functional homogeneity along the dorso-ventral axis of CA3, but not CA1. *Neurobiology of Learning and Memory*, *111*, 56–64.

Bestgen, A. K., Schulze, P., Kuchinke, L., Suchan, B., Derdak, T., Otto, T., Jettkant, B., & Sucker, K. (2016). An extension of olfactometry methods: An expandable, fully automated, mobile, MRI-compatible olfactometer. *Journal of Neuroscience Methods*, *261*, 85–96.

Binder, S., Dere, E., & Zlomuzica, A. (2015). A critical appraisal of the what-where-when episodic-like memory test in rodents: Achievements, caveats and future directions. *Progress in Neurobiology*, *130*, 71–85.

Bird, C. M. (2017). The role of the hippocampus in recognition memory. *Cortex*, *93*(0), 155–165.

Bonhomme, V., Boveroux, P., Hans, P., Brichant, J. F., Vanhaudenhuyse, A., Boly, M., & Laureys, S. (2011). Influence of anesthesia on cerebral blood flow, cerebral metabolic rate, and brain functional connectivity. *Current Opinion in Anaesthesiology*, *24*(5), 474–479.

Bowles, B., Crupi, C., Mirsattari, S. M., Pigott, S. E., Parrent, A. G., Pruessner, J. C., Yonelinas, A. P., & Köhler, S. (2007). Impaired familiarity with preserved recollection after anterior temporal-lobe resection that spares the hippocampus. *Proceedings of the National Academy of Sciences of the United States of America*, *104*(41), 16382–16387.

Bowles, B., Crupi, C., Pigott, S. E., Parrent, A. G., Wiebe, S., Janzen, L., & Köhler, S. (2010). Double dissociation of selective recollection and familiarity impairments following two different surgical treatments for temporal-lobe epilepsy. *Neuropsychologia*, *48*(9), 2640–2647.

Bramham, C. R., Worley, P. F., Moore, M. J., & Guzowski, J. F. (2008). The immediate early gene *Arc*/Arg3.1: Regulation, mechanisms, and function. *Journal of Neuroscience*, *28*(46), 11760–11767.

Brandt, K. R., Eysenck, M. W., Nielsen, M. K., & von Oertzen, T. J. (2016). Selective lesion to the entorhinal cortex leads to an impairment in familiarity but not recollection. *Brain and Cognition*, *104*, 82–92.

Brett, M., Anton, J.-L., Valabregue, R., & Poline, J.-B. (2002). Region of Interest Analysis Using an SPM Toolbox. *NeuroImage*, *16*(2), 769–1198.

Brown, M. W., & Aggleton, J. P. (2001). Recognition memory: What are the roles of the perirhinal cortex and hippocampus? *Nature Reviews Neuroscience*, *2*(1), 51–61.

Brown, M. W., Warburton, E. C., & Aggleton, J. P. (2010). Recognition memory: Material, processes, and substrates. *Hippocampus*, *20*(11), 1228–1244.

Brydges, N. M., Whalley, H. C., Jansen, M. A., Merrifield, G. D., Wood, E. R., Lawrie, S. M., Wynne, S.-M., Day, M., Fleetwood-Walker, S., Steele, D., Marshall, I., Hall, J., & Holmes, M. C. (2013). Imaging Conditioned Fear Circuitry Using Awake Rodent fMRI. *PLoS ONE*, *8*(1), e54197.

Burwell, R. D. (2000). The parahippocampal region: Corticocortical connectivity. *Annals of the New York Academy of Sciences*, *911*(401), 25–42.

Burwell, R. D., & Amaral, D. G. (1998). Cortical afferents of the perirhinal, postrhinal, and entorhinal cortices of the rat. *The Journal of Comparative Neurology*, *398*(2), 179–205.

Chen, X., Tong, C., Han, Z., Zhang, K., Bo, B., Feng, Y., & Liang, Z. (2020). Sensory evoked fMRI paradigms in awake mice. *NeuroImage*, *204*(September 2019), 116242.

Chung, K., & Deisseroth, K. (2013). CLARITY for mapping the nervous system. *Nature Methods*, *10*(10), 1035–1035.

Chwiesko, C. (2017). Bridging human and animal recognition memory: In search of hippocampal fMRI BOLD responses to familiarity and novelty in awake rats.

Clark, R. E., West, A. N., Zola, S. M., & Squire, L. R. (2001). Rats with lesions of the hippocampus are impaired on the delayed nonmatching-to-sample task. *Hippocampus*, *11*(2), 176–186.

Courtiol, E., & Wilson, D. A. (2015). The olfactory thalamus: Unanswered questions about the role of the mediodorsal thalamic nucleus in olfaction. *Frontiers in Neural Circuits*, *9*(September), 1–8.

Crystal, J. D. (2009). Elements of episodic-like memory in animal models. *Behavioural Processes*, *80*(3), 269–277.

Csapo, I., Davis, B., Shi, Y., Sanchez, M., Styner, M., & Niethammer, M. (2012). Longitudinal Image Registration with Non-uniform Appearance Change. In *Medical Image Computing and Computer-Assisted Intervention* (pp. 280–288).

Csapo, I., Davis, B., Shi, Y., Sanchez, M., Styner, M., & Niethammer, M. (2013). Longitudinal Image Registration With Temporally-Dependent Image Similarity Measure. *IEEE Transactions on Medical Imaging*, *32*(10), 1939–1951.

Daselaar, S. M., Fleck, M. S., Dobbins, I. G., Madden, D. J., & Cabeza, R. (2006). Effects of healthy aging on hippocampal and rhinal memory functions: An event-related fMRI study. *Cerebral Cortex*, *16*(12), 1771–1782.

Diana, R. A., Yonelinas, A. P., & Ranganath, C. (2010). Medial Temporal Lobe Activity during Source Retrieval Reflects Information Type, not Memory Strength. *Journal of Cognitive Neuroscience*, *22*(8), 1808–1818.

Dias, R., & Honey, R. C. (2002). Involvement of the rat medial prefrontal cortex in novelty detection. *Behavioral Neuroscience*, *116*(3), 498–503.

Diez, Y., Oliver, A., Cabezas, M., Valverde, S., Martí, R., Vilanova, J. C., Ramió-Torrentà, L., Rovira, À., & Lladó, X. (2014). Intensity Based Methods for Brain MRI Longitudinal Registration. A Study on Multiple Sclerosis Patients. *Neuroinformatics*, *12*(3), 365–379.

Dinh, T. N. A., Jung, W. B., Shim, H. J., & Kim, S. G. (2021). Characteristics of fMRI responses to visual stimulation in anesthetized vs. awake mice. *NeuroImage*, *226*(October 2020), 117542.

Donaldson, D. I., Petersen, S. E., & Buckner, R. L. (2001). Dissociating memory retrieval processes using fMRI: Evidence that priming does not support recognition memory. *Neuron*, *31*(6), 1047–1059.

Duverne, S., Habibi, A., & Rugg, M. D. (2008). Regional specificity of age effects on the neural correlates of episodic retrieval. *Neurobiology of Aging*, *29*(12), 1902–1916.

Eichenbaum, H. (2006). Remembering: Functional Organization of the Declarative Memory System. *Current Biology*, *16*(16), R643–R645.

Eichenbaum, H., Fagan, A., Mathews, P., & Cohen, N. J. (1988). Hippocampal System Dysfunction and Odor Discrimination Learning in Rats: Impairment or Facilitation Depending on Representational Demands. *Behavioral Neuroscience*, *102*(3), 331–339.

Eichenbaum, H., Sauvage, M. M., Fortin, N. J., Komorowski, R., & Lipton, P. (2012). Towards a functional organization of episodic memory in the medial temporal lobe. *Neuroscience and Biobehavioral Reviews*, *36*, 1597–1608.

Eichenbaum, H., Yonelinas, A. P., & Ranganath, C. (2007). The medial temporal lobe and recognition memory. *Annual Review of Neuroscience*, *30*, 123–152.

Ennaceur, A., & Delacour, J. (1988). A new one-trial test for neurobiological studies of memory in rats. 1: Behavioral data. *Behavioural Brain Research*, *31*(1), 47–59.

Epp, J. R., Niibori, Y., (Liz) Hsiang, H.-L., Mercaldo, V., Deisseroth, K., Josselyn, S. A., & Frankland, P. W. (2015). Optimization of CLARITY for Clearing Whole-Brain and Other Intact Organs. *ENeuro*, *2*(3), ENEURO.0022-15.2015.

Faraji, J., Lehmann, H., Metz, G. A., & Sutherland, R. J. (2008). Rats with hippocampal lesion show impaired learning and memory in the ziggurat task: A new task to evaluate spatial behavior. *Behavioural Brain Research*, *189*(1), 17–31.

Farovik, A., Place, R. J., Miller, D. R., & Eichenbaum, H. (2011). Amygdala lesions selectively impair familiarity in recognition memory. *Nature Neuroscience*, *14*(11), 1416–1417.

Ferris, C. F., Febo, M., & Kulkarni, P. (2013). Small Animal Imaging as a Tool for Modeling CNS Disorders. In *Translational Neuroimaging* (pp. 59–85). Elsevier.

Flasbeck, V., Atucha, E., Nakamura, N. H., Yoshida, M., & Sauvage, M. M. (2018). Spatial information is preferentially processed by the distal part of CA3: implication for memory retrieval. *Behavioural Brain Research*, *347*(November 2017), 116–123.

Fonseca, M. S., Bergomi, M. G., Mainen, Z. F., & Shemesh, N. (2020). Functional MRI of large scale activity in behaving mice. *BioRxiv*, 04.16.044941.

Fortin, N. J., Wright, S. P., & Eichenbaum, H. (2004). Recollection-like memory retrieval in rats is dependent on the hippocampus. *Nature*, *431*(7005), 188–191.

Fouquet, C., Tobin, C., & Rondi-Reig, L. (2010). A new approach for modeling episodic memory from rodents to humans: The temporal order memory. *Behavioural Brain Research*, *215*(2), 172–179.

Fyhn, M., Molden, S., Witter, M. P., Moser, E. I., & Moser, M. B. (2004). Spatial representation in the entorhinal cortex. *Science*, *305*(5688), 1258–1264.

Gao, Y. R., Ma, Y., Zhang, Q., Winder, A. T., Liang, Z., Antinori, L., Drew, P. J., & Zhang, N. (2017). Time to wake up: Studying neurovascular coupling and brain-wide circuit function in the un-anesthetized animal. *NeuroImage*, *153*(November 2016), 382–398.

Giovanello, K. S., Keane, M. M., & Verfaellie, M. (2006). The contribution of familiarity to associative memory in amnesia. *Neuropsychologia*, *44*(10), 1859–1865.

Groenewegen, H.J. & Witter, M.P. (2004) Thalamus. In Paxinos, G., (ed.), The Rat Nervous System, 3rd edn, Elsevier, San Diego, pp. 407–435.

Gronlund, S. D., Edwards, M. B., & Ohrt, D. D. (1997). Comparison of the retrieval of item versus spatial position information. *Journal of Experimental Psychology: Learning, Memory, and Cognition*, *23*(5), 1261–1274.

Guzowski, J. F., McNaughton, B. L., Barnes, C. A., & Worley, P. F. (1999). Environment-specific expression of the immediate-early gene *Arc* in hippocampal neuronal ensembles. *Nature Neuroscience*, *2*(12), 1120–1124.

Guzowski, J. F., McNaughton, B. L., Barnes, C. A., & Worley, P. F. (2001). Imaging neural activity with temporal and cellular resolution using FISH. *Current Opinion in Neurobiology*, *11*(5), 579–584.

Guzowski, J. F., Setlow, B., Wagner, E. K., & McGaugh, J. L. (2001). Experience-dependent gene expression in the rat hippocampus after spatial learning: A comparison of the immediate-early genes *Arc*, c-*fos*, and *zif268*. *Journal of Neuroscience*, *21*(14), 5089–5098.

Guzowski, J. F., Timlin, J. A., Roysam, B., McNaughton, B. L., Worley, P. F., & Barnes, C. A. (2005). Mapping behaviorally relevant neural circuits with immediate-early gene expression. *Current Opinion in Neurobiology*, *15*(5), 599–606.

Hafting, T., Fyhn, M., Molden, S., Moser, M. B., & Moser, E. I. (2005). Microstructure of a spatial map in the entorhinal cortex. *Nature*, *436*(7052), 801–806.

Han, Z., Chen, W., Chen, X., Zhang, K., Tong, C., Zhang, X., Li, C. T., & Liang, Z. (2019). Awake and behaving mouse fMRI during Go/No-Go task. *NeuroImage*, *188*, 733–742.

Harris, A. P., Lennen, R. J., Marshall, I., Jansen, M. A., Pernet, C. R., Brydges, N. M., Duguid, I. C., & Holmes, M. C. (2015). Imaging learned fear circuitry in awake mice using fMRI. *European Journal of Neuroscience*, *42*(5), 2125–2134.

Haskins, A. L., Yonelinas, A. P., Quamme, J. R., & Ranganath, C. (2008). Perirhinal Cortex Supports Encoding and Familiarity-Based Recognition of Novel Associations. *Neuron*, *59*(4), 554–560.

Heun, R., Freymann, K., Erb, M., Leube, D. T., Jessen, F., Kircher, T. T., & Grodd, W. (2006). Successful verbal retrieval in elderly subjects is related to concurrent hippocampal and posterior cingulate activation. *Dementia and Geriatric Cognitive Disorders*, *22*(2), 165–172.

Hintzman, D. L., Caulton, D. A., & Levitin, D. J. (1998). Retrieval dynamics in recognition and list discrimination: Further evidence of separate processes of familiarity and recall. *Memory & Cognition*, *26*(3), 449–462.

Hitti, F. L., & Siegelbaum, S. A. (2014). The hippocampal CA2 region is essential for social memory HHS Public Access. *Nature*, *508*(7494), 88–92.

Holt, D. J., Kunkel, L., Weiss, A. P., Goff, D. C., Wright, C. I., Shin, L. M., Rauch, S. L., Hootnick, J., & Heckers, S. (2006). Increased medial temporal lobe activation during the passive viewing of emotional and neutral facial expressions in schizophrenia. *Schizophrenia Research*, *82*(2–3), 153–162.

Horner, A. J., Bisby, J. A., Bush, D., Lin, W. J., & Burgess, N. (2015). Evidence for holistic episodic recollection via hippocampal pattern completion. *Nature Communications*, *6*(May), 1–11.

Howard, M. W., Bessette-Symons, B., Zhang, Y., & Hoyer, W. J. (2006). Aging selectively impairs recollection in recognition memory for pictures: Evidence from modeling and ROC curves. *Psychological Aging*, *21*(1), 96–106.

Inoue, C., & Bellezza, F. S. (1998). The detection model of recognition using know and remember judgments. *Memory & Cognition*, *26*(2), 299–308.

Insausti, R., Herrero, M. T., & Witter, M. P. (1997). Entorhinal cortex of the rat: Cytoarchitectonic subdivisions and the origin and distribution of cortical efferents. *Hippocampus*, *7*(2), 146–183.

Jenkins, T. A., Dias, R., Amin, E., Brown, M. W., & Aggleton, J. P. (2002). Fos Imaging Reveals that Lesions of the Anterior Thalamic Nuclei Produce Widespread Limbic Hypoactivity in Rats. *Journal of Neuroscience*, *22*(12), 5230–5238.

Jennings, J. M., & Jacoby, L. L. (1997). An opposition procedure for detecting age-related deficits in recollection: Telling effects of repetition. *Psychology and Aging*, *12*(2), 352–361.

Johnson, B. A., Ho, S. L., Xu, Z., Yihan, J. S., Yip, S., Hingco, E. E., & Leon, M. (2002). Functional mapping of the rat olfactory bulb using diverse odorants reveals modular responses to functional groups and hydrocarbon structural features. *Journal of Comparative Neurology*, *449*(2), 180–194.

Johnson, B. A., & Leon, M. (2000). Modular representations of odorants in the glomerular layer of the rat olfactory bulb and the effects of stimulus concentration. *Journal of Comparative Neurology*, *422*(4), 496–509.

Jonckers, E., Shah, D., Hamaide, J., Verhoye, M., & Van der Linden, A. (2015). The power of using functional fMRI on small rodents to study brain pharmacology and disease. *Frontiers in Pharmacology*, *6*(OCT), 1–19.

Kafkas, A., & Montaldi, D. (2018). How do memory systems detect and respond to novelty? *Neuroscience Letters*, *680*(February), 60–68.

Kajiwara, R., Takashima, I., Mimura, Y., Witter, M. P., & Iijima, T. (2003). Amygdala input promotes spread of excitatory neural activity from perirhinal cortex to the entorhinal-hippocampal circuit. *Journal of Neurophysiology*, *89*(4), 2176–2184.

Kalthoff, D. (2012). Functional Connectivity of the Rat Brain in Magnetic Resonance Imaging.

Kalthoff, D., Seehafer, J. U., Po, C., Wiedermann, D., & Hoehn, M. (2011). Functional connectivity in the rat at 11.7 T: Impact of physiological noise in resting state fMRI. *NeuroImage*, *54*(4), 2828–2839.

Kelley, W. M., Miezin, F. M., McDermott, K. B., Buckner, R. L., Raichle, M. E., Cohen, N. J., Ollinger, J. M., Akbudak, E., Conturo, T. E., Snyder, A. Z., & Petersen, S. E. (1998). Hemispheric Specialization in Human Dorsal Frontal Cortex and Medial Temporal Lobe for Verbal and Nonverbal Memory Encoding. *Neuron*, *20*(5), 927–936.

Kesner, R. P. (2013). A process analysis of the CA3 subregion of the hippocampus. *Frontiers in Cellular Neuroscience*, *7*(MAY), 1–17.

Kesner, R. P., Lee, I., & Gilbert, P. (2004). A behavioral assessment of hippocampal function based on a subregional analysis. *Reviews in the Neurosciences*, *15*(5), 333–351.

Kesner, R. P., & Rolls, E. T. (2015). A computational theory of hippocampal function, and tests of the theory: New developments. *Neuroscience and Biobehavioral Reviews*, *48*, 92–147.

Kim, J. J., Andreasen, N. C., O'leary, D. S., Wiser, A. K., Boles Ponto, L. L., Watkins, G. L., & Hichwa, R. D. (1999). Direct comparison of the neural substrates of recognition memory for words and faces. In *Brain* (Vol. 122).

Kinnavane, L., Amin, E., Horne, M., & Aggleton, J. P. (2014). Mapping parahippocampal systems for recognition and recency memory in the absence of the rat hippocampus. *European Journal of Neuroscience*, *40*(12), 3720–3734.

Koen, J. D., & Yonelinas, A. P. (2011). From humans to rats and back again: Bridging the divide between human and animal studies of recognition memory with receiver operating characteristics. *Learning & Memory*, *18*(8), 519–522.

Koen, J. D., & Yonelinas, A. P. (2014). The Effects of Healthy Aging, Amnestic Mild Cognitive Impairment, and Alzheimer's Disease on Recollection and Familiarity: A Meta-Analytic Review. *Neuropsychology Review*, *24*(3), 332–354.

Köhler, S., & Martin, C. B. (2020). Familiarity impairments after anterior temporal-lobe resection with hippocampal sparing: Lessons learned from case NB. *Neuropsychologia*, *138*, 107339.

Kozlovskiy, S. A., Vartanov, A. V., Pyasik, M. M., & Velichkovsky, B. M. (2012). The Cingulate Cortex and Human Memory Process. *Psychology in Russia: State of Art*, *5*(1), 231.

Kubik, S., Miyashita, T., & Guzowski, J. F. (2007). Using immediate-early genes to map hippocampal subregional functions. *Learning and Memory*, *14*(11), 758–770.

Kumaran, D., & Maguire, E. A. (2007). Match-mismatch processes underlie human hippocampal responses to associative novelty. *Journal of Neuroscience*, *27*(32), 8517–8524.

Lambers, H., Segeroth, M., Albers, F., Wachsmuth, L., van Alst, T. M., & Faber, C. (2020). A cortical rat hemodynamic response function for improved detection of BOLD activation under common experimental conditions. *NeuroImage*, *208*(December 2019), 116446.

Leitner, F. C., Melzer, S., Lütcke, H., Pinna, R., Seeburg, P. H., Helmchen, F., & Monyer, H. (2016). Spatially segregated feedforward and feedback neurons support differential odor processing in the lateral entorhinal cortex. *Nature Neuroscience*, *19*(7), 935–944.

Liang, Z., Liu, X., & Zhang, N. (2015). Dynamic resting state functional connectivity in awake and anesthetized rodents. *NeuroImage*, *104*(1), 89–99.

Liang, Z., Watson, G. D. R., Alloway, K. D., Lee, G., Neuberger, T., & Zhang, N. (2015). Mapping the functional network of medial prefrontal cortex by combining optogenetics and fMRI in awake rats. *NeuroImage*, *117*, 114–123.

Logothetis, N. K., & Wandell, B. A. (2004). Interpreting the BOLD signal. *Annual Review of Physiology*, *66*, 735–769.

Lorenzini, C., Baldi, E., Bucherelli, C., & Tassoni, G. (1995). Time-Dependent Deficits of Rat's Memory Consolidation Induced by Tetrodotoxin Injections into the Caudate-Putamen, Nucleus Accumbens, and Globus Pallidus. *Neurobiology of Learning and Memory*, *63*(1), 87–93.

Maass, A., Berron, D., Libby, L. A., Ranganath, C., & Düzel, E. (2015). Functional subregions of the human entorhinal cortex. *ELife*, *4*(JUNE), 1–20.

Mahnke, L., Atucha, E., Pina-Fernàndez, E., Kitsukawa, T., & Sauvage, M. M. (2021). Lesion of the hippocampus selectively enhances LEC's activity during recognition memory based on familiarity. *Scientific Reports*, *11*(1), 19085.

Manns, J. R., & Eichenbaum, H. (2006). Evolution of declarative memory. *Hippocampus*, *16*(9), 795–808.

Martin, C., Grenier, D., Thévenet, M., Vigouroux, M., Bertrand, B., Janier, M., Ravel, N., & Litaudon, P. (2007). fMRI visualization of transient activations in the rat olfactory bulb using short odor stimulations. *NeuroImage*, *36*(4), 1288–1293.

Martin, C. J., Martindale, J., Berwick, J., & Mayhew, J. (2006). Investigating neural–hemodynamic coupling and the hemodynamic response function in the awake rat. *NeuroImage*, *32*(1), 33–48.

Mason, G., Wilson, D., Hampton, C., & Würbel, H. (2004). Non-invasively Assessing Disturbance and Stress in Laboratory Rats by Scoring Chromodacryorrhoea. *Alternatives to Laboratory Animals*, 32(1), 153–159.

Meibach, R. C., & Siegel, A. (1977). Subicular projections to the posterior cingulate cortex in rats. *Experimental Neurology*, *57*(1), 264–274.

Melzer, S., Michael, M., Caputi, A., Eliava, M., Fuchs, E. C., Whittington, M. A., & Monyer, H. (2012). Long-Range-Projecting GABAergic Neurons Modulate Inhibition in Hippocampus and Entorhinal Cortex. *Science*, *335*(6075), 1506–1510.

Mhuircheartaigh, R. N., Rosenorn-Lanng, D., Wise, R., Jbabdi, S., Rogers, R., & Tracey, I. (2010). Cortical and subcortical connectivity changes during decreasing levels of consciousness in humans: A functional magnetic resonance imaging study using propofol. *Journal of Neuroscience*, *30*(27), 9095–9102.

Murray, E. A., Bussey, T. J., & Saksida, L. M. (2007). Visual perception and memory: A new view of medial temporal lobe function in primates and rodents. *Annual Review of Neuroscience*, *30*, 99–122.

Nakamura, N. H., Flasbeck, V., Maingret, N., Kitsukawa, T., & Sauvage, M. M. (2013). Proximodistal segregation of nonspatial information in CA3: Preferential recruitment of a proximal CA3-distal CA1 network in nonspatial recognition memory. *Journal of Neuroscience*, *33*(28), 11506–11514.

Nakamura, N. H., & Sauvage, M. M. (2016). Encoding and reactivation patterns predictive of successful memory performance are topographically organized along the longitudinal axis of the hippocampus. *Hippocampus*, *26*(1), 67–75.

Navarroo Schröder, T., Haak, K. V., Zaragoza Jimenez, N. I., Beckmann, C. F., & Doeller, C. F. (2015). Functional topography of the human entorhinal cortex. *ELife*, *4*(JUNE), 1–17.

Nigrosh, B. J., Slotnick, B. M., & Nevin, J. A. (1975). Olfactory discrimination, reversal learning, and stimulus control in rats. *Journal of Comparative and Physiological Psychology*, *89*(4), 285–294.

O'Keefe, J., & Nadel, L. (1978). The Hippocampus as a Cognitive Map. In *Philosophical Studies* (Vol. 27).

O'Mara, S. (2005). The subiculum: what it does, what it might do, and what neuroanatomy has yet to tell us. *Journal of Anatomy*, *207*(3), 271–282.

Paasonen, J., Stenroos, P., Salo, R. A., Kiviniemi, V., & Gröhn, O. (2018). Functional connectivity under six anesthesia protocols and the awake condition in rat brain. *NeuroImage*, *172*(January), 9–20.

Packard, M. G., & Knowlton, B. J. (2002). Learning and memory functions of the basal ganglia. *Annual Review of Neuroscience*, *25*, 563–593.

Palkovits, M. (1983). The rat brain in stereotaxic coordinates. In *Neuropeptides* (Vol. 3, Issue 4). Elsevier Inc.

Pawela, C. P., Biswal, B. B., Hudetz, A. G., Schulte, M. L., Li, R., Jones, S. R., Cho, Y. R., Matloub, H. S., & Hyde, J. S. (2009). A protocol for use of medetomidine anesthesia in rats for extended studies using task-induced BOLD contrast and resting-state functional connectivity. *NeuroImage*, *46*(4), 1137–1147.

Peeters, R. R., Tindemans, I., De Schutter, E., & Van der Linden, A. (2001). Comparing BOLD fMRI signal changes in the awake and anesthetized rat during electrical forepaw stimulation. *Magnetic Resonance Imaging*, *19*(6), 821–826.

Peng, S. L., Chen, C. M., Huang, C. Y., Shih, C. T., Huang, C. W., Chiu, S. C., & Shen, W. C. (2019). Effects of hemodynamic response function selection on rat fMRI statistical analyses. *Frontiers in Neuroscience*, *13:400*.

Prull, M. W., Dawes, L. L. C., Martin, A. M. L., Rosenberg, H. F., & Light, L. L. (2006). Recollection and familiarity in recognition memory: Adult age differences and neuropsychological test correlates. *Psychology and Aging*, *21*(1), 107–118.

Ramus, S. J., & Eichenbaum, H. (2000). Neural correlates of olfactory recognition memory in the rat orbitofrontal cortex. *Journal of Neuroscience*, *20*(21), 8199–8208.

Ranganath, C., & Rainer, G. (2003). Cognitive neuroscience: Neural mechanisms for detecting and remembering novel events. *Nature Reviews Neuroscience*, *4*(3), 193–202.

Rempel-Clower, N. L., Zola, S. M., Squire, L. R., & Amaral, D. G. (1996). Three Cases of Enduring Memory Impairment after Bilateral Damage Limited to the Hippocampal Formation. *The Journal of Neuroscience*, *16*(16), 5233–5255.

Robitsek, R. J., Fortin, N. J., Ming, T. K., Gallagher, M., & Eichenbaum, H. (2008). Cognitive aging: A common decline of episodic recollection and spatial memory in rats. *Journal of Neuroscience*, *28*(36), 8945–8954.

Rolls, E. T. (2019). The cingulate cortex and limbic systems for action, emotion, and memory. In *Handbook of Clinical Neurology* (1st ed., Vol. 166). Elsevier B.V.

Sabatino, M., La Grutta, V., Ferraro, G., & La Grutta, G. (1986). Relations between basal ganglia and hippocampus: Action of substantia nigra and pallidum. *Rev. E.E.G. Neurophysiol. clin.*, *16*(2), 179–190.

Sauvage, M. M. (2010). ROC in animals: Uncovering the neural substrates of recollection and familiarity in episodic recognition memory. *Consciousness and Cognition*, *19*(3), 816–828.

Sauvage, M. M., Beer, Z., & Eichenbaum, H. (2010). Recognition memory: Adding a response deadline eliminates recollection but spares familiarity. *Learning and Memory*, *17*(2), 104–108.

Sauvage, M. M., Beer, Z., Ekovich, M., Ho, L., & Eichenbaum, H. (2010). The Caudal Medial Entorhinal Cortex: a Selective Role in Recollection-Based Recognition Memory. *Journal of Neuroscience*, *30*(46), 15695–15699.

Sauvage, M. M., Fortin, N. J., Owens, C. B., Yonelinas, A. P., & Eichenbaum, H. (2008). Recognition memory: Opposite effects of hippocampal damage on recollection and familiarity. *Nature Neuroscience*, *11*(1), 16–18.

Sauvage, M. M., Kitsukawa, T., & Atucha, E. (2019). Single-cell memory trace imaging with immediate-early genes. *Journal of Neuroscience Methods*, *326*, 108368.

Sauvage, M. M., Nakamura, N. H., & Beer, Z. (2013). Mapping memory function in the medial temporal lobe with the immediate-early gene *Arc*. *Behavioural Brain Research*, *254*, 22–33.

Schafer, J. R., Kida, I., Xu, F., Rothman, D. L., & Hyder, F. (2006). Reproducibility of odor maps by fMRI in rodents. *NeuroImage*, *31*(3), 1238–1246.

Scherf, T., & Angenstein, F. (2017). Hippocampal CA3 activation alleviates fMRI-BOLD responses in the rat prefrontal cortex induced by electrical VTA stimulation. *PLoS ONE*, *12*(2), 1–16.

Shepard, R. N. (1967). Recognition memory for words, sentences, and pictures. *Journal of Verbal Learning and Verbal Behavior*, *6*(1), 156–163.

Shepherd, J. D., & Bear, M. F. (2011). New views of *Arc*, a master regulator of synaptic plasticity. *Nature Neuroscience*, *14*(3), 279–284.

Sirmpilatze, N., Baudewig, J., & Boretius, S. (2019). Temporal stability of fMRI in medetomidine-anesthetized rats. *Sci Rep*. Nov 13;9(1):16673.

Smith, J. B., Liang, Z., Watson, G. D. R., Alloway, K. D., & Zhang, N. (2017). Interhemispheric resting-state functional connectivity of the claustrum in the awake and anesthetized states. *Brain Structure and Function*, *222*(5), 2041–2058.

Squire, L. R. (1992). Nondeclarative Memory: Multiple Brain Systems Supporting Learning. *Journal of Cognitive Neuroscience*, *4*(3), 232–243. h

Squire, L. R., Wixted, J. T., & Clark, R. E. (2007). Recognition memory and the medial temporal lobe: a new perspective. *Nature Reviews Neuroscience*, *8*(11), 872–883.

Squire, L. R., & Zola, S. M. (1998). Episodic memory, semantic memory, and amnesia. *Hippocampus*, *8*(3), 205–211.

Stark, C. E. L., & Squire, L. R. (2000). Functional magnetic resonance imaging (fMRI) activity in the hippocampal region during recognition memory. *Journal of Neuroscience*, *20*(20), 7776–7781.

Stenroos, P., Paasonen, J., Salo, R. A., Jokivarsi, K., Shatillo, A., Tanila, H., & Gröhn, O. (2018). Awake rat brain functional magnetic resonance imaging using standard radio frequency coils and a 3D printed restraint kit. *Frontiers in Neuroscience*, *12*(AUG).

Steward, O., & Scoville, S. A. (1976). Cells of origin of entorhinal cortical afferents to the hippocampus and fascia dentata of the rat. *The Journal of Comparative Neurology*, *169*(3), 347–370.

Sugiura, M., Shah, N. J., Zilles, K., & Fink, G. R. (2005). Cortical representations of personally familiar objects and places: Functional organization of the human posterior cingulate cortex. *Journal of Cognitive Neuroscience*, *17*(2), 183–198.

Tomás Pereira, I., Agster, K. L., & Burwell, R. D. (2016). Subcortical connections of the perirhinal, postrhinal, and entorhinal cortices of the rat. I. afferents. *Hippocampus*, *26*(9), 1189–1212.

Van Strien, N. M., Cappaert, N. L. M., & Witter, M. P. (2009). The anatomy of memory: An interactive overview of the parahippocampal- hippocampal network. *Nature Reviews Neuroscience*, *10*(4), 272–282.

Vazdarjanova, A., & Guzowski, J. F. (2004). Differences in Hippocampal Neuronal Population Responses to Modifications of an Environmental Context: Evidence for Distinct, Yet Complementary, Functions of CA3 and CA1 Ensembles. *Journal of Neuroscience*, *24*(29), 6489–6496.

Vazdarjanova, A., McNaughton, B. L., Barnes, C. A., Worley, P. F., & Guzowski, J. F. (2002). Experience-dependent coincident expression of the effector immediate-early genes *Arc* and *Homer 1a* in hippocampal and neocortical neuronal networks. *Journal of Neuroscience*, *22*(23), 10067–10071.

Vazdarjanova, A., Ramirez-Amaya, V., Insel, N., Plummer, T. K., Rosi, S., Chowdhury, S., Mikhael, D., Worley, P. F., Guzowski, J. F., & Barnes, C. A. (2006). Spatial exploration induces *ARC*, a plasticity-related immediate-early gene, only in calcium/calmodulin-dependent protein kinase II-positive principal excitatory and inhibitory neurons of the rat forebrain. *The Journal of Comparative Neurology*, *498*(3), 317–329.

West, M. J. (1993). New stereological methods for counting neurons. *Neurobiology of Aging*, *14*(4), 275–285.

West, M. J. (1999). Stereological methods for estimating the total number of neurons and synapses: issues of precision and bias. *Trends in Neurosciences*, *22*(2), 51–61.

Witter, M. P., Amaral, D. G., MP, W., & DG, A. (2021). The entorhinal cortex of the monkey: VI. Organization of projections from the hippocampus, subiculum, presubiculum, and parasubiculum. In *Journal of Comparative Neurology* (Vol. 529, Issue 4). J Comp Neurol.

Wixted, J. T., & Squire, L. R. (2011). The medial temporal lobe and the attributes of memory. *Trends in Cognitive Sciences*, *15*(5), 210–217.

World Health Organisation. (2001). The world health report 2001 — Mental health: new understanding, new hope. *Bulletin of the World Health Organization*, *79*(11), 1085–1085.

Xu, F., Kida, I., Hyder, F., & Shulman, R. G. (2000). Assessment and discrimination of odor stimuli in rat olfactory bulb by dynamic functional MRI. *Proceedings of the National Academy of Sciences of the United States of America*, *97*(19), 10601–10606.

Xu, F., Liu, N., Kida, I., Rothman, D. L., Hyder, F., & Shepherd, G. M. (2003). Odor maps of aldehydes and esters revealed by functional MRI in the glomerular layer of the mouse olfactory bulb. *Proceedings of the National Academy of Sciences*, *100*(19), 11029–11034.

Yonelinas, A. P. (2001). Components of episodic memory: The contribution of recollection and familiarity. *Philosophical Transactions of the Royal Society B: Biological Sciences*, *356*(1413), 1363–1374.

Yonelinas, A. P. (2002). The nature of recollection and familiarity: A review of 30 years of research. *Journal of Memory and Language*, *46*(3), 441–517.

Yonelinas, A. P., & Jacoby, L. L. (1994). Dissociations of processes in recognition memory: effects of interference and of response speed. *Canadian Journal of Experimental Psychology*, *48*(4), 516–535.

Yonelinas, A. P., Kroll, N. E. A., Quamme, J. R., Lazzara, M. M., Sauvé, M. J., Widaman, K., & Knight, R. T. (2002). Effects of extensive temporal lobe damage or mild hypoxia on recollection and familiarity. *Nature Neuroscience*, *5*(11), 1236–1241

Yonelinas, A. P., Otten, L. J., Shaw, R. N., & Rugg, M. D. (2005). Separating the brain regions involved in recollection and familiarity in recognition memory. *Journal of Neuroscience*, *25*(11), 3002–3008.

Yonelinas, A. P., & Parks, C. M. (2007). Receiver Operating Characteristics (ROCs) in Recognition Memory: A Review. *Psychological Bulletin*, *133*(5), 800–832.

Yonelinas, A. P., Widaman, K., Mungas, D., Reed, B., Weiner, M. W., & Chui, H. C. (2007). Memory in the aging brain: Doubly dissociating the contribution of the hippocampus and entorhinal cortex. *Hippocampus*, *17*(11), 1134–1140.

Young, B. J., Otto, T., Fox, G. D., & Eichenbaum, H. (1997). Memory representation within the parahippocampal region. *Journal of Neuroscience*, *17*(13), 5183–5195.

Chapter 7

7. Appendix

7.1 Supplementary material

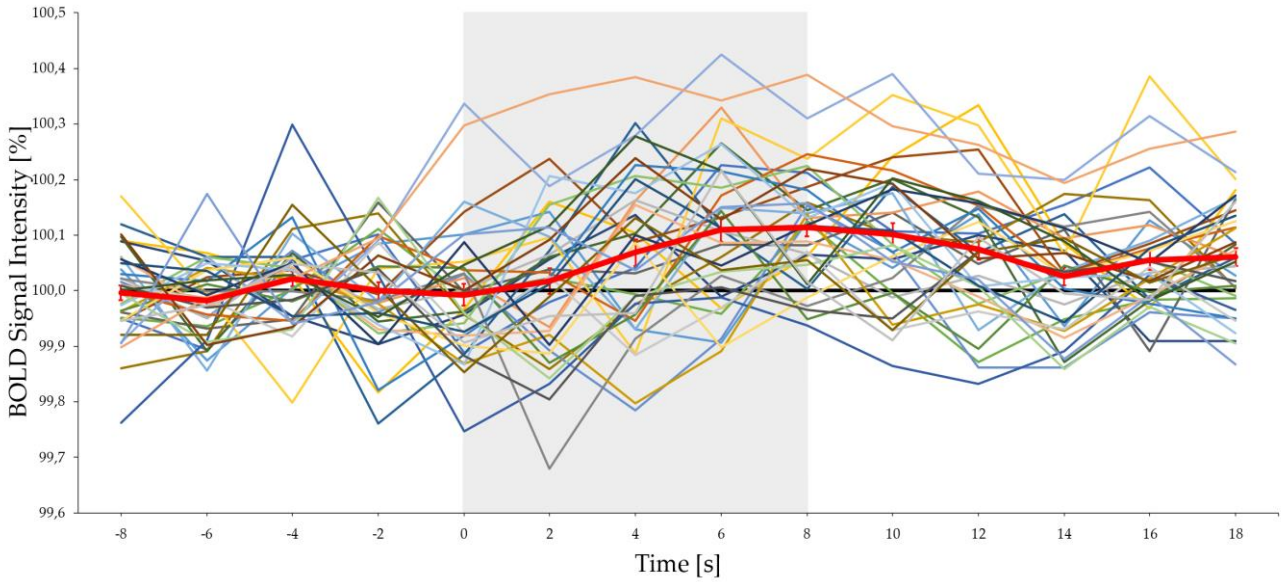

Supplementary Figure 1: Chapter 2 - Summary of BOLD responses from each of the 37 channels that presented the odor 'cherry' once (only one presentation of channel 1 is included here) in experiment 2. Despite individual differences, an increase of BOLD signal can be found for all channels. Indicated by the broad red line is the average BOLD response of all 37 channels (mean±SEM). Grey background indicates the stimulus presentation.

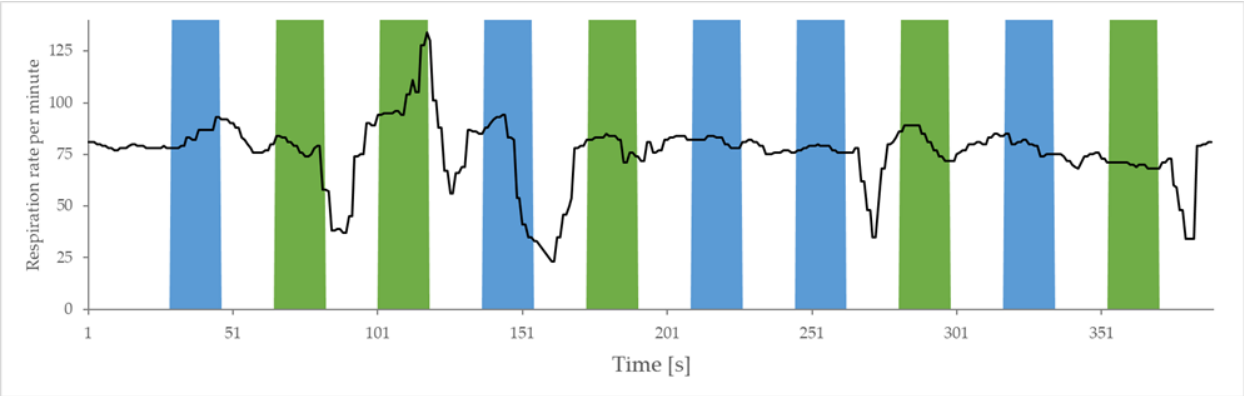

Supplementary Figure 2: Chapter 3 - Respiration rate. Representative time series of the respiration rate of an awake rat exposed to odors. Green background represents the delivery of `old´, blue that of `new´ odors, and white that of `air´ (no odor). No significant differences could be detected between the respiration rates during `old´, `new´, or `air´ presentation.

Table 2: Chapter 3 - Overview of mean breathing during the different stimulus conditions. The respiration rate does not show a significant difference in response to the presentation of `old´ odors, `new´ odors, or `air´ during the awake rat fMRI scans.

	Average respiration rate per minute
old	92±3
new	90±3
air	90±3

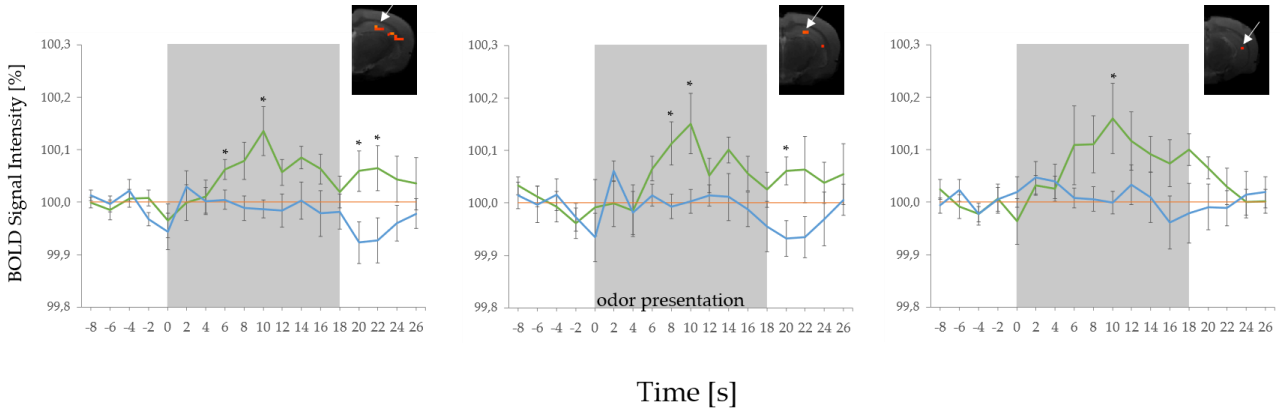

Supplementary Figure 3: Chapter 3 - Averaged HIP BOLD responses of awake rats at other levels than that depicted in Figure 15. Voxel size of clusters of ROIs ranges from 7 to 10 voxels (left&middle: 7 voxels; right: 10 voxels). Grey background indicates the stimulus presentation. White arrows indicate clusters from which the signal was extracted. Asterisks indicate a significant difference in BOLD intensity between `old´ (green) to `new´ (blue) odor presentation. * p<0.05

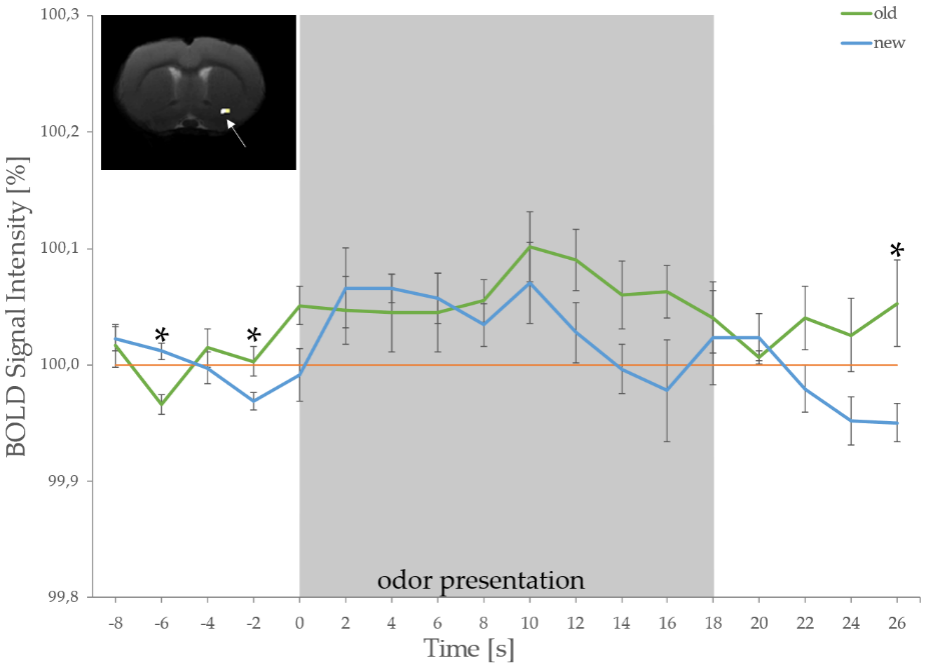

Supplementary Figure 4: Chapter 3 - Example of an averaged BOLD response of an activated area, where no significant difference of BOLD signal intensity between the `new´ and `old´ odor block during odor presentation or subsequently was found (cluster from `new>old´ contrast, see **Figure 16).** The white arrow indicates the cluster from which the signal was extracted. Grey background indicates the stimulus presentation. Asterisks indicate a significant difference in BOLD signal intensity between `old´ and `new´ odor presentation. *p<0.05.

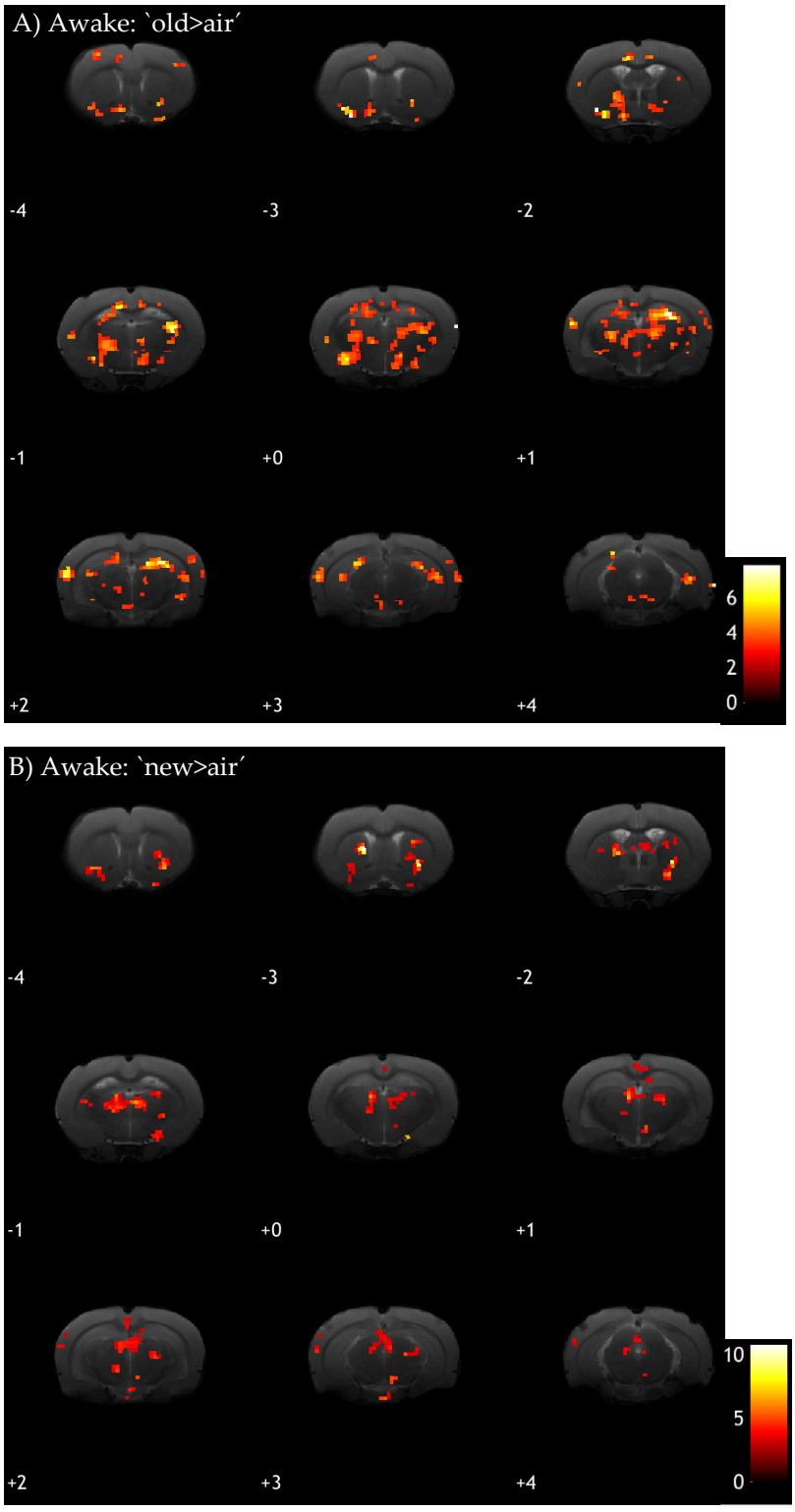

Supplementary Figure 5: Chapter 3 - GLM analysis for the response to `old´ (*A*) or `new´ (*B*) odor presentation versus `air´ in awake rat fMRI** (n=7). Data shown with a p value of <0.01 uncorrected and cluster size >3 voxels. Various regions are similarly activated for `old>air´ and `new>air´ contrasts (parts of the laterodorsal thalamic nucleus, piriform cortex, olfactory tubercle, ventral, and globus pallidus). Extended significant activation of the HIP and the VPL was only found for the `old>air´ contrast (A**). In contrast, the anteromedial/mediodorsal thalamic nucleus and retrosplenial granular cortex were only largely activated in the `new>air´ contrast (**B**).

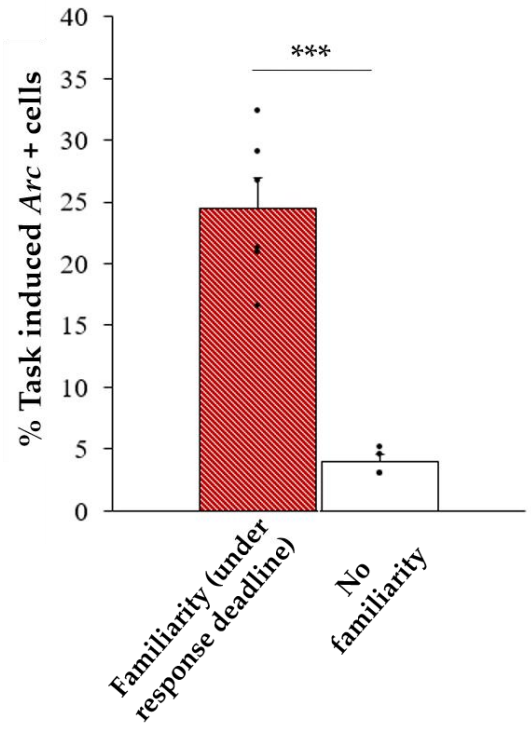

Supplementary Figure 6: Chapter 4 - Adapted from Atucha et al., 2017: Proportions of *Arc* positive cells in the LEC of rats subjected to a response deadline also leading to familiarity judgments in the DNMS task: evidence that activity in the LEC is tight to the contribution of familiarity to memory performance and not to the contribution of other non-cognitive processes occurring during memory retrieval. Rats were trained to perform the DNMS task described in **Figure 18** but to respond within a response deadline of 2 sec. Implementing this response deadline biases judgments towards relying on familiarity (Gronlund et al., 1997; Hintzman et al., 1998; Koen & Yonelinas, 2011; Sauvage, Beer, & Eichenbaum, 2010; Yonelinas & Jacoby, 1994) as opposed to relying both on recollection and familiarity for retrieving memories in animals and humans. In this study, LEC was overwhelmingly engaged in rats relying on familiarity (light red bar) when compared to control rats (white bar) that were trained according to the same scheme but were randomly-rewarded instead of following a DNMS rule (i.e., no demands were imposed on the familiarity process for this group). Results indicate that the difference in LEC activity levels between groups likely stems from a difference in the contribution of familiarity to memory performance rather than from the contribution of other non-cognitive processes occurring at retrieval (Familiarity vs. No familiarity: $t_{(8)} = 6.747$, $p < 0.001$; comparisons to 0: Familiarity: $t_{(5)} = 16.163$, $p < 0.001$; No familiarity: $t_{(3)} = 7.23$, $p = 0.005$). Of note, both experimental manipulations leading to familiarity judgments in this DNMS task (implementing a response deadline in Atucha et al., 2017 or lesioning the hippocampus in the present study) yield similar levels of activation in the LEC (response deadline vs. HIP lesion: $t_{(10)} = 0.724$; $p = 0.486$). Bars represent means ± SEM. ***$p < 0.001$. Proportions of *Arc* positive cells are normalized by LEC proportions of *Arc* positive cells of respective home-caged control groups.

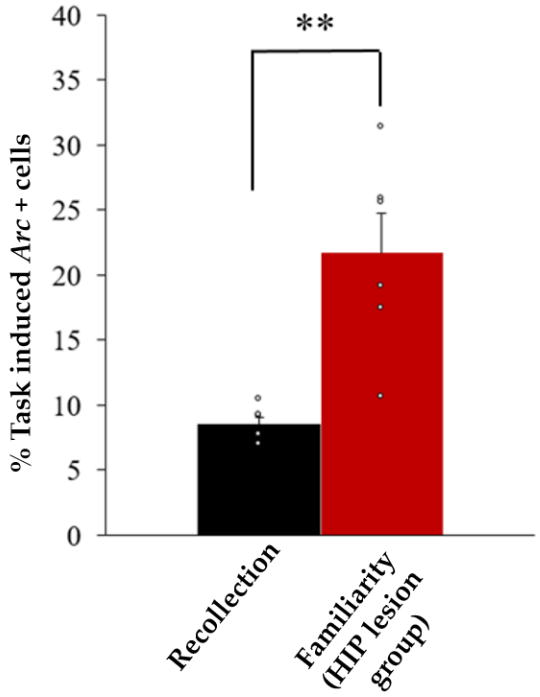

Supplementary Figure 7: Chapter 4 - Proportions of *Arc* positive cells in the LEC of rats using either recollection or familiarity to solve the DNM task: evidence that activity in the LEC is tight to the contribution of familiarity to recognition memory and not to the contribution of the second cognitive process contributing to recognition memory; recollection. Associative recognition memory, the memory for associated stimuli, relies on recollection in the present DNMS task (Sauvage et al., 2008), whereas the performance of rats with hippocampal lesion in the same task relies on familiarity (Fortin et al., 2004). LEC's activity level in rats relying on recollection (black bar) was low, whereas it was significantly higher in rats with HIP lesion relying on familiarity (red bar) (Recollection vs. familiarity (HIP lesion): $t_{(10)} = 4.29$, $p < 0.01$). This result further supports the claim that activity in the LEC during the retrieval phase of the DNMS task depends on the contribution of familiarity to recognition memory and not on the contribution of other cognitive processes. Bars represent means ± SEM; ** $p < 0.01$. Proportions of *Arc* positive cells are normalized by LEC proportions of *Arc* positive cells of respective home-caged control groups.

7.2 Publications

Mahnke, L., Atucha, E., Pina-Fernàndez, E., Kitsukawa, T., & Sauvage, M. M. (2021). Lesion of the hippocampus selectively enhances LEC's activity during recognition memory based on familiarity. *Scientific Reports*, 11(1), 19085. https://doi.org/10.1038/s41598-021-98509-4

Krautwald, K., **Mahnke, L.**, & Angenstein, F. (2019). Electrical stimulation of the lateral entorhinal cortex causes a frequency-specific BOLD response pattern in the rat brain. *Frontiers in Neuroscience*, 13(MAY), 1–13. https://doi.org/10.3389/fnins.2019.00539

Ku, S. P., Nakamura, N. H., Maingret, N., **Mahnke, L.**, Yoshida, M., & Sauvage, M. M. (2017). Regional specific evidence for memory-load dependent activity in the dorsal subiculum and the lateral entorhinal cortex. *Frontiers in Systems Neuroscience*, 11(July), 1–10. https://doi.org/10.3389/fnsys.2017.00051

7.3 Ehrenerklärung

Ich versichere hiermit, dass ich die vorliegende Arbeit ohne unzulässige Hilfe Dritter und ohne Benutzung anderer als der angegebenen Hilfsmittel angefertigt habe; verwendete fremde und eigene Quellen sind als solche kenntlich gemacht.

Ich habe insbesondere nicht wissentlich:

- Ergebnisse erfunden oder widersprüchliche Ergebnisse verschwiegen,
- statistische Verfahren absichtlich missbraucht, um Daten in ungerechtfertigter Weise zu interpretieren,
- fremde Ergebnisse oder Veröffentlichungen plagiiert,
- fremde Forschungsergebnisse verzerrt wiedergegeben.

Mir ist bekannt, dass Verstöße gegen das Urheberrecht Unterlassungs- und Schadensersatzansprüche des Urhebers sowie eine strafrechtliche Ahndung durch die Strafverfolgungsbehörden begründen kann.

Ich erkläre mich damit einverstanden, dass die Arbeit ggf. mit Mitteln der elektronischen Datenverarbeitung auf Plagiate überprüft werden kann.

Die Arbeit wurde bisher weder im Inland noch im Ausland in gleicher oder ähnlicher Form als Dissertation eingereicht und ist als Ganzes auch noch nicht veröffentlicht.

Zerbst, den 21.10.2021